2016

AN EXPERIMENTAL INVESTIGATION INTO THE EFFECT OF PARTICULATE MATTER ON NOx REDUCTION IN A SCR CATALYST ON A DPF

Saksham Gupta
Michigan Technological University, sakshamg@mtu.edu

AN EXPERIMENTAL INVESTIGATION INTO THE EFFECT OF PARTICULATE MATTER ON NO_x REDUCTION IN A SCR CATALYST ON A DPF

By

Saksham Gupta

A REPORT

Submitted in partial fulfillment of the requirements for the degree of

MASTER OF SCIENCE

In Mechanical Engineering

MICHIGAN TECHNOLOGICAL UNIVERSITY

2016

This report has been approved in partial fulfillment of the requirements for the Degree of MASTER OF SCIENCE in Mechanical Engineering

Department of Mechanical Engineering- Engineering Mechanics

Report Co-Advisor: *Dr. Jeffrey Naber*

Report Co-Advisor: *Dr. John Johnson*

Committee Member: *Dr. David Shonnard*

Department Chair: *Dr. William Predebon*

Table of Contents

Table of Contents i
List of Figures iii
List of Tables iv
Acknowledgements v
Common Terms and Abbreviations vi
Abstract viii
Chapter 1. Introduction 1
1.1 Overview of Research 1
1.2 Goals and Objectives 3
1.3 Overview of Report 3
Chapter 2. Experimental Setup, Instrumentation, and Test Procedures 4
2.1 Experimental Setup 4
Engine and Dynamometer 6
Aftertreatment System 7
2.2 Fuel Properties 9
2.3 Test Cell Instrumentation 9
Air and Fuel Flow Measurement 9
Pressure Measurement 10
Temperature Measurement 10
Data Acquisition 11
Emissions Measurement 12
Particulate Matter Sampling and Measurement 12
2.4 Test Points 13
2.5 Test Procedure 14
Tests with PM Loading in the SCRF® 15
Tests without PM Loading in the SCRF® 19
Chapter 3. Results 20
3.1 NO_x Reduction 20
SCRF® Inlet Conditions 20
NO Conversion across DOC 23
NO_2 Decrease and NO_x Conversion across SCRF® 24
3.2 NH_3 Slip and Nitrogen Balance 30

Chapter 4. Summary and Conclusions 32
4.1 Summary 32
Loading Stages 32
NO_x Reduction Stage 32
4.2 Conclusions 33
References 34
Appendix A. Particulate Matter Sampling 35
Appendix B. SCRF® Weighing 37
Appendix C. Engine, Exhaust Conditions and PM Mass Balance for Each Stage 38
Stage 1 and Stage 2 at 2 g/L Loading 39
Stage 1 and Stage 2 at 4 g/L Loading 43
Appendix D. Gaseous Emissions by Stage 48
Stage 1 and Stage 2 Loading at 2 g/L 48
Stage 1 and Stage 2 Loading at 4 g/L 49
NO_x Reduction Stage 50
Appendix E. SCRF® Pressure Drops 52
Loading at 0 g/L 52
Loading at 2 g/L 54
Loading at 4 g/L 56
Appendix F. SCRF® Temperature Distributions 59
Stage 2 Loading at 2 g/L and 4 g/L 60
NO_x Reduction Stage 70
Loading at 0 g/L 71
Loading at 2 g/L 77
Loading at 4 g/L 83
Appendix G. Permission to Use Copyrighted Material 89

List of Figures

Figure 1.1 Overview of aftertreatment system [2] 2
Figure 2.1 Engine system in the test cell 4
Figure 2.2 Experimental setup showing the location of sampling lines, pressure port lines, and the dynamometer in the test cell 5
Figure 2.3 Aftertreatment system with sensors and instrumentation..... 6
Figure 2.4 SCRF® thermocouple arrangement – Dimensions are in mm.....11
Figure 2.5 Schematic representation of the process of testing with PM loading in the SCRF®.....15
Figure 2.6 Pressure drop curve for Stage 1, Stage 2 and repeat loading in between the NO_x Reduction Stage 18
Figure 2.7 Urea dosing cycle for SCRF® 19
Figure 2.8 Schematic representation of the process of testing without PM loading in the SCRF® 19
Figure 3.1 Inlet SCRF® NO_2 /NO_x ratio at different SCRF® inlet temperatures (test points).....21
Figure 3.2 Change in NO_2/NO_x ratio at inlet and outlet of the SCRF® with different SCRF® inlet temperatures for 0, 2, and 4g/L loading ANR - 0 24
Figure 3.3 Variation of NO_x conversion efficiency (%) with ANR – 0.8 for NO_x reduction test points and SCRF® inlet temperatures 26
Figure 3.4 Variation of NO_x conversion efficiency (%) with ANR - 1 for NO_x reduction test points and SCRF® inlet temperatures.....28
Figure 3.5 Variation of NO_x conversion efficiency (%) with ANR – 1.2 for NO_x reduction test point.....29
Figure 3.6 NH_3 slip from SCRF® for NO_x reduction test points at ANR - 0.8 31
Figure 3.7 NH_3 slip from SCRF® for NO_x reduction test points at ANR - 1 31
Figure 3.8 NH_3 slip from SCRF® for NOx reduction test points at ANR – 1.2 Repeat (Rpt.).....31

List of Tables

Table 2.1 Specifications of the Cummins ISB 2013 engine..... 7
Table 2.2 Eddy current dynamometer specifications..... 7
Table 2.3 Specifications of the DOC, CPF and SCRF®..... 8
Table 2.4 Specification of fuel used for testing [2] 9
Table 2.5 Specifications of pressure transducer.....10
Table 2.6 Specification of thermocouples 11
Table 2.7 Specifications of IMR-MS 12
Table 2.8 Specifications of Mettler Toledo UMT2 microbalance [2] 13
Table 2.9 Specifications of weighing apparatus [2].....13
Table 2.10 Test matrix of baseline SCR tests for NO_x reduction experiments.....14
Table 3.1 Engine and SCRF® inlet conditions at different test points for NO_x reduction test 22
Table 3.2 NO and NO_2 species concentration at the inlet and outlet DOC for different test points.....23
Table 3.3 DOC inlet temperature, space velocity and NO conversion efficiency for different test points.....24
Table 3.4 Species concentration at upstream and downstream SCRF® for NO_x reduction test points at ANR-0.8.....26
Table 3.5 Species conversion efficiency across SCRF® for NO_x reduction test points at ANR-0.8.....26
Table 3.6 Species concentration at upstream and downstream SCRF® for NO_x reduction test points at ANR-1.....28
Table 3.7 Species conversion efficiency across SCRF® for NO_x reduction test points at ANR-1.....28
Table 3.8 Species concentration at upstream and downstream SCRF® for NO_x reduction test points at ANR-1.2.....29
Table 3.9 Species conversion efficiency across SCRF® for NO_x reduction test points at ANR-1.2.....29

Acknowledgements

I wish to express my sincere gratitude to several people who were associated with this research study directly or indirectly, from my personal and professional life, without whom I would have never been able to finish my report. I am thankful to my committee members, student research group, friends, and my parents for their continued guidance and support in my research.

I would like to thank my advisors Dr. John Johnson and Dr. Jeffrey Naber for providing me this excellent opportunity to work in this Consortium project and providing me continued guidance and support during the course of my research. I thank the MTU Consortium for providing me support during the course of my research. I am thankful to Dr. David Shonnard for being part of my defense committee. Dr. John Johnson provided immense guidance on analyzing the data critically and providing close feedback on report writing. I would like to thank Dr. Jeffrey Naber, who helped me better understand the instrumentation and experimentation in the test cell and provided me the guidance on troubleshooting instrumental failures in the test cell. Krishna Chilumukuru, currently at Cummins, was helpful in providing information about the components, instruments and procedures used for testing.

My thanks are extended to my research group colleagues at Michigan Tech, Vaibhav Kadam for helping me understand the test cell and test procedure, Erik Gustafson and Sagar Sharma for their assistance during the testing. Thanks are also extended to Steve Lehmann and Christopher Pinnow from Michigan Tech for guiding me in setting up and troubleshooting electrical wires and connection in the test cell.

Common Terms and Abbreviations

This section lists the terms/abbreviations used commonly throughout this report

Abbreviations

LFE:	Laminar Flow Element
ULSD:	Ultra Low Sulphur Diesel
DOC:	Diesel Oxidation Catalyst
DPF:	Diesel Particulate Filter
CPF:	Catalyzed Particulate Filter
SCR:	Selective Catalytic Reduction
SCRF®:	Selective Catalytic Reduction Filter (produced by Johnson-Matthey)
MTU:	Michigan Technological University
MST:	Manual Sampling Train
DGM:	Dry Gas Meter
PM:	Particulate Matter
H/C:	Hydrogen to Carbon ratio
NO, NO_2, NO_x:	Nitric Oxide, Nitrogen Dioxide, (NO + NO_2)
CO, CO_2, O_2:	Carbon Monoxide, Carbon Dioxide, Oxygen
NH_3:	Ammonia
NH_3 Slip:	Ammonia coming out of the system
NO_2/NO_x:	Ratio of NO_2 concentration to NO_x concentration
S1:	Stage 1
S2:	Stage 2
Std.:	Standard
Act.:	Actual
Conc.:	Concentration
ANR:	Ammonia to NO_x ratio
Vel.:	Velocity
MW:	Molecular Weight

UDOC:	Upstream DOC
DDOC:	Downstream DOC
USCRF:	Upstream SCRF®
DSCRF:	Downstream SCRF®
SCRF®- 0:	SCRF® loaded to 0 g/L PM
SCRF®- 2:	SCRF® loaded to 2 g/L PM
SCRF®- 4:	SCRF® loaded to 4 g/L PM
MFR:	Mass Flow Rate
NO_2/PM:	Ratio of NO_2 (mg) to PM (mg)
Conv.:	Conversion
hr.:	Hour
P:	Pressure
Temp.:	Temperature
V:	Volume
mg/scm:	milligram /standard cubic meter

Symbols

®:	Registered Trademark
ρ:	Density
%:	Percent
°:	Degrees
W/:	With
W/O:	Without
±:	Plus or minus
ΔX:	Overall change in quantity 'X'

Abstract

The study of NO_x reduction across the SCRF® is presented in this report to understand the inlet and outlet NO, NO_2, NH_3 species from the SCRF®. The SCRF® is a prototype SCR catalyst on a Diesel Particulate Filter (DPF) that reduces NOx and PM at the downstream location. The SCRF® reduces the packaging volume of the aftertreatment components in order to reduce the cost, volume and weight of the aftertreatment system. A total of 12 experiments were performed on a Cummins ISB 2013 280 hp engine and the aftertreatment system. The tests were performed to investigate the NO_x reduction performance of the SCRF® under various Particulate Matter loading.

The loading phase has been divided into two stages: Stage 1 and Stage 2. Stage 1 begins after all the PM has been removed from the SCRF®, which is then followed by Stage 2 loading. The engine is run at 2400 rpm and 200 Nm load with different fuel rail pressures for a duration to achieve PM loadings of 0, 2, and 4 g/L (grams of PM per volume of the SCRF®) in the SCRF®.

For the testing of the SCRF® without PM loading, a Catalyzed Particulate Filter (CPF) was placed before the SCRF®. After the loading phase, NO_x reduction stage was run at different engine conditions. The engine speed and load conditions were selected for the NO_x reduction stage, named as test points 1, 3, 6, and 8, in order to attain a wide range in space velocities, inlet temperatures and NO_2/NO_x ratios in the SCRF®, which are the major parameters determining NO_x reduction efficiency in the SCRF®. The exhaust temperature varied from 206 to 443 °C, inlet NO_2/ NO_x ratio varied from 0.22 to 0.46, and space velocity varied from 13.5 to 48.2 k/hr. Urea was dosed in the decomposition tube before the SCRF® to determine the NO_x conversion efficiency at different ammonia to NO_x ratio (ANR) values. The ANR values considered for the NO_x reduction and NH_3 slip were 0, 0.8, 1, 1.2, and 1.2 repeat. The ANR of 1.2 was repeated in the urea dosing cycle.

It was found that the NO_x conversion efficiency across the SCRF® is maximum for test points 3 and 6 i.e. for the temperature range of 300-350 °C. The NO_2/NO_x ratio at those points was around 0.42-0.46. It is observed that the loading in the SCRF® does not affect the NO_x conversion efficiency at low (205 °C) and high (440 °C) temperature points but affects in between. The NO_x conversion efficiency improved with PM

loading until 300°C SCRF® inlet temperature and decreased (with PM loading) after 350 °C. There is noticeable ammonia oxidation at temperatures above 400 °C in the SCRF® that affects NO_x conversion efficiency [1]. At higher temperature of about 440 °C, NH_3 slip is observed varying with PM loading in the SCRF®. With PM loading, NO_2 assisted oxidation increases the concentration of NO [2] and affects the NO_x conversion efficiency.

It is concluded from the results that the NO_2 concentration across the SCRF® decreased with PM loading and SCRF® temperature due to NO_2 assisted PM oxidation. The impact of PM loading on NO_x reduction in the SCRF® was insignificant below 300 °C. NO_x conversion decreased by 3 – 5 % above 350 °C with increase in PM loading from 0 to 2 and 4 g/L, due to consumption of NO_2 via passive oxidation of PM. The NO_x concentration is not completely converted across the SCRF® at temperatures above 350 °C even if dosed with an ANR value of 1.2.

Chapter 1. Introduction

Emissions from diesel engines have always been an area of research due to their impact on the environment. To mitigate pollution, control of engine emissions is a statutory requirement, standards of which are set by US EPA. One of the techniques to control NO_x emissions practically and economically is by having a Selective Catalytic Reduction (SCR) catalyst on a Diesel Particulate Filter (DPF), called a SCRF®. The SCRF® is one of the latest technologies, which is a combination of SCR and DPF that results in both Particulate Matter (PM) Oxidation and NO_x reduction. This technology has proved to efficiently reduce NO_x emissions by 95% and has helped in preventing ammonia slip at the downstream location [3]. A flow through SCR can be added in the engine exhaust to diminish NO_x emissions and to reduce fuel consumption while engines are run at higher load.

This part of the research was carried out on a Cummins 2013 ISB diesel engine that was fitted with an aftetreatment system comprising of a Diesel Oxidation Catalyst (DOC), Catalyzed Particulate Filter (CPF), and SCRF® (SCR catalyst on a DPF). Experiments were carried out to study the NO_x conversion efficiency of the SCRF® and the experimental data will also be used for the calibration of the SCRF® model.

1.1 Overview of Research

The Diesel Engine Aftertreatment Consortium project aims to conduct experimental and modeling research on advanced aftertreatment systems. The study focuses on PM oxidation and NO_x reduction characteristics of CPF, SCR, and SCRF®. SCRF® is a substrate developed by Johnson Matthey and is being used in the Consortium project for testing. The objective of this research is to study the reactions for the NO_x reduction in the SCRF® with and without PM loading. The observations and results of the experimental tests of the SCRF® with and without PM were analyzed, compared, and the experimental data will be used to calibrate the system model.

The aftertreatment system configuration is shown in Figure 1.1. The first component is the DOC whose function is to oxidize CO, NO, and the hydrocarbons present in the exhaust stream. The Figure 1.1 describes two layouts:

1. Without PM loading – As shown in figure, the CPF is placed downstream the DOC such that the CPF filters all the PM coming in the exhaust.
2. With PM loading – Spacer, an empty block, is placed downstream DOC (in place of the CPF as done in Figure 1.1) that allows all PM to pass through it.

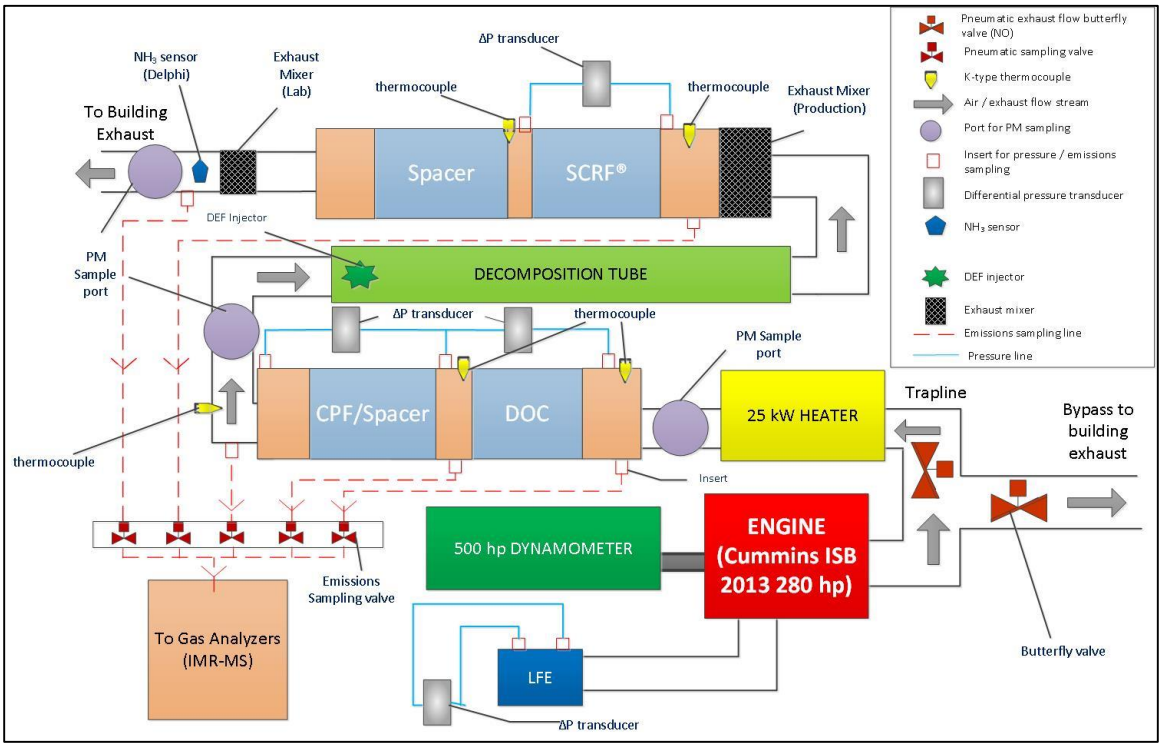

Figure 1.1 Overview of aftertreatment system [2]

1.2 Goals and Objectives

The goal of the research project is to understand the performance of the DPF with an SCR catalyst coated on the substrate by experimental studies.

To achieve efforts towards this goal, experimental studies were conducted on the SCRF® to determine the NO_x reduction efficiency of the SCRF® with and without PM loading in order to understand the effect of PM on the kinetics of the SCR catalyst. Various parameters such as NO, NO_2, and NH_3 (at the upstream and downstream locations of the SCRF®), pressure drop (across the SCRF®), and temperature distribution (across the SCRF®) were studied to determine the NO_x reduction efficiency of the SCRF® with and without PM loading.

The SCRF® experimental data collected will be used to develop and calibrate the MTU SCR-F model.

The following are the specific objectives:

1. To develop procedures for testing the SCRF® under engine load conditions and collect the data to support the SCRF® model calibration effort.
2. To use the Cummins 2013 ISB diesel engine at selected engine conditions to attain desired exhaust parameters of temperature, space velocities, NO_2/NO_x ratios and NO_2/PM ratios and study if PM has an effect on the NO_x reduction trend and the SCR reactions.
3. To compare the data collected for the SCRF® tests with and without PM loading.

1.3 Overview of Report

The report discusses the experimental study conducted in the Heavy Duty Diesel Lab at MTU to understand the NO_x reduction and NH_3 slip in the SCRF®. Chapter 2 discusses the experimental setup, and the instrumentation used to collect the data. Chapter 3 contains the results of the research for the tests on the SCRF®. Chapter 4 summarizes and determines the findings of the research and discusses future work.

Chapter 2. Experimental Setup, Instrumentation, and Test Procedures

This chapter discusses the experimental setup, instrumentation, and procedures used for conducting the experiments. The Heavy Duty Diesel Lab at Michigan Technological University contains the engine, dynamometer, fuel flow meter, data acquisition system, aftertreatment system, Pierburg emission bench, mass spectrometer and other measuring instruments.

2.1 Experimental Setup

This section discusses the engine and the aftertreatment system used for the testing. Figure 2.1 and 2.2 show the layout of the engine and the aftertreatment system components along with various sensors, ports, and other instrumentation in the test cell.

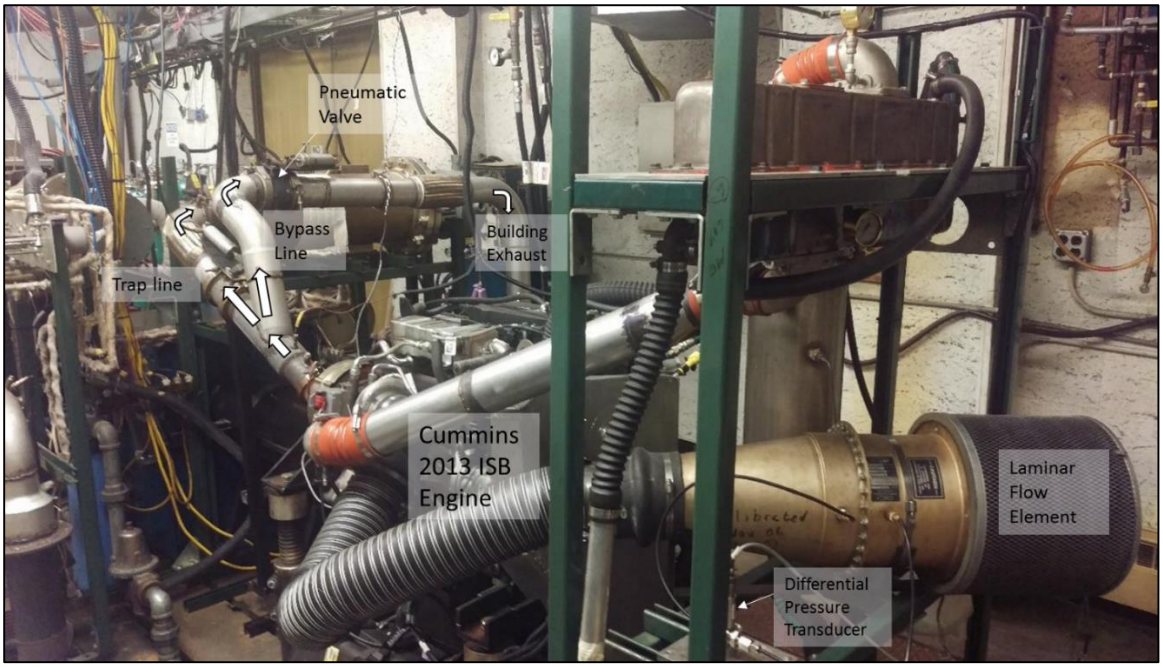

Figure 2.1 Engine system in the test cell

Ambient air was supplied to the test cell from the building ventilation system, so that the exhaust gases that might leak from any of the systems within the setup would not go in to the test cell. The engine exhaust system was maintained under a relatively negative pressure for the removal of the exhaust gases. Intake air was flown through

the Laminar Flow Element (LFE) to the intake manifold of the engine. Exhaust coming out from the engine was diverted to the aftertreatment system by pneumatically controlled butterfly valves through the trap line as shown in Figure 2.1. The exhaust gas was then heated using an electric heater prior to going into the DOC. After the DOC, the exhaust flowed to the CPF for tests without PM loading or directly to the decomposition tube for tests with PM loading. For the latter, an empty block (called the spacer) was provided in place of the CPF. In the CPF, particulate matter was retained and oxidized. Urea in the decomposition tube was injected and the exhaust was then fed to the exhaust mixer located upstream of the SCRF® to enable proper mixing. The stream then flowed to the SCRF® and finally, the exhaust was directed through the building exhaust.

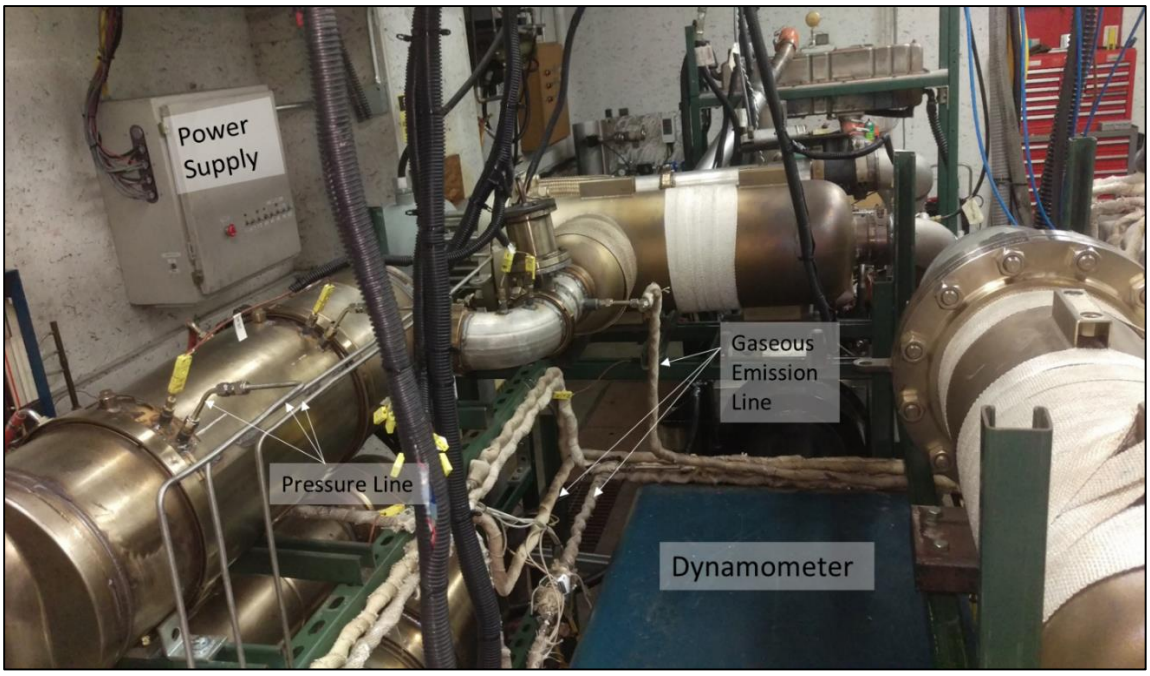

Figure 2.2 Experimental setup showing the location of sampling lines, pressure port lines, and the dynamometer in the test cell

The pressure drops across the LFE, DOC, CPF and SCRF® were measured by delta pressure transducers as shown in Figure 2.2, whereas the temperatures of the exhaust at the inlet and the outlet of components were measured by K-type thermocouples as shown in Figure 2.3. PM sampling ports were located at upstream DOC and downstream SCRF® for particulate matter sampling. Sample probes were inserted at various locations of the aftertreatment system for gaseous sampling. The probes were

connected to a Mass Spectrometer (from V & F Gmbh) through stainless steel sample lines. The production engine system provided various sensors to acquire information about temperature, pressure and NO_x concentration in the exhaust which was communicated to the Cummins proprietary calibration tool (Calterm). The concentrations of NO_x and O_2 entering and leaving the aftertreatment system were measured at turbo out and SCRF® out location.

The experimental setup comprises of various components which will be described in the next parts of this section.

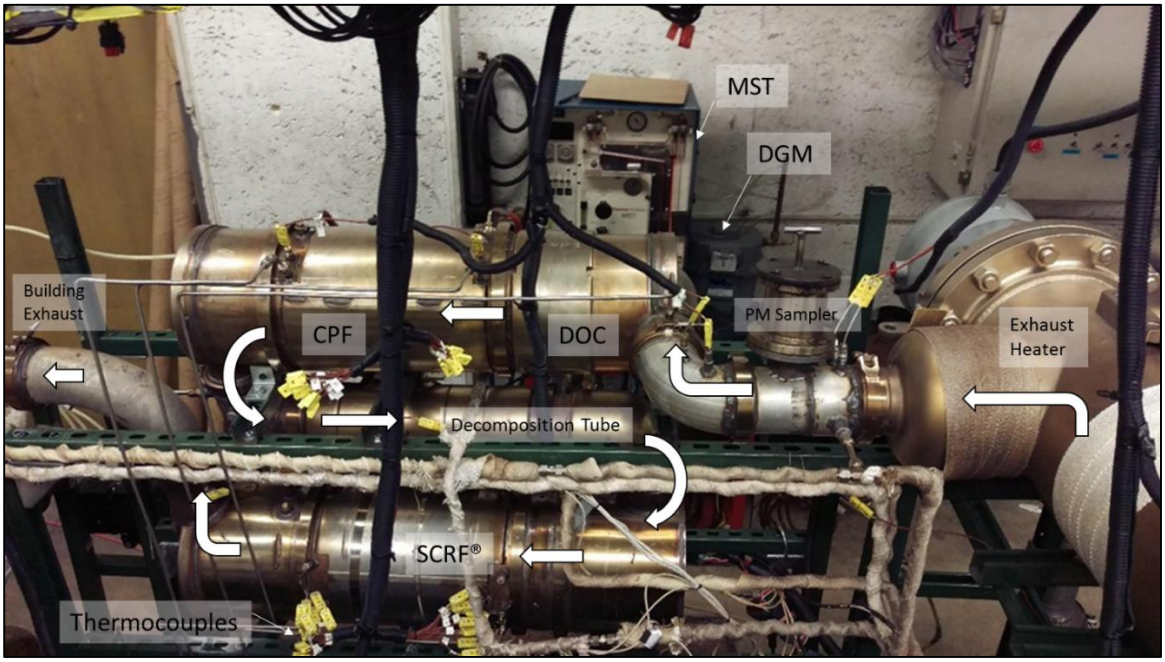

Figure 2.3 Aftertreatment system with sensors and instrumentation

Engine and Dynamometer

The test cell has the Cummins 2013 ISB engine which meets the 2013 emission standards, and 2014 greenhouse gas (GHG) and fuel efficiency regulations. The specifications of the engine are shown in Table 2.1. The engine is equipped with a High-Pressure Common Rail (HPCR) fuel injection system. A single high-capacity Electronic Control Module (ECM) controls the engine and the aftertreatment system for optimum performance and fuel efficiency [4].

Table 2.1 Specifications of the Cummins ISB 2013 engine

Model	Cummins 2013 ISB 208 kW (280 hp)
Bore and Stroke	107 X 124 mm
Displacement	409 in^3 (6.7 L)
Aspiration	Turbocharged
Controls	Electronic Control Module
Config/Cylinders	Variable Geometry Turbocharger Inline 6 cylinder
Aftercooling	Cummins Charge Air Cooler
Rated Power and Speed	208 kW and 2400 RPM
Peak Torque	895 Nm @1600 RPM
EGR System	Electronically controlled and cooled

The dynamometer installed in the test cell shown in Figure 2.2 is an eddy current dynamometer with specifications shown in Table 2.2. The load and engine speed on the engine were controlled using a Digital model 1022A dynamometer controller. It can be set to two operating modes, 'Speed' and 'Load' mode. Keeping one of the parameters set to a value, the other parameter can be regulated using the throttle (potentiometer).

Table 2.2 Eddy current dynamometer specifications

Manufacturer	Dynamitic
Type of Dynamometer	Eddy Current
Model	DM8121HS
Power (kW)	373 @ 1750 - 7000 RPM
Torque (Nm)	2035 @ 1750 RPM

Aftertreatment System

The various components of the aftertreatment system shown in Figures 1.1, and 2.3 are described below with specifications given in Table 2.3.

a) SDVs: Shutdown valves, which are pneumatically controlled butterfly valves installed in the exhaust lines to direct the exhaust coming out of the engine either towards building exhaust (through the bypass line) or towards the aftertreatment system (through the trap line) before exiting the building exhaust system.

b) Electric Heater: Heater is required to increase the temperature of the exhaust gas passing through the trap line independent of the engine condition.

c) DOC: DOC stands for Diesel Oxidation Catalyst that is required to oxidize CO, NO, and hydrocarbons present in the exhaust stream.

d) CPF: CPF stands for Catalyzed Particulate Filter, which is incorporated in the setup as shown in Figure 2.3 to remove the PM when testing the SCRF® without PM.

e) SCRF®: It is a DPF with an SCR catalyst, which performs the function of PM filtration, PM oxidation, and NO_x reduction. SCRF® was produced and supplied by the companies "Corning" and "Johnson Matthey".

f) Decomposition Tube: Urea solution is injected using an injector in the decomposition tube so that it gets decomposed to NH_3, which then enters the SCRF®.

g) Exhaust Mixer: Its function is to ensure proper mixing and in turn provide an exhaust gas mixture for accurate measurements.

Table 2.3 Specifications of the DOC, CPF and SCRF®

Substrate	DOC	CPF	SCRF®
Material	Cordierite	Cordierite	Cordierite
Diameter (inch)	9	9	10.5
Length (inch)	4	10	12
Cell Geometry	Square	Square	Square
Total Volume (L)	4.17	10.4	17.04
Open Volume (L)	3.5	7.3	10.2
Cell Density/in^2	400	200	200
Cell Width (mil)	46	59	55
Filtration Area (in^2)	N/A	9886	11370
Open Frontal Area (in^2)	53.9	24.7	25.9
Channel Wall Thickness (mil)	4	12	16
Porosity (%)	35	59	50
Mean Pore Size (μm)	N/A	15	16
Numbers of Cells	25447	12723	17318
Number of Inlet Cells	25447	6362	8659

2.2 Fuel Properties

For the testing, Ultra Low Sulphur Diesel Number 2 (ULSD #2) summer blend fuel was used that was supplied to MTU by Krans Oil at Lake Linden, MI. Since the fuel used for the testing in this report was the same as that for the CPF testing, fuel properties data in Table 2.4 were taken from reference [2].

Table 2.4 Specification of fuel used for testing [2]

Fuel Type	ULSD -2
API. Gravity at 15.6°C	35.4
SP. Gravity at 15.6°C	0.848
Viscosity at 40°C (cst)	3
Total Sulfur (ppm)	7
Initial Boiling Point (°C)	184
Final Boiling Point (°C)	363
Cetane Index	48.7
Water Content (ppm)	34
Higher Heating Value[1] [MJ/kg]	45.68
Lower Heating Value[1] [MJ/kg]	42.89
H/C[1]	1.833

[1] These values were obtained from reference [5] since they were not available from the analysis at Cummins.

2.3 Test Cell Instrumentation

The test cell is installed with various instruments and sensors to acquire data as described in this section. The parameters were measured, logged and displayed using the Data Acquisition System.

Air and Fuel Flow Measurement

The air flow into the intake system of the engine was measured by a Meriam Instruments Laminar Flow Element (Model number 50MC2-06F). The flow rate was calculated using the pressure drop data and the ambient temperature and humidity. The accuracy was in the range of 0.72% to 0.86% with repeatability of 0.1%.

The fuel flow rate was measured by the Micromotion flowmeter installed in the laboratory. The exhaust flow is the sum of the air flow and fuel flow rate. The exhaust mass flow was also indicated by the engine ECM.

Pressure Measurement

The pressure drop across the LFE, the DOC, and the SCRF® was measured using differential pressure transducers. The specifications of the pressure transducer used for the air flow and various components in the aftertreatment system is given in Table 2.5.

Table 2.5 Specifications of pressure transducer

	ΔP LFE	ΔP DOC	ΔP CPF	ΔP SCRF®
Sensor Brand	**Omega Engineering**	**Omega Engineering**	**Omega Engineering**	**Omega Engineering**
Model Number	PX-429-10WDWU10V	PX-409-2.5DWU5V	PX-429-2.5DWU10V	PX-429-005DWU10V
Sensor Type	Differential	Differential	Differential	Differential
Range	0 - 10	0-17.24	0-17.25	0-34.47
Units	in. H_2O	kPa	kPa	kPa
Output Voltage Range (V)	0-10	0-10	0-10	0-10

Temperature Measurement

An Omega HX94V temperature and relative humidity (RH) transmitter were used to measure ambient temperature and humidity of the test cell. The accuracy of temperature measurement was ±0.6 % with a repeatability of ±0.3 %. The accuracy of RH measurement was ±0.2 % and a repeatability of ±1 %.

The exhaust gas temperatures at different locations of the engine and aftertreatment system were measured using K-type thermocouples with the specifications as shown in Table 2.6. In the SCRF®, thermocouples were arranged in axial and radial positions at the upstream and downstream locations as shown in Figure 2.4. The inlet of the SCRF® had thermocouples named S1 to S5 whereas the outlet had thermocouples named S16 to S20. The thermocouple temperature readings were used to analyze temperature distribution in the SCRF®.

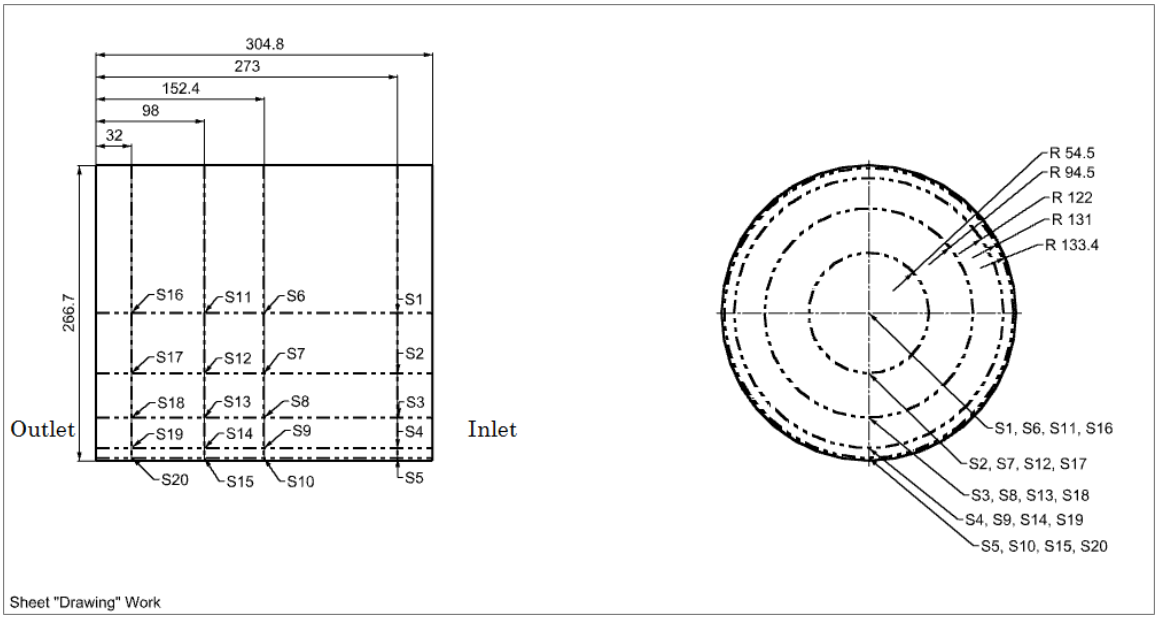

Figure 2.4 SCRF® thermocouple arrangement – Dimensions are in mm

Table 2.6 Specification of thermocouples

Manufacturer [-]	Location [-]	Diameter [in.]	Length [in.]	Part # [-]	Accuracy [%]
Omega	Air Intake, Exhaust stream, Coolant	0.125	6	KMQSS125U-6	± 2.2 °C
Omega	SCRF®	0.02	12	K-MQSS-020-U-12	± 2.2 °C
Omega	SCRF®	0.02	16	K-MQSS-020-U-16	± 2.2 °C

Data Acquisition

The measured values of temperature, pressure, speed and load were measured and communicated to desktop computers using National Instruments DAQ chassis (two NI CDAQ-9178). The fuel flow measured by Micro Motion Coriolis flow meter was communicated via RS-485 driver using the transmitter. [5]

NI Labview interface was used on the desktop computer in the control room to log the acquired data and to operate the electro-pneumatic butterfly valves for exhaust sampling from different locations. Engine data was acquired via CAN communication (J1939 protocol) with the ECM. Calterm was used to display and control various parameters of the engine.

Emissions Measurement

The emission samples were collected from three locations i.e. upstream DOC, upstream SCRF®, and downstream SCRF® as shown in Figure 2.2. The samples were directed to the Mass Spectrometer located in the control room to analyze the concentration of gas species in the exhaust system. The V&F air sense Ion Molecule Reaction Mass Spectrometer (IMR-MS) was used to determine the concentration of NO, NO_2, and NH_3. The specifications of the IMR-MS is given in Table 2.7.

Table 2.7 Specifications of IMR-MS

Components	Detection level at 100 ms	Monitoring mass	Ionizator	Span Gas	Span gas concen-tration	Accuracy
[-]	[ppb]	[amu]	[-]	[-]	[ppm]	[%]
NO	100	30	Hg	NO, N_2	515.4	± 1
NO_2	50	46	Hg	NO_2, Air	99.05	± 2
NH_3	120	17	Hg	NH_3,N_2 balance	103.8	± 2

The two NO_x and NO_x/O_2 sensors from the production aftertreatment system were used to take NO_x measurements. The sensor consists of an NGK sensing element with a Continental control unit. The measured value is displayed through Calterm.

Particulate Matter Sampling and Measurement

A PM filter (A/E type 47 mm diameter, glass fiber, manufactured by Pall Corporation, WA) was used to collect PM in the exhaust at upstream DOC and downstream SCRF® location in the aftertreatment system. The Dry Gas Meter (DGM) was connected to the Manual Sampling Train (MST) as shown in Figure 2.3.

The MST is equipped with a vacuum gauge, K-type thermocouples, a DGM, a manometer and a timer to determine the value of sample pump vacuum, temperature, volume of exhaust gas sampled, pressure drop and time respectively. The duration, volume and temperature of exhaust sampled was measured using the data from the dry gas meter. The mass of the PM sampled on the glass fiber filter is weighed using a Mettler Toledo UMT2 microbalance. The procedure of sampling and PM filter weighing is given in Appendix A.

The specification of the weighing scale is given in Table 2.8.

Table 2.8 Specifications of Mettler Toledo UMT2 microbalance [2]

Readability	0.1 µg
Weight capacity	2100 mg
Repeatability	0.25 µg
Linearity	± 1 µg
Linearity referred to 500 mg	± 0.5 µg
Stabilization Time	10-24 s depending on vibration adapter setting
Sensitivity Drift (5-40 °C)	±0.00015 %

The PM retained in the SCRF® in the tests during PM loading was measured. The engine was shut down and the loading in the SCRF® was weighed during the test procedure. The mass measurement was done on an Ohaus Ranger Scale and the specifications of the scale are given in Table 2.9. The detailed procedure to weigh the SCRF® is given in Appendix B.

Table 2.9 Specifications of weighing apparatus [2]

Manufacturer	**Ohaus**
Model	Ranger RD35LM
Capacity	35 kg
Resolution	0.1 g
Repeatability	± 0.1 g
Certified Accuracy	± 1.0 g

2.4 Test Points

The test cell setup and instruments described in Sections 2.1 and 2.3 were used to collect the data to analyze NO_x reduction efficiency and NH_3 slip of the SCRF® in the aftertreatment system. To achieve this goal, the engine was run at test points, selected from the test matrix of baseline SCR, as shown in Table 2.10. The engine conditions were decided from the table so as to obtain flow rate, space velocities, SCRF® inlet temperatures and NO_x out of the engine which are same as in the experiments performed for baseline SCR testing of the production system [6].

The test points were selected in order to determine the NO_x reduction performance of the SCRF® over a range of NO_2/NO_x ratios at different SCRF® inlet temperatures and space velocities. The test points 1, 3, 6, and 8 were selected out of the table matrix for the tests in this report which cover both the lower and higher values of SCRF® inlet temperatures and inlet NO_2/NO_x ratio. The different SCRF® conditions were achieved by varying engine conditions and heater temperature. The ammonia to NO_x ratios (ANRs) were set based on the urea dosing cycle developed for conducting the tests. This allowed for calibration of the model for similar exhaust conditions. At the same time, these points cover a range of inlet NO_2/NO_x ratios.

Table 2.10 Test matrix of baseline SCR tests for NO_x reduction experiments

Test Point	Speed	Torque	Exhaust Flow rate	SCR Inlet Temp.	SCR Std. Space Vel.	SCR Inlet NO_2	SCR Inlet NO_x	SCR Inlet NO_2/NO_x
[-]	[RPM]	[N-m]	[kg/min]	[°C]	[k/hr]	[-]	[ppm]	[-]
1*	1200	203	4.9	208	14.6	301	492	0.61
2	1650	203	6.5	231	19.4	184	306	0.6
3*	2200	325	10	310	29.9	217	341	0.64
4	2100	377	0.4	331	28.1	230	372	0.62
5	1660	529	7.8	353	23.3	356	662	0.54
6*	1200	580	6.4	354	19.1	922	1712	0.54
7	2100	750	13	404	38.8	242	546	0.44
8*	2400	813	16	455	47.8	233	596	0.39

* The test points marked with asterisk (*) were selected for conducting the SCRF® tests in the report.

2.5 Test Procedure

The aftertreatment system configuration studied in this work includes a DOC, CPF, and SCRF®, where the experiments were aimed to determine the NO_x reduction of the SCRF®. The tests for the SCRF® were performed with 0, 2, and 4 g/L (grams of PM per volume of the SCRF®). The test procedure planned to conduct the testing included SCRF® cleanout stage to remove PM completely from the SCRF®, PM Loading stage to load PM into the SCRF®, and NO_x reduction stage to analyze the SCRF® NO_x reduction performance and NH_3 slip at a particular engine condition. The engine conditions for test point 1, 3, 6, and 8 discussed in Section 2.4 were run for NO_x reduction stage. Loading stages were eliminated for tests without PM loading. The CPF was placed to filter the PM after the DOC and upstream of SCRF® (see Figure

1.1) during the NO_x reduction stage. The air intake temperature was controlled at 50˚± 2˚C by directing the building water supply to the heat exchanger for cooling the air. The PM loading of the SCRF® test procedure is similar to the procedure used in the past for baseline CPF testing [2]. The rail pressure was reduced by 30% to increase the engine-out PM and to load PM in a practical time (330 minutes).

Tests with PM Loading in the SCRF®

Figure 2.5 shows the schematic representation of the test sequence for PM loading in the SCRF®.

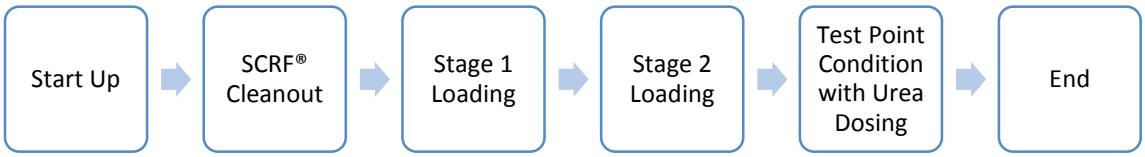

Figure 2.5 Schematic representation of the process of testing with PM loading in the SCRF®

Experiments were conducted in different stages as mentioned below:

1. **Start Up and SCRF® Cleanout**

The engine was warmed up by running it at 900 RPM at idle load conditions for 3 to 5 minutes and readings of data displayed on Labview and Calterm were checked for correctness. The engine was then raised to a higher speed of 1200 RPM at 200 Nm load in the subsequent 2 minutes. The engine was then brought to an intermediate engine condition (1600 RPM and 475 Nm load). The engine was run in this state for 30 minutes to have stabilized engine out emission samples. Parameters were again noted in this condition to check for variations.

PM accumulated in the SCRF® was cleaned out using in-cylinder fuel dosing that raises the temperature for the PM oxidation process. The fuel was dosed at 36 mg/stroke. The temperature was maintained above 550˚C at the upstream SCRF® location for complete clean out. The slope of pressure drop displayed on Labview interface reaches a balance point (a point where the rate of PM oxidation and accumulation are the same) with time, thus concluding the clean out stage.

2. Particulate Matter Loading

The particulate matter loading was done in two stages, Stage 1 and Stage 2. The selection of the loading test condition was taken from reference [2]. The loading conditions were decided based on exhaust mass flow rates, space velocities, PM concentrations, and NO_x/PM ratios to achieve PM loading in a reasonable amount of time.

In Stage 1, the engine load condition was changed to 2400 RPM and 218 Nm after the completion of the SCRF® cleanout stage. The emission samples were taken at upstream DOC (UDOC), upstream SCRF® (USCRF), and downstream SCRF® (DSCRF). For PM analysis, samples were collected at UDOC and DSCRF®. Loading was done for 30 minutes. The exhaust was then directed to the 'bypass' line, the engine was shut down and the SCRF® was disassembled from the aftertreatment system and weighed by the procedure as discussed in Appendix B. The weight of the SCRF® changes with temperature and hence consistency was maintained by recording the temperature of the SCRF® thermocouples above 220 ± 20 ˚C (shown in Figure 2.3) prior to weighing.

The SCRF® was assembled back into the system and the engine was restarted for Stage 2 loading. The engine was brought to the same condition as that of Stage 1 loading condition. Once the engine-out temperature had stabilized, exhaust was routed to the 'trapline' using the pneumatic valve.

In Stage 2 loading, the engine was run until the system was loaded to 2 or 4 g/L. It took 330 and 500 minutes approximately for 2 and 4 g/L respectively. Emissions were sampled at UDOC, USCRF and DSCRF locations for a duration of approximately 60 minutes each and PM was sampled at UDOC and DSCRF location for a duration of 10 and 60 minutes respectively. After the loading, exhaust was shifted to the 'bypass' line and the same shut down procedure was adopted.

3. NO_x Reduction

The purpose of this stage is to observe the NO_x reduction capability of the SCRF® at each of the engine conditions mentioned in Section 2.4 over a range of NO_2/NO_x ratios and NH_3/NO_x ratios (ANR) at the inlet of the SCRF® at different SCRF® inlet temperatures and space velocities. It was done by injecting an appropriate amount of

urea to achieve desired ANR values. The urea dosing cycle depicts SCRF® inlet ANR values (0.8, 1,1.2, and 1.2 repeat) and their sequence adopted, for the study of transient response of ANR on NO_x reduction efficiency and NH_3 slip, as shown in Figure 2.4. The ANR values around 1 were selected to study for high NO_x reduction efficiencies.

The engine conditions were similar to those used for SCR testing as was discussed in Section 2.4. Since flow rates and temperatures were similar, the conversion efficiency of the DOC should produce similar amounts of NO_2 and the SCRF® inlet NO_2/NO_x ratio should be similar. The engine was run at test points 1, 3, 6, and 8 for the study of the effects of PM loading on NO_x reduction as discussed in Section 2.4. Test points 1 and 3 (218 and 304 ˚C) have less PM oxidation during the urea dosing cycle whereas test points 6 and 8 (354 and 455 ˚C) have higher PM oxidation during the same. The PM was added and oxidized simultaneously in the SCRF® during these engine conditions. The rate of PM oxidation is higher for high inlet SCRF® temperatures and vice versa. At higher temperatures, PM loading was done in the SCRF® to maintain the PM concentration at approximately 2 or 4 g/L in the SCRF®. Figure 2.6 shows the two loading stages represented by "Repeated loading-I" and "Repeated loading-II" done in the test point 6 NO_x reduction stage in order to maintain 2 g/L in the SCRF®. The urea is dosed in order to obtain required ANR values during the repeated loading stages as shown in Figure 2.6.

The engine was run at set conditions with urea dosing in the decomposition tube to get particular SCRF® inlet temperatures and ANR values. The emission samples were taken from upstream and downstream locations of the SCRF® and upstream location of DOC with a mass spectrometer. The sampling was done for each of these ANR values for approximately 20 minutes until stabilized NO_x concentration and NH_3 slip was achieved at the downstream SCRF® location. The dosing rate was then changed to achieve different ANR values and downstream SCRF® measurements were taken. The process was repeated for the rest of the ANR values as per the urea dosing cycle in Figure 2.7. Once the required ANR points were achieved, the engine was brought back to baseline condition, then down to idle and then shut down.

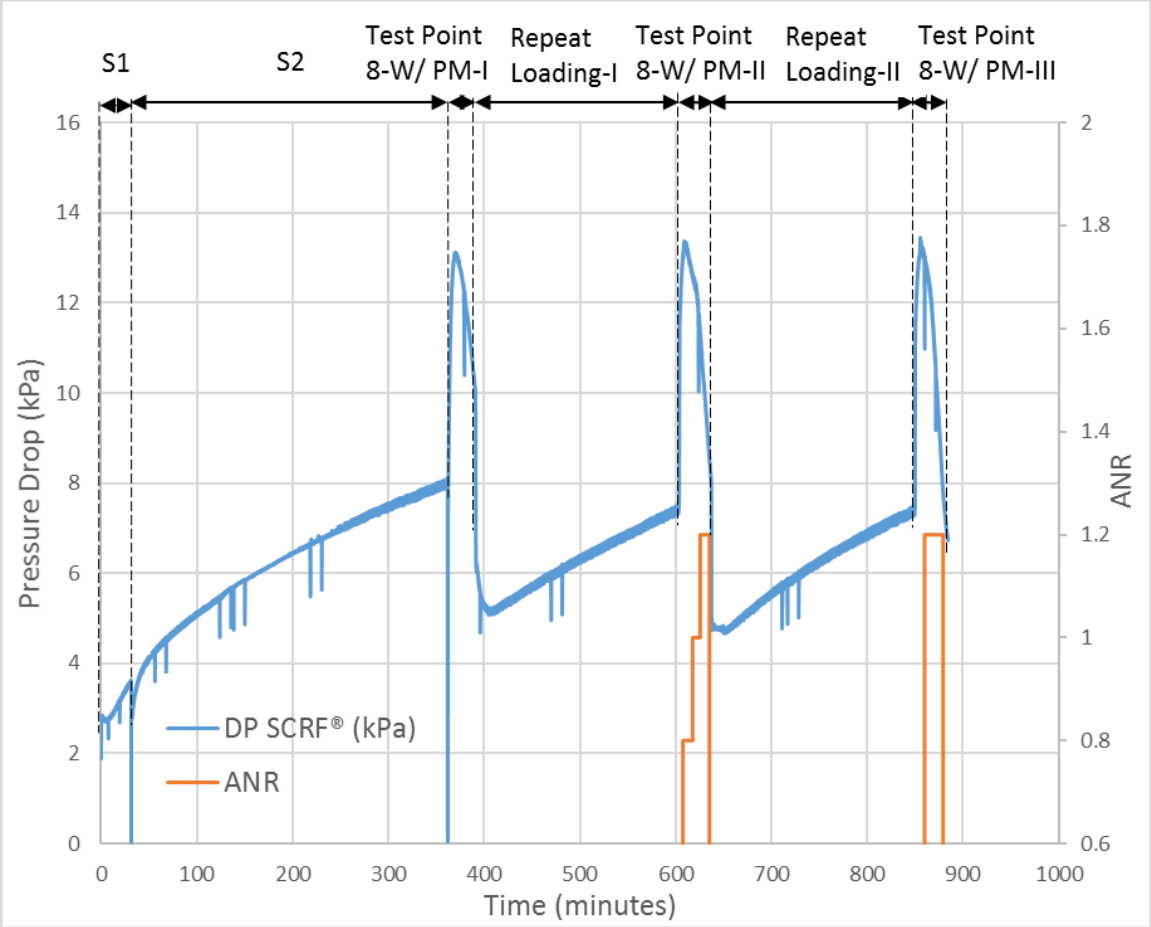

Figure 2.6 Pressure drop curve for Stage 1, Stage 2 and repeat loading in between the NO_x Reduction Stage

The species concentration was calculated by averaging out the stable range of the sample. The ANR value of 1.2 was repeated in the urea dosing cycle, to obtain further empirical data for NH_3 adsorption measurement and to ensure repeatability, as shown in Figure 2.7. The PM sample was taken at UDOC with the Manual Sampling Train. Its concentration was maintained at 2.0 ± 0.2 or 4.0 ± 0.4 g/L in the SCRF® by loading it in between the urea dosing cycle (whenever necessary) for high SCRF® inlet temperature test points (test point 6 and 8 for 2 g/L and 4 g/L). The loading was done at the engine conditions described in Particulate Matter Loading section to load SCRF® up to the desired 2 or 4 g/L PM concentration. The SCRF® was then weighed to confirm the PM concentration.

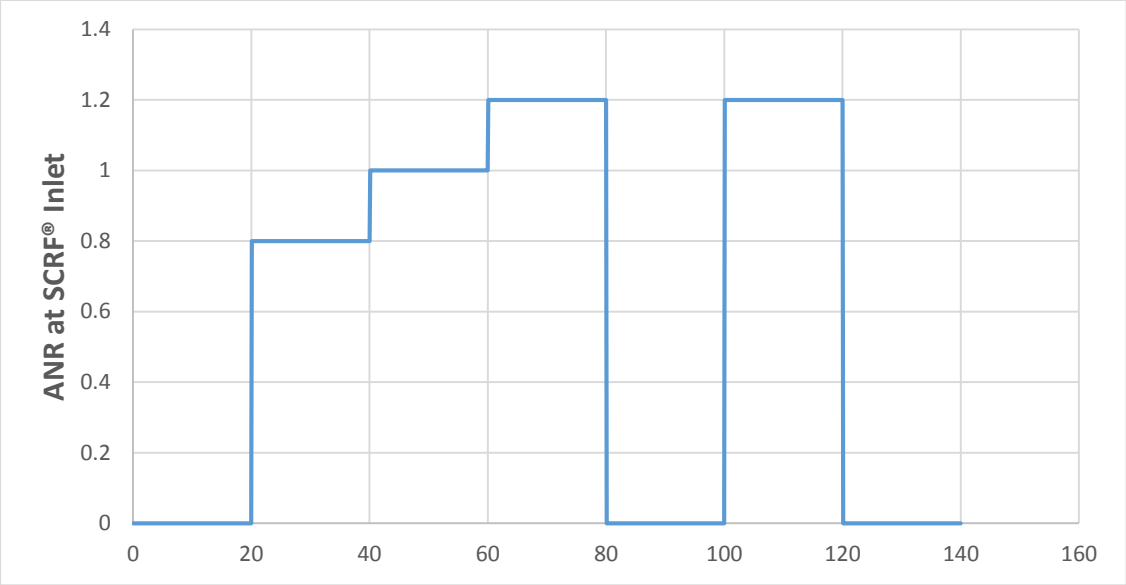

Figure 2.7 Urea dosing cycle for SCRF®

Tests without PM Loading in the SCRF®

The test procedure to perform NO_x reductions in the SCRF® without PM is different from tests with PM loading in the sense that the CPF is placed downstream of the DOC to filter PM loading. This was done so as to reduce the possibility of PM interfering with the NH_3 adsorption capacity of the SCRF® as shown in Figure 2.8. The stages for these tests consist of SCRF® cleanout and NO_x reduction only. The loading phase was not required since there was no PM accumulation or PM oxidation in the SCRF®. When the emission samples of NO, NO_2, and NH_3 stabilized, the NO_x reduction stage was completed and the engine was shut down followed by saving the data.

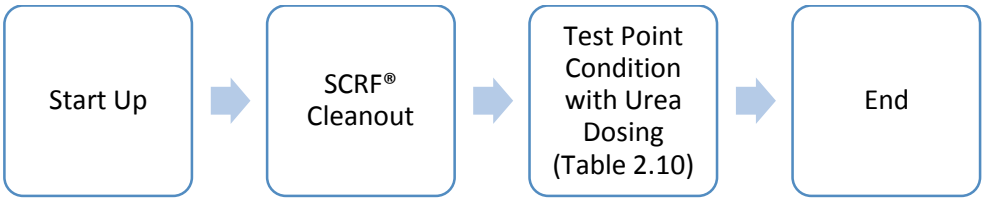

Figure 2.8 Schematic representation of the process of testing without PM loading in the SCRF®

Chapter 3. Results

Chapter 2 discussed the experimental setup, test points and procedures used in this report. This chapter presents the findings of the research and discusses the significance of the data analysis. The analysis of the data from the engine and aftertreatment system configuration, is presented in terms of stage wise gaseous emissions and their conversion efficiency across the DOC and the SCRF®.

A total of 12 runs were conducted in which loading constituted Stage-1, Stage-2 and repeated loading stages done in between the NO_x reduction stage (with PM in the SCRF®). Stage - 1 and Stage - 2 loading were carried out only for PM loaded SCRF® testing. The SCRF® was loaded to 2.0 ± 0.2 g/L and 4.0 ± 0.4 g/L before the NO_x reduction stage. The notation SCRF® - 0, SCRF® - 2, and SCRF® - 4 represent PM loading of 0 g/L, 2 g/L, and 4 g/L in the SCRF® respectively.

From the results presented, NO_x reductions efficiency and the amount of NH_3 slip is determined and compared for loaded and unloaded SCRF® at different ANR values. Appendix C, E, and F discusses the stage wise PM balance, pressure drops, and temperature profiles respectively. The analyzed results obtained for SCRF® performance tests are then compared with the baseline SCR tests [6].

3.1 NO_x Reduction

This section discusses the results of the NO_x reduction test data at different test points. The test data for PM loading of 0, 2, and 4 g/L in the SCRF® are analyzed and compared to determine the performance of the SCRF® at different loading conditions. The analysis is done with respect to different ammonia to NO_x ratio values (ANR – 0, 0.8, 1, 1.2, 1.2 rpt.) at the inlet of the SCRF®. The gaseous emissions for loading stages and NO_x reduction stages (ANR - 0 and 1.2 rpt.) are presented in Appendix D.

SCRF® Inlet Conditions

The exhaust flows through the DOC, CPF or spacer, decomposition tube and the SCRF®. The engine was run at a particular speed and load condition to achieve the desired SCRF® inlet temperatures and exhaust flow rates and in turn the space velocities.

Space Velocity is defined as the number of volumes of the substrate per unit time processed by the substrate. The unit used in this study is [k/hr]. It is formulated as

$$Space\ Velocity = \frac{Mass\ Flow\ Rate_{exh}\ [kg/hr]}{\rho_{exh}[kg/m^3] * V_{substrate}[m^3]} * \frac{1}{1000}$$

(Equation 3.1)

Where, ρ_{exh} is the density of exhaust gas [kg/m^3] and $V_{substrate}$ is substrate volume

$$\rho_{exh} = \frac{P}{R * T}$$

Where, P is pressure at the inlet of SCRF® [kPa], R is the gas constant for exhaust [0.287 kJ/kg/K], taken same as that of air, T is absolute temperature [K]. For standard space velocity calculations, the temperature and pressure are taken as 298 K and 101.32 kPa respectively, and $\rho_{exh,standard}$ = 1.29 kg/m^3.

Table 3.1 shows the inlet conditions of the SCRF® for the test points, selected from SCR baseline test matrix shown in Table 2.10. In Table 3.1, the SCRF® inlet temperature is 207-218, 302-305, 340-347, and 441-443 °C for test point 1, 3, 6, and 8 respectively. The exhaust flow rate and space velocity were in the range of 5-17.7 kg/min. and 13.5 -48.2 k/hr respectively where the lowest and highest values are for test point 1 and 8 respectively. Figure 3.1 shows the variation of inlet SCRF® NO_2 /NO_x ratio at different SCRF® inlet temperatures (test points). It is observed that the highest concentration of NO_x into the SCRF® is for test point 6 with a highest NO_2/NO_x ratio of 0.43-0.46.

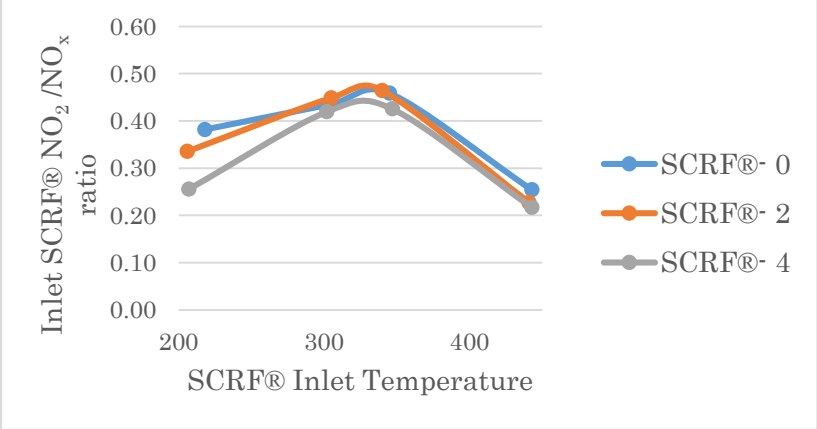

Figure 3.1 Inlet SCRF® NO_2 /NO_x ratio at different SCRF® inlet temperatures (test points)

Table 3.1 Engine and SCRF® inlet conditions at different test points for NO_x reduction test

Parameter	PM Loading	Test Point			
		1	3	6	8
Speed [RPM]	SCRF®- 0	1199	2200	1202	2401
	SCRF®- 2	1200	2101	1200	2398
	SCRF®- 4	1200	2203	1200	2401
Load [Nm]	SCRF®- 0	201	330	580	826
	SCRF®- 2	208	329	588	820
	SCRF®- 4	203	331	587	818
Exhaust Flow [kg/min]	SCRF®- 0	5.0	10.7	6.9	17.0
	SCRF®- 2	5.0	9.9	6.8	17.6
	SCRF®- 4	5.0	10.9	6.8	17.7
SCRF® Inlet Temperature [°C]	SCRF®- 0	218	304	345	443
	SCRF®- 2	206	305	340	441
	SCRF®- 4	207	302	347	443
SCRF® Std. Space Vel. [k/hr]	SCRF®- 0	13.7	29.1	18.8	46.3
	SCRF®- 2	13.7	27.0	18.6	48.0
	SCRF®- 4	13.5	29.8	18.6	48.2
SCRF® Act. Space Vel. [k/hr]	SCRF®- 0	24.5	60.2	42.0	115
	SCRF®- 2	22.6	53.8	39.3	118
	SCRF®- 4	22.7	56.4	39.9	108
SCRF® Inlet NO [ppm]	SCRF®- 0	345	158	795	411
	SCRF®- 2	403	161	743	424
	SCRF®- 4	453	198	793	415
SCRF® Inlet NO_2 [ppm]	SCRF®- 0	213	121	674	140
	SCRF®- 2	203	131	644	125
	SCRF®- 4	146	124	588	115
SCRF® Inlet NO_x [ppm]	SCRF®- 0	558	279	1468	551
	SCRF®- 2	607	292	1387	548
	SCRF®- 4	599	322	1381	530
Upstream NO_2/NO_x	SCRF®- 0	0.38	0.43	0.46	0.25
	SCRF®- 2	0.34	0.45	0.46	0.23
	SCRF®- 4	0.24[1]	0.39	0.43	0.22
Engine Out PM [mg/scm][3]	SCRF®- 0	N/A	N/A	N/A	N/A
	SCRF®- 2	2.14	4.30	3.59	7.39
	SCRF®- 4	1.97	4.93	2.85	4.97[2]

[1] NO_2/NO_x ratio is inconsistent with other SCRF®- 0 and 2 loading tests because of inaccurate reading of NO and NO_x species concentration from mass spectrometer

[2] The engine out PM is lower than expected because the filter papers had moisture prior to PM collection

[3] scm is a volume of the exhaust (cubic meter) sampled which is converted to standard conditions of 298 K and 101.32 kPa

NO Conversion across DOC

The NO conversion across the DOC determines the species concentration of NO and NO_2 at the outlet of the SCRF®. The conversion depends on the inlet temperature and space velocity of the exhaust flowing through the DOC.

The species conversion efficiencies are calculated from inlet and outlet species concentrations as given by Equation 3.2

$$DOC\ or\ SCRF®\ (NO/NO_x)\ Conversion\ efficiency\ (\%) = \frac{Inlet\ (NO/NO_x) - \ Outlet\ (NO/NO_x)}{Inlet\ (NO/NO_x)} * 100$$

(Equation 3.2)

Table 3.2 gives the NO and NO_2 species concentration at upstream and downstream location of the DOC. The concentrations of NO and NO_2 are in agreement for individual test points at 0, 2, and 4 g/L loading since the PM loading in the SCRF® is not related with the DOC performance.

Table 3.3 gives the DOC inlet temperature, DOC space velocity and DOC NO conversion efficiency. It was observed that the NO conversion efficiency was higher in temperature range of 300-350 °C (test point 3 and 6) and decreased as temperature approached 440 °C (test point 8). The trend for NO conversion efficiency is discussed in Reference [7] where the maxima lies close to 325 °C and decreases at temperatures higher or lower than 325 °C.

Table 3.2 NO and NO_2 species concentration at the inlet and outlet DOC for different test points

Test Point	NO						NO_2					
	SCRF® - 0		SCRF® - 2		SCRF® - 4		SCRF® - 0		SCRF® - 2		SCRF® - 4	
	In	Out	In	Out	In	Out	In	Out	In	Out	In	Out
[-]	[ppm]	[ppm]	[ppm]	[ppm]	[ppm]	[ppm]	[ppm]	[ppm]	[ppm]	[ppm]	[ppm]	[ppm]
1	575	345	581	403	563	453	5	213	2	203	37	146
3	257	160	288	161	324	198	18	120	0	131	1	124
6	1336	795	1484	743	1483	793	18	674	4	644	14	588
8	542	411	556	424	507	415	1	140	2	125	8	115

Table 3.3 DOC inlet temperature, space velocity and NO conversion efficiency for different test points

Test Point	DOC Inlet Temp. [°C]			SCRF® Space Velocity [k/hr]			NO Conv. % across DOC		
	SCRF® - 0	SCRF® - 2	SCRF® - 4	SCRF® - 0	SCRF® - 2	SCRF® - 4	SCRF® - 0	SCRF® - 2	SCRF® - 4
1	221	218	214	55.7	56.1	55.2	40	31	20
3	306	315	316	119.1	110.4	121.7	38	44	39
6	346	355	362	76.8	76.1	75.9	40	50	46
8	439	442	449	189.3	196.3	196.9	24	24	18

NO_2 Decrease and NO_x Conversion across SCRF®

The concentrations of both NO and NO_2 decrease across the SCRF® when dosed with urea due to the reduction reaction of NO and NO_2 with ammonia to form nitrogen. The effects of ANR on the NO_x conversion efficiency is discussed in this section.

Figure 3.2 shows the trend of NO_2/NO_x ratio at inlet or outlet of the SCRF® with SCRF® inlet temperatures and loading, without urea dosing. This can be explained by increased participation of NO_2 in PM oxidation at high temperature with PM in the filter [2].

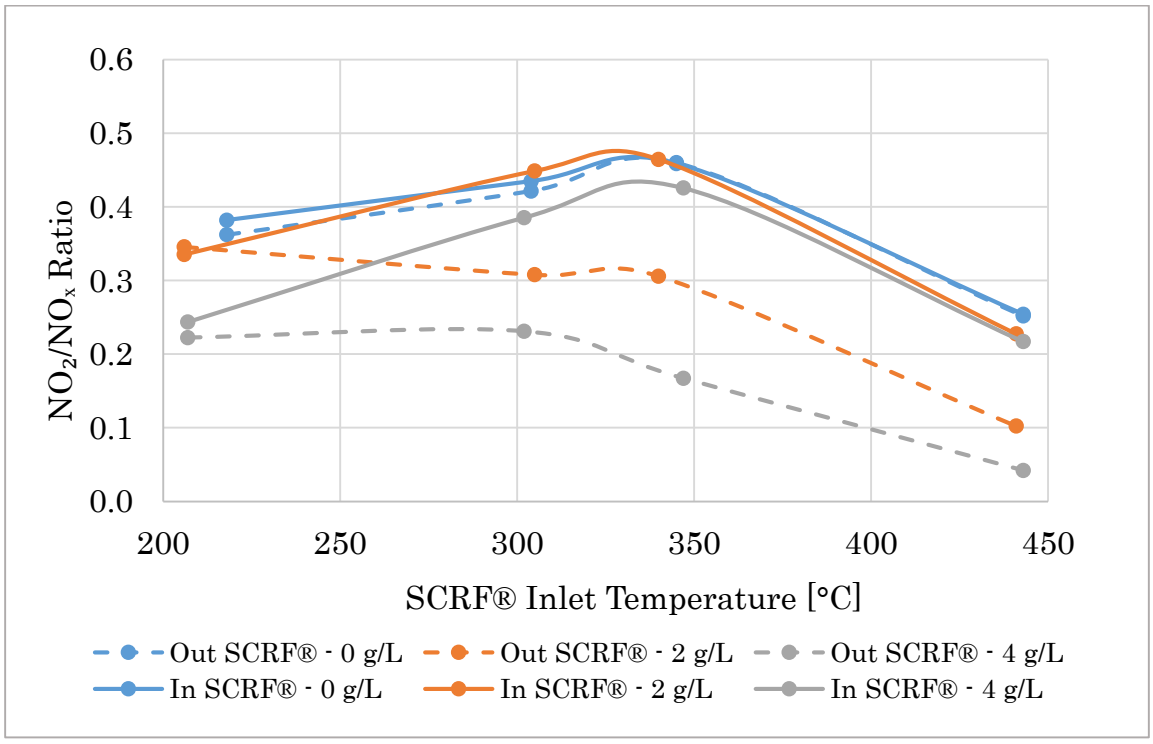

Figure 3.2 Change in NO_2/NO_x ratio at inlet and outlet of the SCRF® with different SCRF® inlet temperatures for 0, 2, and 4g/L loading ANR - 0

Tables 3.4, 3.6, and 3.8 show the NO and NO_2 concentrations at the inlet and outlet of the SCRF® (loaded with 0, 2, and 4 g/L) at ANR – 0.8, 1, and 1.2 respectively. It is observed from these tables that, with urea dosing, the NO_2 concentration decreases with PM loading for all test points. Also, the NO concentration downstream of the SCRF® is affected by the conversion of NO_2 to NO during NO_2 assisted PM oxidation. At ANR – 1 and 1.2, the NO_2 concentration downstream of the SCRF® is negligible.

The NO_x conversion efficiency data for the test points at different ANR values are shown in Tables 3.7 and 3.9. Figures 3.3, 3.4, and 3.5 show the NO_x conversion efficiency plots of SCRF® as a function of SCRF® inlet temperatures when loaded with 0, 2, and 4 g/L for ANR – 0.8, 1, 1.2 respectively. The factors affecting NO_x conversion efficiency are SCRF® inlet temperature, PM loading (0, 2, and 4 g/L) in SCRF®, and NO_2/NO_x at inlet to the SCRF®. Figure 3.4 shows the highest NO_x conversion efficiency of 99% for test point 6 without PM loading at ANR - 1. Figure 3.5 shows nearly constant NO_x conversion efficiency for test points 1, 3, and 6.

In Figures 3.3, 3.4, and 3.5, there is a slight decrease in the NO_x conversion efficiency for test points 6 and 8 with loading. The major portion of the NO_x concentration comprises NO since the NO_2 concentration at the downstream SCRF®, for ANR -0.8, 1 and 1.2, is negligible. There is high NO_2 to NO conversion for loaded SCRF®.

In Table 3.5, the NO_x conversion efficiency for SCRF® loaded at 4 g/L compared to 0 g/L is 4% higher for test point 3 and is 7% lower for test point 8. The decrement in NO_x conversion efficiency for 4g/L loading compared to 0 g/L will be less than 7% since the actual ANR dosed was lower than 0.8. For test point 6, SCRF® loaded with 0 g/L, the actual ANR was 0.77 and therefore gives lower NO_x conversion efficiency of 83%. It is observed that the NO_x reduction efficiency improved with loading until the temperature around 300 °C and then decreased for temperatures above 350 °C.

Table 3.4 Species concentration at upstream and downstream SCRF® for NO_x reduction test points at ANR-0.8

Test Point	NO [ppm]						NO_2 [ppm]						NH_3 [ppm]					
	SCRF®- 0		SCRF®- 2		SCRF®- 4		SCRF®- 0		SCRF® - 2		SCRF®- 4		SCRF®- 0		SCRF®- 2		SCRF®- 4	
	In	Out	In	Out	In	Out	In	Out	In	Out	In	Out	In	Out	In	Out	In	Out
1	345	136	403	142	453	124	213	6	203	1	146	1	446	1	486	2	481	2
3	158	44	161	63	198	55	121	18	131	2	124	1	220	2	231	1	274	0
6	795	108	743	273	793	275	674	149	644	10	588	7	1125	0	1096	0	1093	2
8	411	99	424	117	415	147	140	6	125	1	115	1	438	12	426	7	399	27

Table 3.5 Species conversion efficiency across SCRF® for NO_x reduction test points at ANR-0.8

Test Point	ANR			NO_x conversion efficiency [%]			Nitrogen Balance [%]		
	SCRF®- 0	SCRF®- 2	SCRF®- 4	SCRF®- 0	SCRF®- 2	SCRF®- 4	SCRF®- 0	SCRF®- 2	SCRF®- 4
1	0.80	0.80	0.80	75	77	79	94	96	89
3	0.79	0.79	0.85	78	78	82	99	99	97
6	0.77	0.79	0.79	83	80	80	108	101	101
8	0.79	0.78	0.75	81	78	72	105	103	102

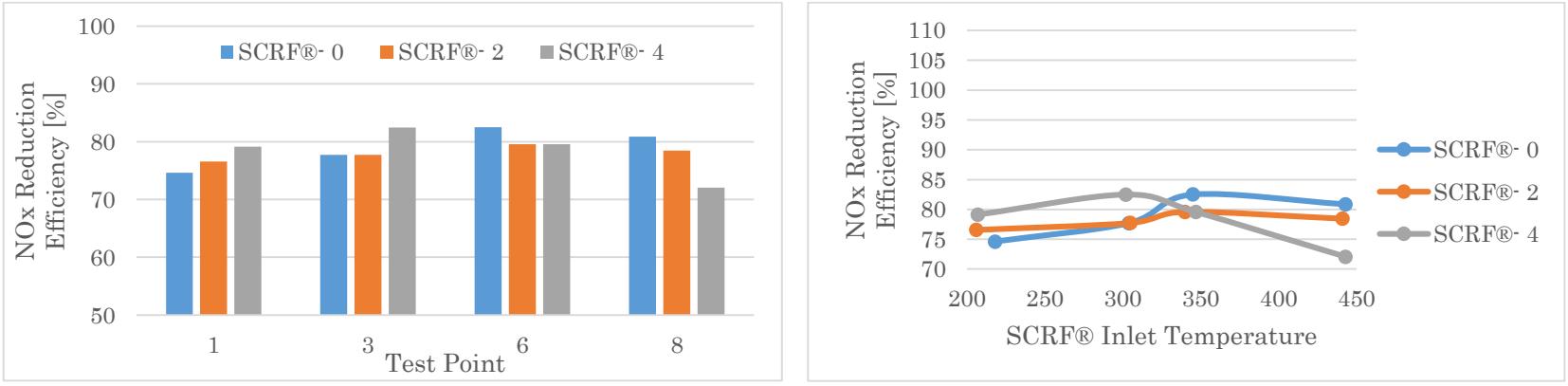

Figure 3.3 Variation of NO_x conversion efficiency (%) with ANR – 0.8 for NO_x reduction test points and SCRF® inlet temperatures

In Figure 3.4, the NO_x conversion efficiency trend for ANR - 1 is similar to the one for ANR 0.8 shown in Figure 3.3. For test point 3, SCRF® loaded with 4 g/L, the NO_x conversion efficiency came out lower i.e. 98% as the actual ANR value was 1.03 at the time of testing. The NO_x conversion efficiency reached 98% and 99% for test point 3 with PM loading of 4 g/L and test point 6 with PM loading of 0 g/L respectively, which are the maxima of their curves in Figure 3.4.

Table 3.9 shows that the NO_x conversion efficiency is above 97% for all test points except test point 8. As shown in Table 3.1, the SCRF® inlet temperature (around 440 °C) and space velocity (around 48 k/hr) are higher for test point 8 compared to other test points (1, 3, and 6). Above 400 °C, the oxidation of NH_3 to N_2 and NO becomes dominant and therefore NO_x conversion efficiency is poor [1].

Table 3.6 Species concentration at upstream and downstream SCRF® for NO_x reduction test points at ANR-1

Test Point	NO [ppm]						NO_2 [ppm]						NH_3 [ppm]					
	SCRF®- 0		SCRF®- 2		SCRF®- 4		SCRF®- 0		SCRF®- 2		SCRF®- 4		SCRF®- 0		SCRF®- 2		SCRF®- 4	
	In	Out	In	Out	In	Out	In	Out	In	Out	In	Out	In	Out	In	Out	In	Out
1	345	61	403	49	453	47	213	0	203	0	146	0	558	2	609	3	600	5
3	158	11	161	13	198	8	121	1	131	0	124	0	275	5	289	1	331	4
6	795	6	743	60	793	85	674	3	644	1	588	2	1404	7	1370	1	1360	9
8	411	43	424	61	415	60	140	3	125	0	115	0	548	35	536	16	522	55

Table 3.7 Species conversion efficiency across SCRF® for NO_x reduction test points at ANR-1

Test Point	ANR			NO_x conversion efficiency [%]			Nitrogen Balance [%]		
	SCRF®- 0	SCRF®- 2	SCRF®- 4	SCRF®- 0	SCRF®- 2	SCRF®- 4	SCRF®- 0	SCRF®- 2	SCRF®- 4
1	1.00	1.00	1.00	89	92	92	89	92	93
3	0.99	0.99	1.03	96	96	98	99	97	96
6	0.96	0.99	0.98	99	96	94	104	97	96
8	0.99	0.98	0.98	92	89	89	99	94	101

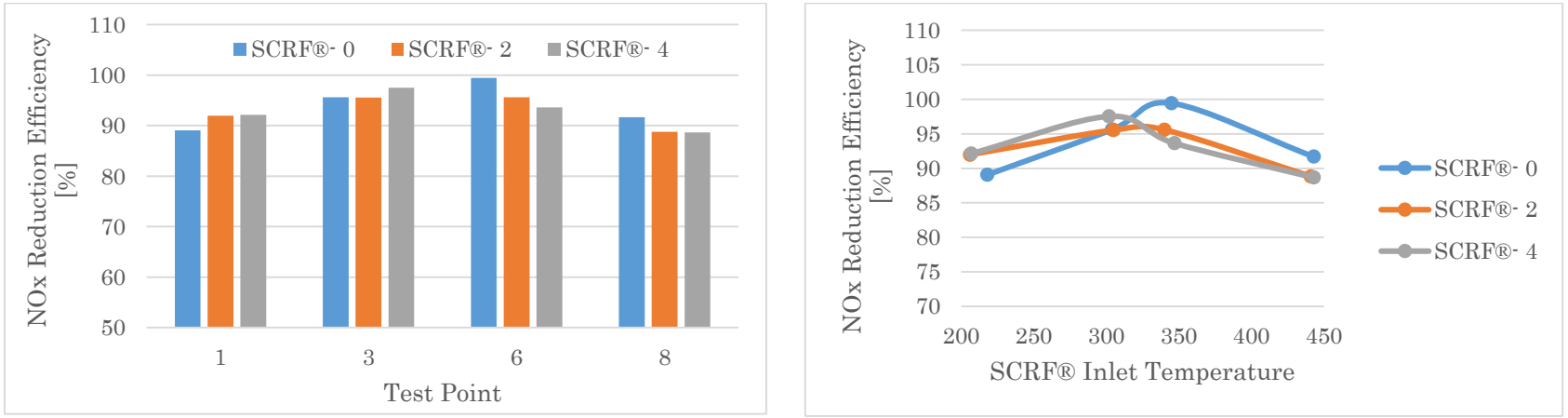

Figure 3.4 Variation of NO_x conversion efficiency (%) with ANR - 1 for NO_x reduction test points and SCRF® inlet temperatures

Table 3.8 Species concentration at upstream and downstream SCRF® for NO_x reduction test points at ANR-1.2

Test Point	NO [ppm]						NO_2 [ppm]						NH_3 [ppm]					
	SCRF®- 0		SCRF®- 2		SCRF®- 4		SCRF®- 0		SCRF®- 2		SCRF®- 4		SCRF®- 0		SCRF®- 2		SCRF®- 4	
	In	Out	In	Out	In	Out	In	Out	In	Out	In	Out	In	Out	In	Out	In	Out
1	345	7	403	7	453	15	213	0	203	0	146	0	669	112	730	141	722	185
3	158	4	161	2	198	3	121	1	131	0	124	0	331	60	347	50	398	68
6	795	2	743	6	793	14	674	-1	644	0	588	2	1685	197	1644	107	1633	106
8	411	36	424	46	415	52	140	2	125	0	115	0	657	84	640	36	626	79

Table 3.9 Species conversion efficiency across SCRF® for NO_x reduction test points at ANR-1.2

Test Point	ANR			NO_x conversion efficiency [%]			Nitrogen Balance [%]		
	SCRF®- 0	SCRF®- 2	SCRF®- 4	SCRF®- 0	SCRF®- 2	SCRF®- 4	SCRF®- 0	SCRF®- 2	SCRF®- 4
1	1.20	1.20	1.21	99	99	98	99	101	107
3	1.19	1.19	1.24	98	99	99	101	98	97
6	1.15	1.19	1.18	100	100	99	99	91	90
8	1.19	1.17	1.18	93	92	90	91	84	89

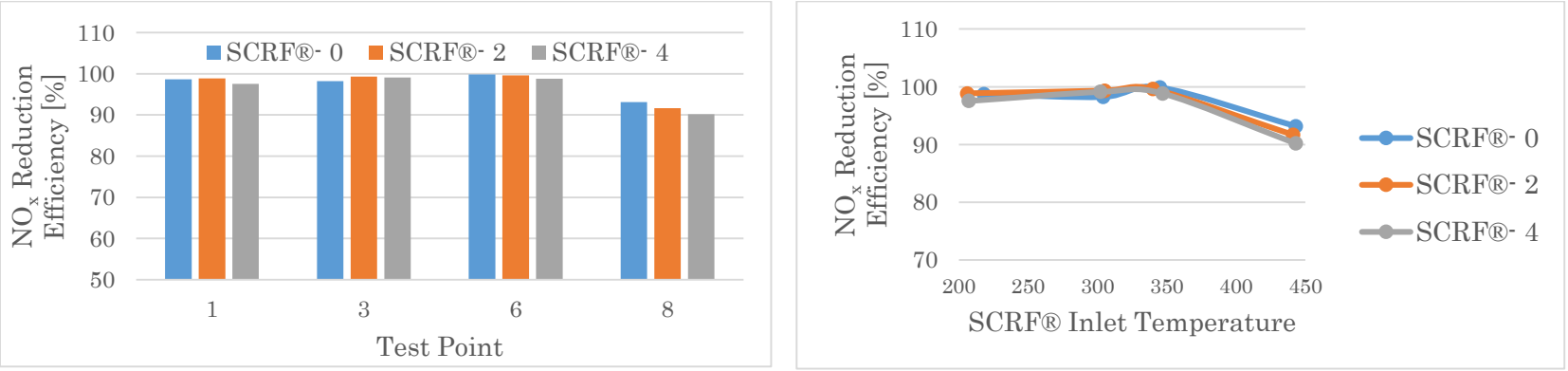

Figure 3.5 Variation of NO_x conversion efficiency (%) with ANR – 1.2 for NO_x reduction test point

3.2 NH_3 Slip and Nitrogen Balance

The NH_3 inlet and outlet concentrations across the SCRF® are shown in Tables 3.4, 3.6, and 3.8. The urea (32.5% concentration in urea-water solution) injected in the decomposition tube decomposes to ammonia (NH_3) and reduces the exhaust NO_x across the SCRF®. The NH_3 entering the SCRF®, if all the urea is converted to NH_3, can be calculated from the values of urea injection rate and the known properties of urea and the exhaust. The NH_3 inlet to SCRF® is formulated as:

$$SCRF® \; Inlet \;\; NH_3(ppm) = \frac{Urea\ injection\ rate * 0.325 * MW\ of\ Exhaust\ gas * Urea\ Density}{Exhaust\ Flow\ rate * MW\ of\ Urea}$$

(Equation 3.3)

Figures 3.6, 3.7, and 3.8 give the NH_3 slip from the SCRF® for different test points at different ANR, for PM loading of 0, 2, and 4 g/L. The NH_3 slip is a function of the urea injected and the ANR value at the inlet of SCRF®. In Figure 3.6, the NH_3 slip at ANR – 0.8 for test points 1, 3, and 6 are below 5 ppm. Figure 3.7 shows the NH_3 slip for ANR – 1 rising with increasing temperature. This can be attributed to NH_3 slip by PM oxidation at high SCRF® inlet temperature because there is more NH_3 storage in the loaded SCRF® [8].

Figures 3.6, 3.7, and 3.8 show that the trend of NH_3 slip with loading is the same with ANR – 0.8, 1, and 1.2 for all individual test points. It is observed that the NH_3 slip for 2 g/L loading is lower than the NH_3 slip for 0 or 4 g/L loading in all figures. Figure 3.8 shows non uniform trend of NH_3 slip with temperature. The duration of test to obtain the NH_3 slip concentration at each ANR value in a test point was 10 minutes only which might not be sufficient enough to stabilize the readings. The oxidation of NH_3 to N_2 and NO is a dominant reaction at temperatures above 400°C [1].

The nitrogen balance across the SCRF® is shown in Tables 3.7 and 3.9 and was calculated and checked to ensure data consistency. The expression for nitrogen balance is given by:

$$SCRF® \; Nitrogen\ Balance\ (\%) = \{1 - \frac{Inlet\ NH_3\ - \left((Inlet\ NO_x - \ Outlet\ NO_x) + \ Oulet\ NH_3\right)}{Inlet\ NH3}\} * 100$$

(Equation 3.4)

In Table 3.9, the nitrogen balance (%) below 100% shows that it could be either measurement error or N_2, N_2O species coming out of SCRF® which are not accounted for in Equation 3.4.

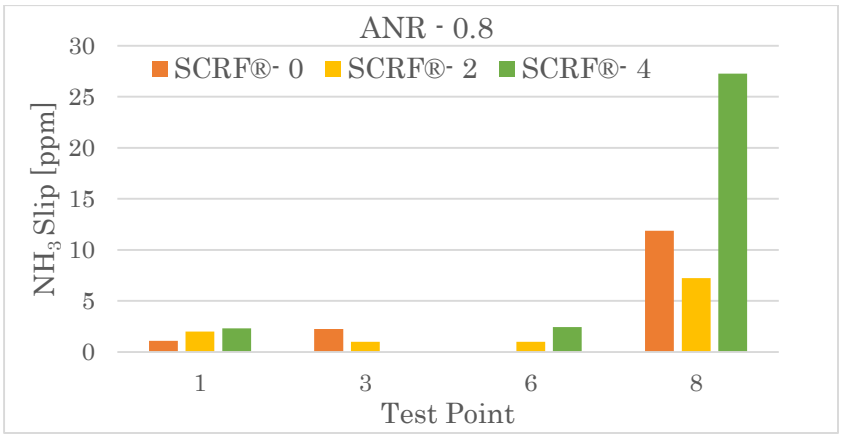

Figure 3.6 NH_3 slip from SCRF® for NO_x reduction test points at ANR - 0.8

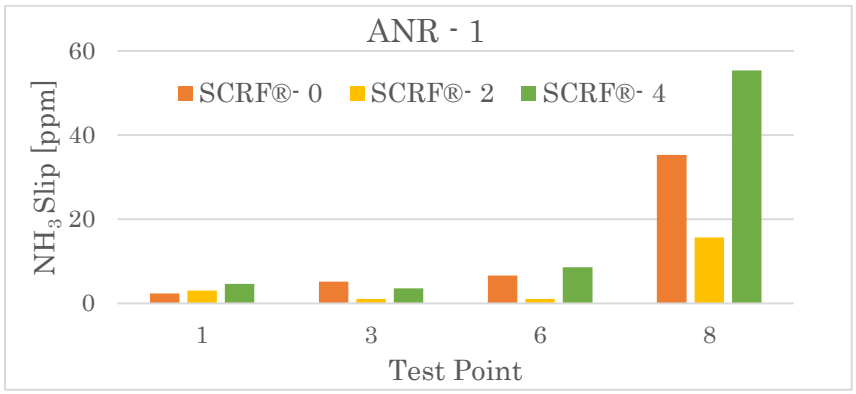

Figure 3.7 NH_3 slip from SCRF® for NO_x reduction test points at ANR - 1

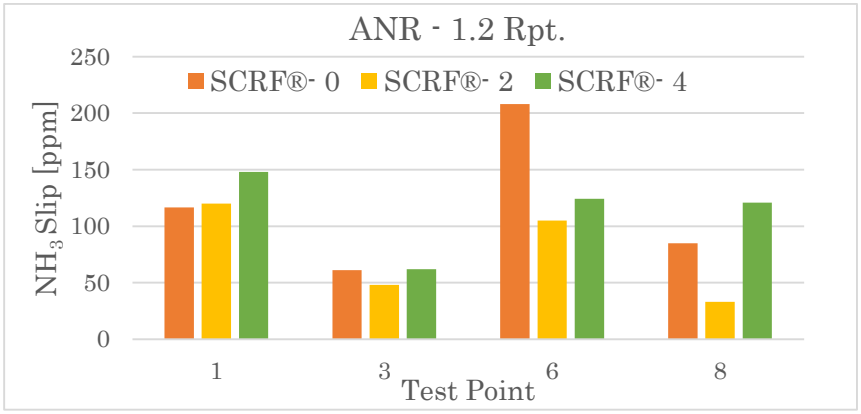

Figure 3.8 NH_3 slip from SCRF® for NOx reduction test points at ANR – 1.2 Repeat (Rpt.)

Chapter 4. Summary and Conclusions

Chapter 3 discussed the results of the tests conducted to analyze NO_x reduction across the SCRF® and NH_3 downstream of the SCRF®. This chapter summarizes the important findings and conclusions of the research presented in this report.

4.1 Summary

The objective of the research was to study the effect of PM loading (0, 2, and 4 g/L) on the NO_x reduction performance of the SCRF®. The aftertreatment system was comprised of the DOC, CPF and SCRF®. Four test points, named as test point 1, 3, 6, and 8, were conducted for each PM loading condition in the SCRF®. For the test without PM loading, the CPF was placed before the SCRF® in order to filter the PM entering the SCRF® whereas for tests with PM loading, the spacer was placed in place of the CPF.

Loading Stages

The engine was run at 2400 rpm engine speed and 200 Nm engine load to load PM in the SCRF®. The fuel rail pressure was reduced to 1050 bar and 750 bar to load PM to 2 g/L and 4 g/L respectively. The exhaust flow rate was 11.2 and 11.5 kg/min for 2 and 4 g/L loading respectively for stage 2. The PM concentration out of engine varied from 17.7 to 21.2 mg/scm and from 11 to 11.8 mg/scm for 2 and 4 g/L respectively during stage 2. The filtration efficiency for tests with PM loading of 2 and 4 g/L had a mean value of 97.4 % and 98.8 %, which shows that filtration efficiency improved with loading.

NO_x Reduction Stage

The NO_x reduction stage is conducted after loading the SCRF® with 0, 2 or 4 g/L for different test points. During this stage, urea is dosed for in order to obtain ANR values of 0, 0.8, 1, and 1.2. The test points were selected from a test matrix to have a wide range of SCRF® inlet conditions such as SCRF® inlet temperature, NO_2/NO_x ratio, and exhaust space velocity. The NO_2/NO_x ratio at SCRF® inlet location varied from 0.22 to 0.46, maximum occurring at 344 °C (mean) inlet temperature. The space velocity for test point 8 was approximately 48 k/hr, which is highest among the test points. The NO_x conversion efficiency across the SCRF® and NH_3 slip at the outlet of the SCRF®

was determined in order to determine the effect of PM loading in the SCRF® on NO_x conversion efficiency and NH_3 slip.

4.2 Conclusions

The following are the conclusions with respect to the objectives of this study:

1. Without urea dosing, the NO_2 concentration at the downstream SCRF® location decreases with increased PM loading and temperature due to NO_2 assisted PM oxidation.
2. The NO_x conversion efficiency of the SCRF® has a maxima for the temperature range of 302-347 °C (test points 3 and 6) where the NO_2/NO_x ratio values and space velocities lie in the range of 0.42-0.46 and 18.6-29.8 k/hr respectively.
3. The impact of PM loading (from 0 to 2 and 4 g/L) on NO_x conversion efficiency is not significant for temperature range below 300 °C however it decreases by 3-5% above 350 °C, due to consumption of NO_2 via passive oxidation of PM.
4. The NO_x conversion efficiency stays below 95% for high temperature (around 450 °C) test point when dosed with urea with ANR value of 1.2.

References

[1] Cavataio, G., Girard, J., and Lambert, C., "Cu/Zeolite SCR on High Porosity Filters: Laboratory and Engine Performance Evaluations," SAE Technical Paper 2009-01-0897, 2009, doi:10.4271/2009-01-0897

[2] Raghavan, Krishnan G., "An Experimental Investigation into the Effect of NO_2 and Temperature on the Passive Oxidation and Active Regeneration of Particulate Matter in a Diesel Particulate Filter", Master's Thesis, Michigan Technological University, 2015.

[3] Inc., E. *DieselNet: Diesel Emission*. 2015; Available from: https://www.dieselnet.com.

[4] "CumminsEngines", https://cumminsengines.com/

[5] Foley, Ryan Kristopher, "Experimental Investigation into Particulate Matter Distribution in Catalyzed Particulate Filters using a 3D Terahertz Wave Scanner", Master's Thesis, Michigan Technological University, 2013.

[6] Vaibhav Kadam, "An Experimental Investigation of the NO_x Reduction Performance of a Cu-Zeolite Flow-through SCR and a SCR Catalyst on a DPF", Master's Thesis, Michigan Technological University, 2016.

[7] Surenahali, H. S., "Dynamic Model Based State Estimation In a Heavy Duty Diesel Aftertreatment System For Onboard Diagnostics And Controls," PhD Dissertation, Michigan Technological University 2013.

[8] Schrade, F., Brammer, M., Schaeffner, J., Langeheinecke, K. et al., "Physico-Chemical Modeling of an Integrated SCR on DPF (SCR/DPF) System," *SAE Int. J. Engines* 5(3):958-974, 2012, DOI: 10.4271/2012-01-1083.

[9] Pidgeon, James, "An Experimental Investigation into the effects of Biodiesel Blends on Particulate Matter Oxidation in a Catalyzed Particulate Filter during Active Regeneration", Master's Thesis, Michigan Technological University, 2013

Appendix A. Particulate Matter Sampling

The Manual Sampling Train (MST) as shown in Figure A.1 was used for sampling PM at upstream of the DOC and downstream of the SCRF®. The MST had a K-type thermocouple to measure exhaust temperature, a vacuum gauge to measure sample pump vacuum, a dry gas meter (DGM) in Figure A.2 to measure exhaust sample volume, a manometer to measure pressure drop at the DGM and a timer to estimate the duration of sampling.

The PM filters were conditioned before the experiment by baking at 850˚F for 45 minutes. It removed any moisture present on the filter which could have affected the initial mass of the filter. The filter papers were then kept in a glove box environment, which was maintained at consistent humidity (60%) and temperature (25 °C) by a tray of desiccant, for 24 hours. The filter papers were weighed using Mettler Toledo UMT2 microbalance before the PM sampling. The filter papers were kept in a box filled with desiccant to avoid moisture absorption by the PM collected on it.

The PM filter probe as shown in Figure A.3 contained the glass fiber filter and was placed at the sample port. To start the sampling, the valve was opened to allow the exhaust to be drawn into the MST. Simultaneously the pump and timer were switched on. The mass of PM retained in the filter is a function of the sampling duration, exhaust flow rate and PM concentration in the exhaust. The valve was then closed and simultaneously the pump and timer were switched off at the end of the sampling duration.

The temperature and the pressure readings were noted at the start and at the end of each PM sample collection. The volume of the exhaust sample was measured by the change in the initial and final reading of DGM. The PM coated filters were weighed using the microbalance after the sampling. The standard concentration of PM (mg/scm) is defined by the PM mass sampled divided by the volume of the exhaust (cubic meter) sampled converted to standard conditions of 25˚C and 1 atm.

Figure A.1 Manual Sampling Train

Figure A.2 Dry Gas Meter

Figure A.3 a) PM sampling probe (left picture) b) Filter paper (right picture)

Appendix B. SCRF® Weighing

The SCRF® was weighed at the end of each loading and NO_x reduction stage of the test as shown in Figure B.1. It was observed that the weight of SCRF® block varies with temperature and therefore the SCRF® was immediately weighed after the engine was shut down [9]. To remove the SCRF® from the aftertreatment system, first the outlet cone was loosened to prevent air suction from the exhaust system. Later the SCRF® was disassembled from the aftertreatment system after disconnecting the thermocouples, pressure lines and electrical connections mounted on the SCRF®.

The calibration weight was measured to ensure scale accuracy and individual thermocouple readings were recorded. Before weighing the SCRF®, the scale was zeroed prior to each measurement reading. Then the SCRF® was placed on the scale and three weight readings were noted. The mass of the SCRF® was calculated by averaging out the three readings.

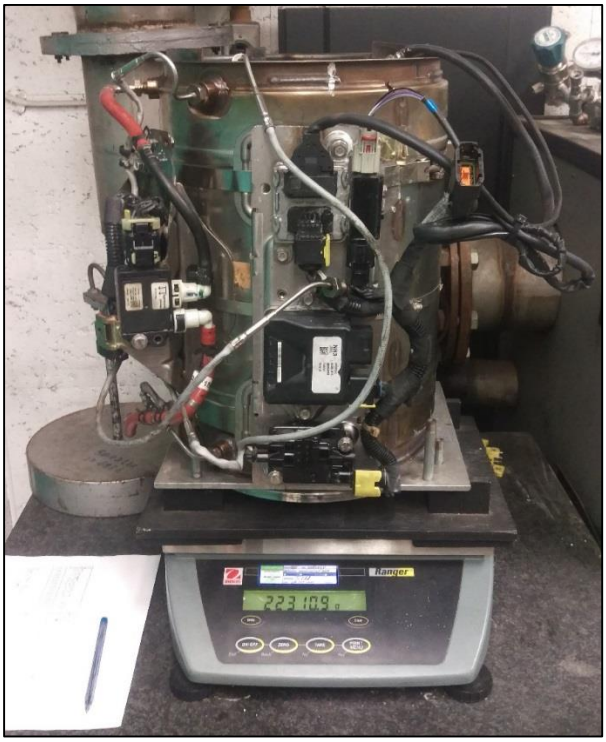

Figure B.1 Weighing of SCRF® using the Ohaus manufacturer weighing scale

Appendix C. Engine, Exhaust Conditions and PM Mass Balance for Each Stage

The engine conditions, SCRF® conditions and PM mass balance across the SCRF® is presented for stage 1, stage 2 and NO_x reduction stage in this appendix. The engine speed, load, the engine out and SCRF® inlet (temperature, $NO/NO_2/NO_x$ concentration, PM concentration) conditions are analyzed and compared for deviation in Table C.1, C.2, C.5, and C.6. The filtration efficiency of the SCRF® and PM oxidation in the SCRF® are summarized in Tables C.3, C.4, C.7, and C.8.

PM $_{in/out}$ (g) of the SCRF® is calculated using the formula:

$$PM_{in/out} = Conc_{in/out} * 10^{-3} * \frac{MFR_{exh}}{1.18} * t_{stage}$$

(Equation C.1)

Where,

$PM_{in/out}$ is the PM mass in/out of the SCRF® [g], $Conc_{in}$ is the PM concentration (PM conc.) into the SCRF® [mg/scm], MFR_{exh} is the mass flowrate of exhaust [kg/min.], 1.18 is the standard exhaust density at 25°C and 1 atm, taken as that of air [kg/m^3], t_{stage} is the duration of the stage [min]

PM $_{retained}$ (g) in the SCRF® for loading stages is determined from the pre and post stage SCRF® weight measurements.

PM $_{available}$ (g) in the SCRF® is the amount of PM entered (PM_{in} from Equation C.1) during the stage in addition to existing PM in the system at the start of the loading stage (m_{start}).

$$PM_{available} = PM_{in} + m_{start}$$

(Equation C.2)

PM $_{oxidized}$ (g) is calculated by the subtracting the amount of PM_{out} of the SCRF® and $PM_{retained}$ in the SCRF® from the PM_{in} during the stage.

$$PM_{oxidized} = PM_{in} - PM_{retained} - PM_{out}$$

(Equation C.3)

Stage 1 and Stage 2 at 2 g/L Loading

It is seen from Tables C.1 and C.2 that the species concentration (NO, NO_2 and NO_x) and engine out PM concentration are consistent for all test points. The speed and load values are kept at constant values of 2400 RPM and 200 Nm and have very small deviation. The average engine-out particulate matter is 11.4 mg/scm (milligrams /standard cubic meter) and is consistent for all tests with a standard deviation of 0.5 mg/scm and 0.3 mg/scm for stage 1 and stage 2 respectively.

The parameters such as PM concentration into SCRF®, NO_2/PM ratio, temperature into SCRF® and loading duration which affected the PM deposition and oxidation in the SCRF® are given in Tables C.3 and C.4. The test point 3 (2401 rpm engine speed, 203 Nm load) has least PM retention of 27.9 g in the SCRF® for the high PM amount coming into the SCRF® and hence high PM available for oxidation. Another reason was that the test point 3 was run for least time period of approximately 300 minutes.

PM oxidation (percentage) in stage 1 as shown in Table C.3 has the similar trend to that of PM oxidation (percentage) in stage 2 as shown in Table C.4. This is because mass loaded in stage 1 is estimated assuming the same rate of loading as in stage 2. The filtration efficiency is obtained using the samples collected during stage 2 which is considered to be same for stage 1.

Table C.1 Engine and SCRF® conditions for Stage 1 at 2 g/L loading

Test Point	Speed	Load	Temp. into SCRF®	Exhaust Flowrate	SCRF® Std. Space Vel.	SCRF® Act. Space Vel.	NO into SCRF®	NO_2 into SCRF®	NO_x into SCRF®	Engine Out PM conc.
[-]	[RPM]	[N-m]	[C]	[kg/min]	[k/hr]	[k/hr]	[ppm]	[ppm]	[ppm]	[mg/scm]
1	2383	205	276	11.2	30.5	57.6	118	62	180	11.0
3	2395	205	274	11.2	33.3	57.3	138	38	176	12.2
6	2400	203	274	11.2	33.5	57.6	118	72	190	11.4
8	2397	201	284	11.3	33.7	59.1	124	66	190	11.0
Mean	2394	204	277	11.2	32.7	57.9	124	59	184	11.4
Std. Dev.	7	2	5	0.1	1.5	0.8	9	15	7	0.5
ULIM 95%	2401	205	282	11.3	34.2	58.7	134	74	191	11.9
LLIM 95%	2387	202	272	11.2	31.3	57.1	115	45	177	10.9
95% CI	14	3	9	0.1	2.9	1.6	18	29	14	1.1

Table C.2 Engine and SCRF® conditions for Stage 2 at 2 g/L loading

Test Point	Speed	Load	Temp. into SCRF®	Exh. Flow-rate	SCRF® Std. Space Vel.	SCRF® Act. Space Vel.	NO into SCRF®	NO_2 into SCRF®	NO_x into SCRF®	Engine Out PM	SCRF® delta P at the end of S2
[-]	[RPM]	[N-m]	[C]	[kg/min]	[k/hr]	[k/hr]	[ppm]	[ppm]	[ppm]	[mg/scm]	[kPa]
1	2401	203	279	11.3	30.7	58.3	114	82	196	11.0	6.6
3	2401	203	274	11.2	30.5	57.3	131	56	187	11.8	6.4
6	2399	200	269	11.3	30.8	57.5	122	65	186	11.4	6.3
8	2399	202	274	11.2	30.6	57.7	127	69	197	11.2	6.2
Mean	2400	202	274	11.2	30.7	57.7	123	68	191	11.4	6.4
Std. Dev.	1	1	4	0.1	0.1	0.4	7	11	6	0.3	0.2
ULIM 95%	2401	203	278	11.3	30.8	58.1	131	79	197	11.7	6.5
LLIM 95%	2399	201	270	11.2	30.5	57.3	116	57	186	11.0	6.2
95% CI	2	2	8	0.1	0.3	0.8	15	21	11	0.7	0.3

Table C.3 Particulate matter mass balance during Stage 1 at 2 g/L loading

Test Point	PM Conc. Into SCRF®	NO_2/PM Ratio	NO_x/PM Ratio	Filtration Efficiency of SCRF®	PM Into SCRF® during S1	PM Mass Out of SCRF® during S1	Total PM deposited in SCRF® by the end of S1	PM Mass Oxidized during S1	PM Mass Retained at the end of S1	Duration	% Oxidized
[-]	[mg/scm]	[mg NO_2: mg PM]	[mg NO_x: mg PM]	[%]	[g]	[g]	[g]	[g]	[g]	[min]	[%]
1	11.0	10.6	30.8	96.9	3.1	0.1	3.1	0.2	2.8	30	7%
3	12.2	5.8	27.1	97.7	3.5	0.1	3.5	0.9	2.6	31	25%
6	11.4	11.8	31.2	97.4	3.3	0.1	3.3	0.7	2.5	31	20%
8	11.0	11.3	32.4	97.8	3.3	0.1	3.3	0.4	2.8	32	13%
Mean	11.4	9.9	30.4	97.4	3.3	0.1	3.3	0.5	2.7	31	16%
Std. Dev.	0.5	2.7	2.3	0.4	0.2	0.0	0.2	0.3	0.2	0	8%
ULIM 95%	11.9	12.6	32.6	97.8	3.5	0.1	3.5	0.8	2.8	31	24%
LLIM 95%	10.9	7.2	28.2	97.1	3.2	0.1	3.2	0.3	2.5	30	8%
95% CI	1.1	5.4	4.4	0.7	0.3	0.0	0.3	0.6	0.3	1	15%

Table C.4 Particulate matter mass balance during Stage 2 at 2 g/L loading

Test Point	PM Conc. Into SCRF®	NO_2/PM Ratio	NO_x/PM Ratio	Filtration Efficiency of SCRF®	PM Into SCRF® during S2	PM Mass Out of SCRF® during S2	Total PM deposited in SCRF® by the end of S2	PM Mass Oxidized during S2	PM Mass Retained at the end of S2	Duration	%Oxidized	PM Loading at the end of S2
[-]	[mg/scm]	[mg NO_2: mg PM]	[mg NO_x: mg PM]	[%]	[g]	[g]	[g]	[g]	[g]	[min]	[%]	[g/L]
1	11.0	14.1	33.5	96.9	34.6	1.1	37.4	3.0	33.3	330	8%	2.0
3	11.8	9.0	29.8	97.7	33.5	0.8	36.1	7.4	27.9	300	21%	1.6
6	11.4	10.6	30.6	97.4	36.6	1.0	39.1	8.0	30.1	334	20%	1.8
8	11.2	11.6	32.9	97.8	35.3	0.8	38.1	4.8	32.5	330	13%	1.9
Mean	11.4	11.3	31.7	97.4	35.0	0.9	37.7	5.8	31.0	323	15%	1.8
Std. Dev.	0.3	2.1	1.8	0.4	1.3	0.1	1.3	2.4	2.5	16	6%	0.1
ULIM 95%	11.7	13.4	33.5	97.8	36.2	1.0	38.9	8.1	33.4	339	22%	2.0
LLIM 95%	11.0	9.2	30.0	97.1	33.7	0.8	36.4	3.5	28.5	308	9%	1.7
95% CI	0.7	4.2	3.5	0.7	2.5	0.3	2.5	4.6	4.9	31	12%	0.3

Stage 1 and Stage 2 at 4 g/L Loading

Tables C.5 and C.6 give the data for engine speed, load, SCRF® inlet species concentration and engine out PM for all test points. The average engine-out particulate matter is 18.7 mg/scm and 19.4 mg/scm for stage 1 and stage 2 respectively.

Table C.8 shows that the percent PM oxidation for Stage 2, which is consistent for all test points with an average of 24% and a standard deviation of 3 %. The PM retention in the SCRF® is 4 g and 69.4 g for stage 1 and stage 2 respectively. A filtration efficiency of 99.1% is obtained using the samples collected during stage 2 and is considered to be same for stage 1.

Table C.5 Engine and SCRF® conditions for Stage 1 at 4 g/L loading

Test Point	Speed	Load	Temp. into SCRF®	Exhaust Flowrate	SCRF® Std. Space Vel.	SCRF® Act. Space Vel.	NO into SCRF®	NO_2 into SCRF®	NO_x into SCRF®	Engine Out PM Conc.	SCRF® delta P
[-]	[RPM]	[N-m]	[C]	[kg/min]	[k/hr]	[k/hr]	[ppm]	[ppm]	[ppm]	[mg/scm]	[kPa]
1	2401	205	285	11.4	31.0	61.1	112	42	154	15.1	3.7
3	2398	205	285	11.4	33.9	61.0	98	46	144	21.2	3.7
6	2396	201	286	11.3	33.8	61.0	101	46	147	18.8	3.7
8	2399	205	294	11.4	34.0	62.2	107	50	157	19.7	3.8
Mean	2399	204	288	11.4	33.2	61.3	105	46	151	18.7	3.7
Std. Dev.	2	2	5	0.0	1.5	0.6	6	3	6	2.6	0.1
ULIM 95%	2400	206	292	11.4	34.6	61.9	111	49	157	21.2	3.8
LLIM 95%	2397	202	283	11.3	31.7	60.8	99	43	145	16.2	3.6
95% CI	4	4	9	0.1	2.9	1.1	12	6	12	5.0	0.1

Table C.6 Engine and SCRF® conditions for Stage 2 at 4 g/L loading

Test Point	Speed	Load	Temp. into SCRF®	Exhaust Flowrate	SCRF® Std. Space Vel.	SCRF® Act. Space Vel.	NO into SCRF®	NO_2 into SCRF®	NO_x into SCRF®	Engine Out PM Conc.	SCRF® delta P at the end of S2
[-]	[RPM]	[N-m]	[C]	[kg/min]	[k/hr]	[k/hr]	[ppm]	[ppm]	[ppm]	[mg/scm]	[kPa]
1	2401	205	288	11.4	31.1	58.5	110	53	163	17.7	9.4
3	2387	202	283	11.3	30.9	57.8	100	53	153	21.2	9.1
6	2402	204	297	11.6	31.5	59.8	122	54	175	19.5	10.0
8	2402	204	298	11.5	31.3	59.6	102	48	150	19.2	9.9
Mean	2398	204	291	11.5	31.2	58.9	109	52	161	19.4	9.6
Std. Dev.	8	1	7	0.1	0.2	0.9	10	3	11	1.4	0.4
ULIM 95%	2405	205	298	11.5	31.5	59.8	118	55	172	20.8	10.0
LLIM 95%	2390	203	284	11.4	31.0	58.0	99	49	149	18.0	9.1
95% CI	15	2	14	0.2	0.5	1.9	19	5	22	2.7	0.9

Table C.7 Particulate matter mass balance during Stage 1 at 4 g/L loading

Test Point	PM Conc. Into SCRF®	NO_2/PM Ratio	NO_x/PM Ratio	Filtration Efficiency of SCRF®	PM Into SCRF® during S1	PM Mass Out of SCRF® during S1	Total PM deposited in SCRF® by the end of S1	PM Mass Oxidized during S1	PM Mass Retained at the end of S1	Duration	%Oxidized
[-]	[mg/scm]	[mg NO_2: mg PM]	[mg NO_x: mg PM]	[%]	[g]	[g]	[g]	[g]	[g]	[min]	[%]
1	15.1	5.2	19.2	99.0	4.5	0.05	4.5	0.5	4.0	31	11%
3	21.2	4.0	12.8	98.3	6.0	0.10	6.0	2.1	3.8	30	35%
6	18.8	4.6	14.7	99.0	5.3	0.05	5.3	1.4	3.9	30	26%
8	19.7	4.8	15.0	99.0[3]	5.9	-0.01	5.9	1.5	4.3	31	26%
Mean	18.7	4.7	15.4	98.8	5.4	0.05	5.4	1.4	4.0	30	25%
Std. Dev.	2.6	0.5	2.7	0.3	0.7	0.04	0.7	0.6	0.2	1	10%
ULIM 95%	21.2	5.1	18.0	99.2	6.1	0.09	6.1	2.0	4.2	31	34%
LLIM 95%	16.2	4.2	12.8	98.5	4.8	0.00	4.8	0.7	3.8	30	15%
95% CI	5.0	1.0	5.2	0.7	1.3	0.09	1.3	1.3	0.4	1	19%

Table C.8 Particulate matter mass balance during Stage 2 at 4 g/L loading

Test Point	PM Conc. Into SCRF®	NO_2/PM Ratio	NO_x/PM Ratio	Filtration Efficiency of SCRF®	PM Into SCRF® during S2	PM Mass Out of SCRF® during S2	Total PM deposited in SCRF® by the end of S2	PM Mass Oxidized during S2	PM Mass Retained at the end of S2	Duration	%Oxidized	PM Loading at the end of S2
[-]	[mg/scm]	[mg NO_2: mg PM]	[mg NO_x: mg PM]	[%]	[g]	[g]	[g]	[g]	[g]	[min]	[%]	[g/L]
1	17.7	5.6	17.3	99.0	87.7	0.9	91.7	21.6	69.2	511	24%	4.1
3	21.2	4.7	13.6	98.3	93.6	1.6	97.4	34.3	61.5	460	21%	3.6
6	19.5	5.2	16.9	99.0	97.5	1.0	101.4	29.3	71.1	510	29%	4.2
8	19.2	4.7	14.7	99.0[1]	95.5	-0.1	99.8	24.2	75.7	510	24%	4.4
Mean	19.4	5.0	15.6	98.8	93.6	0.8	97.6	27.4	69.4	497	24%	4.1
Std. Dev.	1.4	0.4	1.8	0.3	4.2	0.7	4.2	5.6	5.9	25	3%	0.3
ULIM 95%	20.8	5.5	17.3	99.2	97.7	1.5	101.7	32.9	75.2	522	28%	4.4
LLIM 95%	18.0	4.6	13.9	98.5	89.4	0.1	93.4	21.8	63.6	473	21%	3.7
95% CI	2.7	0.9	3.4	0.7	8.3	1.4	8.3	11.1	11.6	49	7%	0.7

[1] The value is taken same as that for test point 6 since the filter paper was damaged at the downstream location during sampling.

Appendix D. Gaseous Emissions by Stage

This appendix discusses the emission species for stage 1 and the NO_x reduction stage runs. The NO_x reduction stage test results for ANR 1 and 1.2 are discussed in Chapter 3 and the results for ANR 0, 0.8, and 1.2 (repeat) are summarized in this section in Tables D.3 through D.8. The positive and negative values of NO conversion efficiency show reduction and increment in NO concentration across the components (DOC, SCRF®) respectively.

All the measurements presented in the table are from Mass Spectrometer (IMR-MS). Due to problems with the Mass Spectrometer emission analyzer, the NO_2 species ppm was not available correctly at the upstream DOC location for the test points. The correct species measurements were obtained in tests with 4g/L loading after the maintenance of IMR-MS by V&F. The NO_x is determined as the sum of NO and NO_2 concentrations at the respective locations. The effect of loading on NO_x reduction efficiency at different test points can be seen in Figure D.1 for ANR-1.2 Repeat.

Stage 1 and Stage 2 Loading at 2 g/L

Table D.1 NO, NO_2, NO_x concentration at upstream and downstream locations of DOC and SCRF® during Stage 1 loading at 2 g/L

Test Point	NO			NO_2			NO_x			NO Conv.	
	U DOC	U SCRF®	D SCRF®	U DOC	U SCRF®	D SCRF®	U DOC	U SCRF®	D SCRF®	DOC	SCRF®
[-]	[ppm]	[ppm]	[ppm]	[ppm]	[ppm]	[ppm]	[ppm]	[ppm]	[ppm]	[%]	[%]
1	182	118	127	1	62	50	183	180	177	35	-8
3	170	138[1]	132[1]	1	38	39	171	176	171	19	4
6	181	118	130	1	72	58	182	190	188	35	-10
8	181	124	129	1	66	55	182	190	184	32	-4
Mean	179	124	130	1	59	50	180	184	180	30	-5
Std. Dev.	6	9	2	0	15	8	6	7	8	8	6
ULIM 95%	184	134	132	1	74	58	185	191	187	38	2
LLIM 95%	173	115	127	1	45	42	174	177	172	23	-11
95% CI	11	18	4	0	29	16	11	14	15	15	12

[1]The concentration of NO at USCRF® and DSCRF® are flagged because of calibration issues with the mass spectrometer during test point 3.

Table D.2 NO, NO_2, NO_x concentration at upstream and downstream locations of DOC and SCRF® during Stage 2 loading at 2 g/L

Test Point	NO			NO_2			NO_x			NO Conv. %	
	U DOC	U SCRF®	D SCRF®	U DOC	U SCRF®	D SCRF®	U DOC	U SCRF®	D SCRF®	DOC	SCRF®
[-]	[ppm]	[ppm]	[ppm]	[ppm]	[ppm]	[ppm]	[ppm]	[ppm]	[ppm]	[%]	[%]
1	172	114	136	1	82	51	173	196	187	34	-20
3	180	131	146	1	56	44	181	187	190	27	-12
6	170	122	145	8	65	37	178	186	182	28	-19
8	185	127	133	6	69	51	191	197	184	31	-5
Mean	177	123	140	4	68	46	181	191	186	30	-14
Std. Dev.	7	7	7	4	11	6	7	6	4	3	7
ULIM 95%	183	131	146	7	79	52	188	197	189	33	-7
LLIM 95%	170	116	133	1	57	40	173	186	182	27	-21
95% CI	14	15	13	7	21	13	15	11	7	6	14

Stage 1 and Stage 2 Loading at 4 g/L

Table D.3 NO, NO_2, NO_x concentration at upstream and downstream locations of DOC and SCRF® during Stage 1 loading at 4 g/L

Test Point	NO			NO_2			NO_x			NO Conv. %	
	U DOC	U SCRF®	D SCRF®	U DOC	U SCRF®	D SCRF®	U DOC	U SCRF®	D SCRF®	DOC	SCRF®
[-]	[ppm]	[ppm]	[ppm]	[ppm]	[ppm]	[ppm]	[ppm]	[ppm]	[ppm]	[%]	[%]
1	147	112	112	1	42	32	148	154	144	24	0
3	138	98	104	0	46	35	138	144	139	29	-6
6	125	101	117	22	46	31	147	147	149	19	-16
8	130	107	114	18	50	34	148	157	148	18	-7
Mean	135	105	112	10	46	33	145	151	145	22	-7
Std. Dev.	10	6	6	11	3	2	5	6	4	5	7
ULIM 95%	144	111	117	22	49	35	150	157	149	27	-1
LLIM 95%	125	99	107	-1	43	32	140	145	141	17	-14
95% CI	19	12	11	23	6	3	10	12	9	10	13

Table D.4 NO, NO_2, NO_x concentration at upstream and downstream locations of DOC and SCRF® during Stage 2 loading at 4 g/L

Test Point	NO			NO_2			NO_x			NO Conv. %	
	U DOC	U SCRF®	D SCRF®	U DOC	U SCRF®	D SCRF®	U DOC	U SCRF®	D SCRF®	DOC	SCRF®
[-]	[ppm]	[ppm]	[ppm]	[ppm]	[ppm]	[ppm]	[ppm]	[ppm]	[ppm]	[%]	[%]
1	133	110	135	18	53	17	152	163	152	17	-22
3	145	100	118	2	53	25	147	153	143	31	-18
6	147	122	156	23	54	23	170	175	179	17	-29
8	135	102	132	17	48	18	152	150	150	24	-29
Mean	140	109	135	15	52	21	155	161	156	23	-24
Std. Dev.	7	10	16	9	3	4	10	11	16	6	6
ULIM 95%	147	118	151	24	55	24	165	172	172	29	-19
LLIM 95%	133	99	120	6	49	17	145	149	140	16	-30
95% CI	14	19	31	18	5	7	20	22	31	12	11

NO_x Reduction Stage

Table D.5 Species concentration at upstream and downstream SCRF® for NO_x reduction test points at ANR-0

Test Point	NO [ppm]						NO_2 [ppm]					
	SCRF®- 0		SCRF®- 2		SCRF®- 4		SCRF®- 0		SCRF®- 2		SCRF®- 4	
	In	Out	In	Out	In	Out	In	Out	In	Out	In	Out
1	345	352	403	387	453	402	213	200	203	205	146	115
3	158	160	161	198	198	249	121	116	131	88	124	75
6	795	808	743	967	793	1151	674	688	644	426	588	231
8	411	415	424	457	415	502	140	139	125	52	115	22

Table D.6 Species concentration at upstream and downstream SCRF® for NO_x reduction test points at ANR-1.2 Rpt.

Test Point	NO [ppm]						NO_2 [ppm]						NH_3 [ppm]					
	SCRF®- 0		SCRF®- 2		SCRF®- 4		SCRF®- 0		SCRF®- 2		SCRF®- 4		SCRF®- 0		SCRF®- 2		SCRF®- 4	
	In	Out	In	Out	In	Out	In	Out	In	Out	In	Out	In	Out	In	Out	In	Out
1	345	7	403	8	453	15	213	0	203	0	146	1	685	117	723	120	722	148
3	158	5	161	2	198	3	121	0	131	0	124	0	331	61	347	48	392	62
6	795	5	743	6	793	9	674	0	644	0	588	1	1685	208	1644	105	1596	124
8	411	35	424	40	415	75	140	0	125	0	115	0	657	85	646	33	642	121

Table D.7 Species conversion efficiency across SCRF® for NO_x reduction test points at ANR-1.2 Rpt.

Test Point	ANR			NO_x conversion efficiency [%]			Nitrogen Balance [%]		
	SCRF®- 0	SCRF®- 2	SCRF®- 4	SCRF®- 0	SCRF®- 2	SCRF®- 4	SCRF®- 0	SCRF®- 2	SCRF®- 4
1	1.23	1.19	1.21	99	99	97	97	99	101
3	1.19	1.19	1.22	98	99	99	101	97	97
6	1.15	1.19	1.16	100	100	99	99	90	94
8	1.19	1.18	1.21	94	93	86	91	84	90

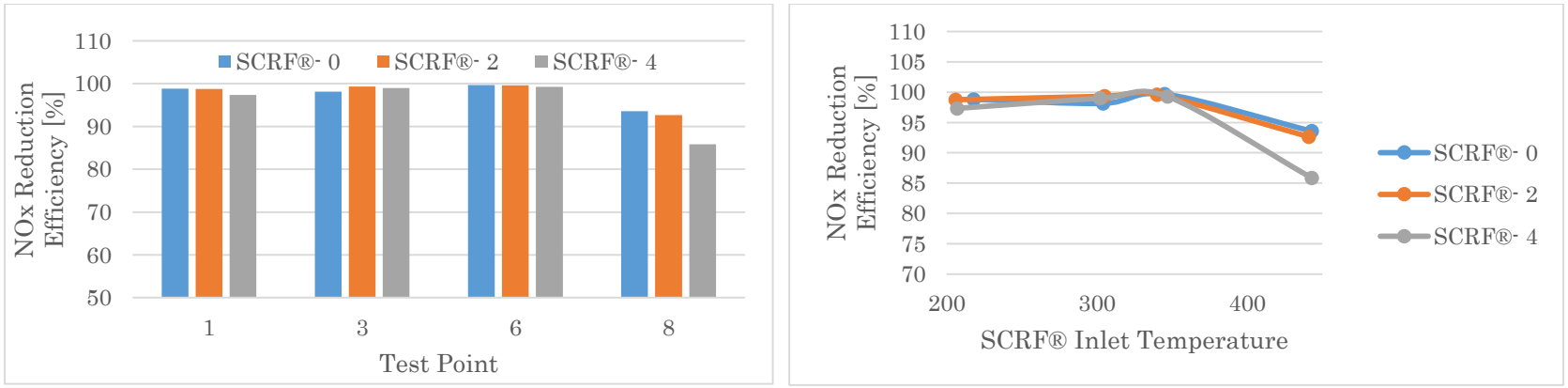

Figure D.1 NO_x conversion efficiency (%) with ANR – 1.2 Repeat for test points with and without loading

Appendix E. SCRF® Pressure Drops

The pressure drops across the SCRF® for each test point with and without PM loading are presented in this section in the figures. The pressure drop curve for tests with 0 g/L PM loading is constant because the PM concentration coming into the SCRF® is low as shown in Figures E.1, E.2, E.3, and E.4.

The test points 6 and 8 have higher PM oxidation rate because of higher SCRF® inlet temperatures and, therefore the SCRF® was loaded again in between the NO_x reduction stage which is denoted by repeat loadings, as shown in Figures E.7 and E.8 for 2 g/L loading. Similar repeat loading was done for the same test points for 4 g/L as shown in Figures E.11 and E.12. In Figures E.5, E.6, E.9, and E.10, the PM oxidation is low and hence repeated loading was not required.

Loading at 0 g/L

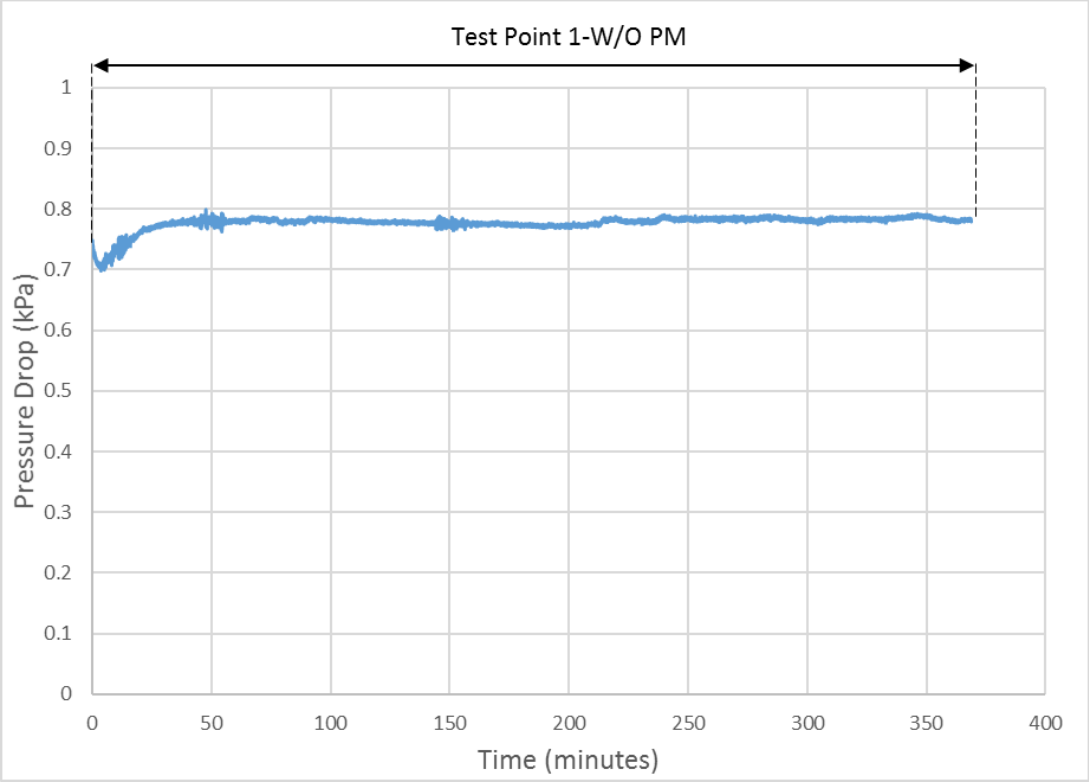

Figure E.1 Pressure drop curve for test point 1 without PM loading in the SCRF®

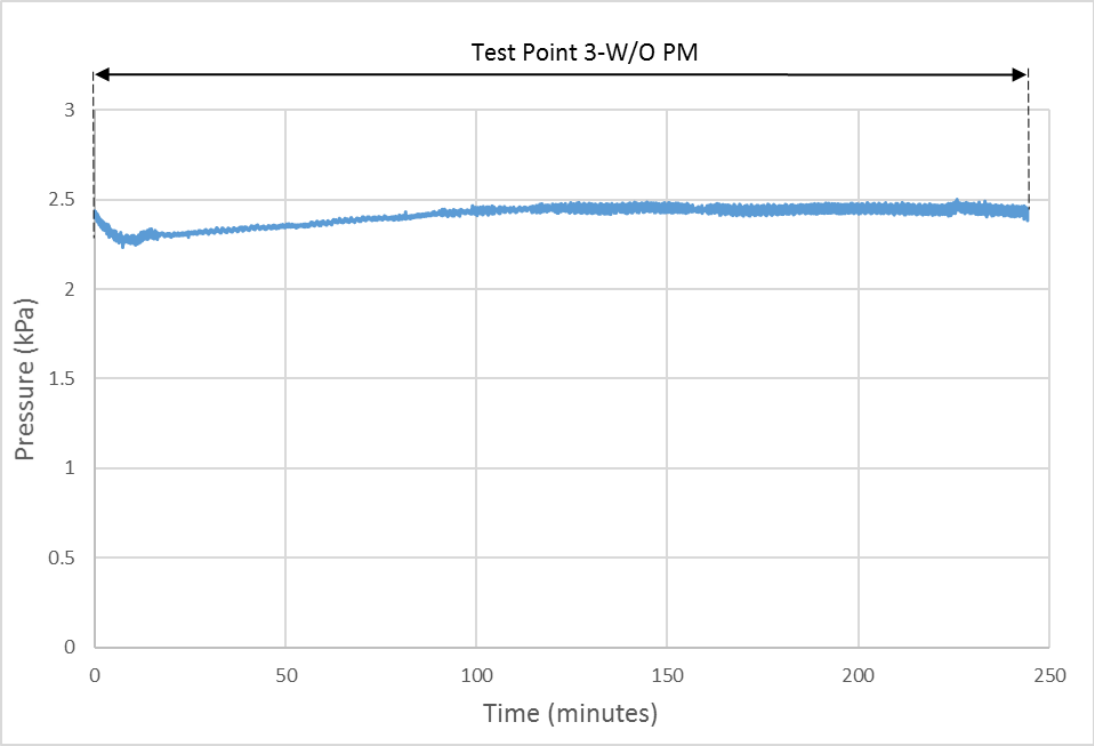

Figure E.2 Pressure drop curve for test point 3 without PM loading in the SCRF®

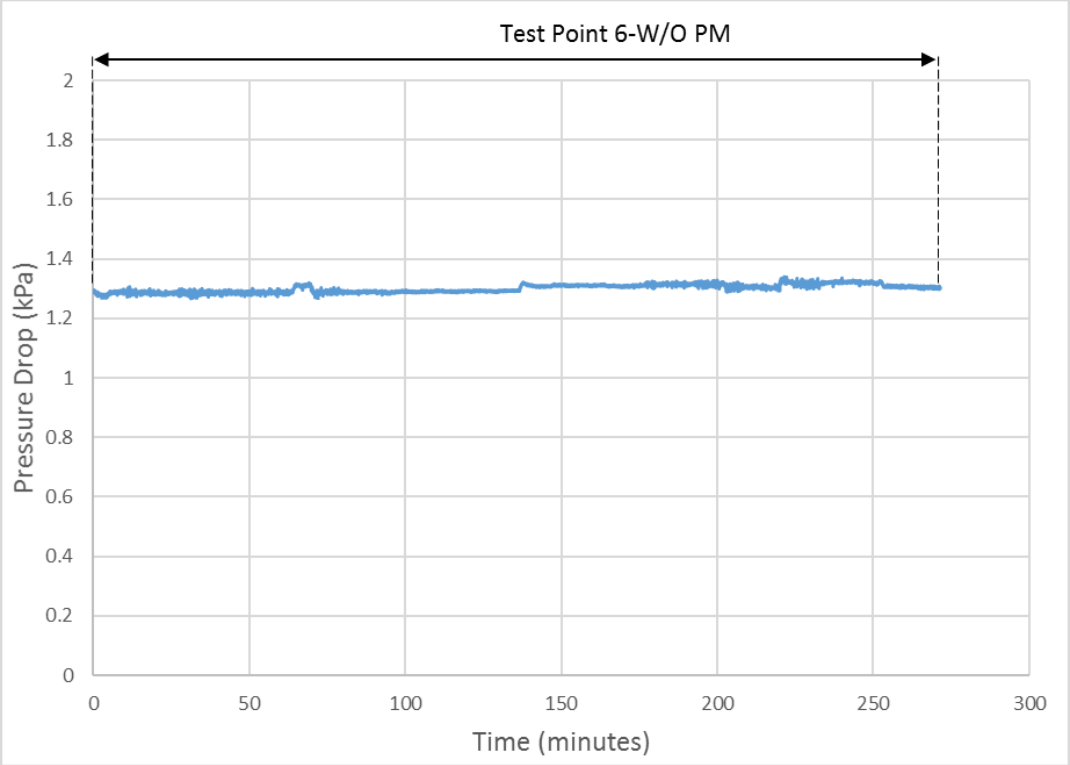

Figure E.3 Pressure drop curve for test point 6 without PM loading in the SCRF®

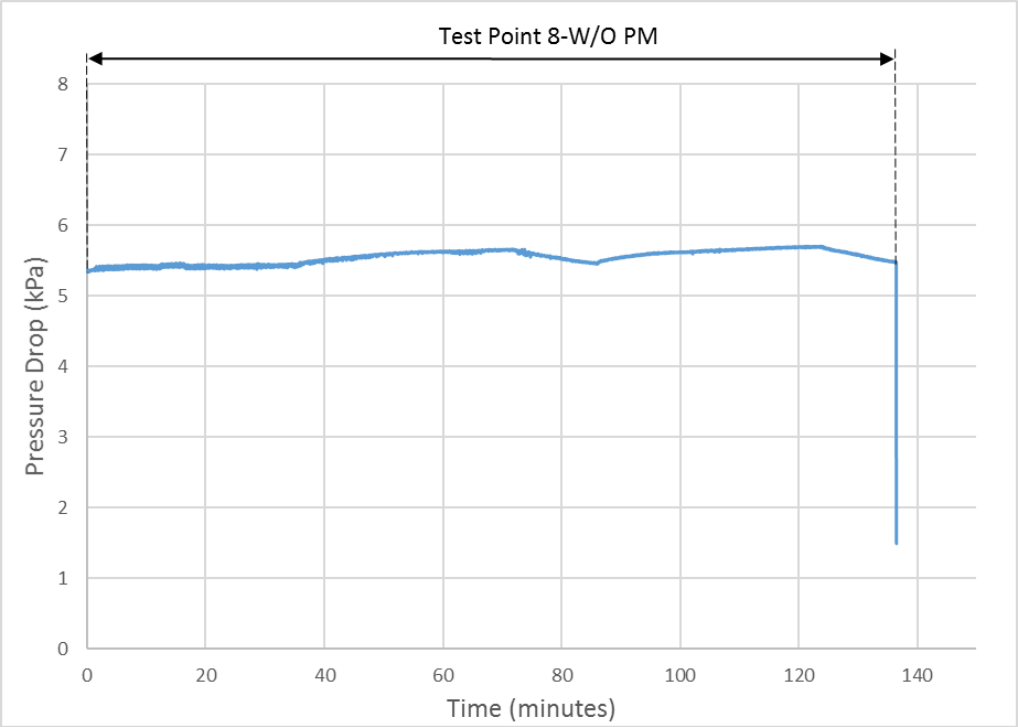

Figure E.4 Pressure drop curve for test point 8 without PM loading in the SCRF®

Loading at 2 g/L

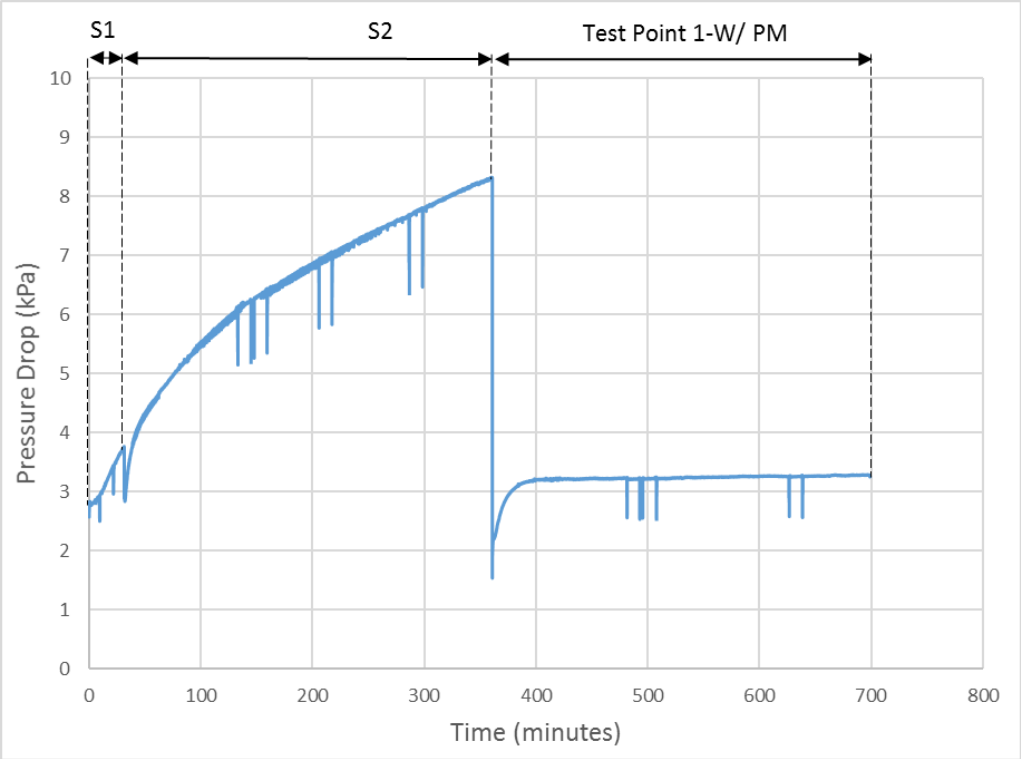

Figure E.5 Pressure drop curve for test point 1 with PM loading 2 g/L in the SCRF®

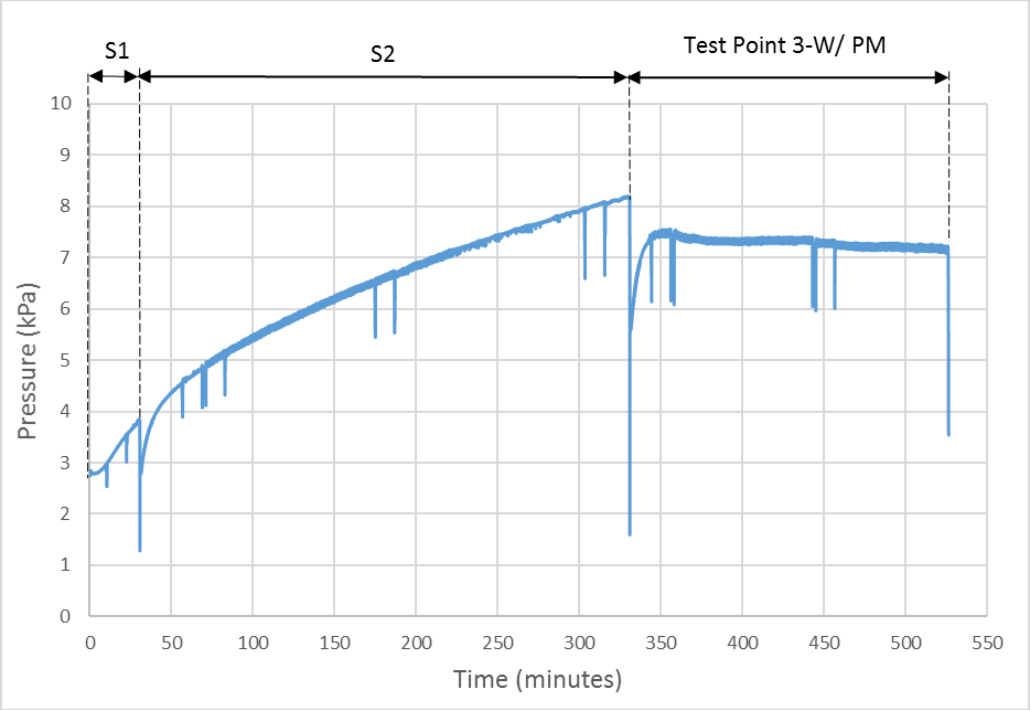

Figure E.6 Pressure drop curve for test point 3 with PM loading 2 g/L in the SCRF®

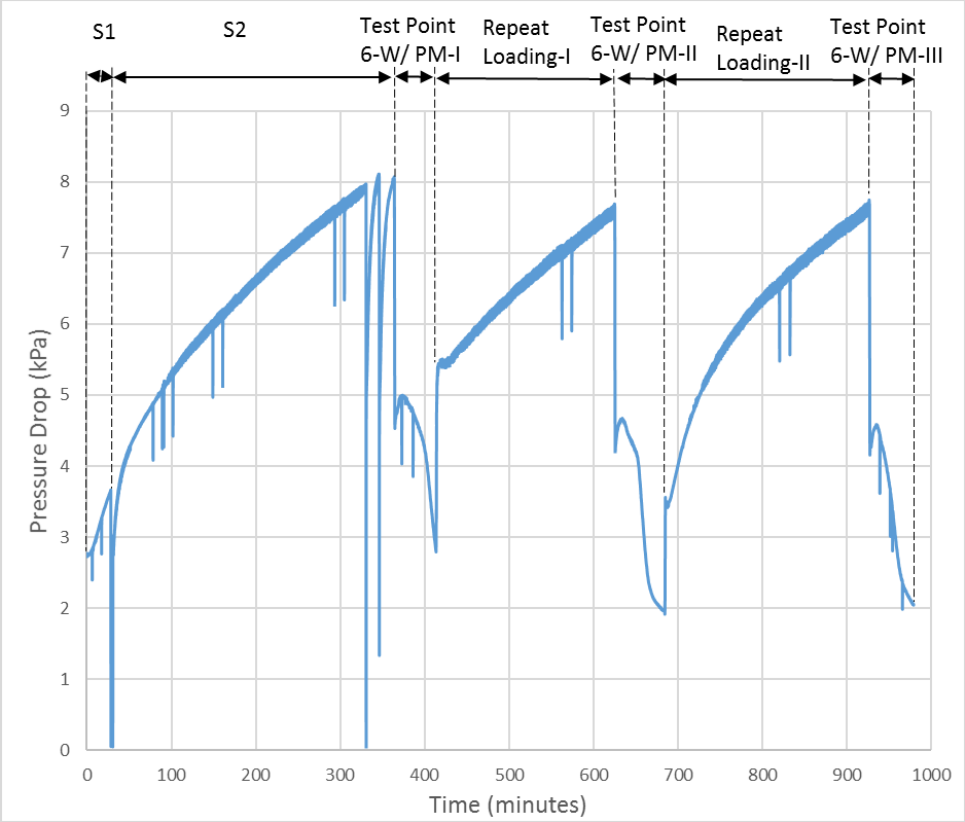

Figure E.7 Pressure drop curve for test point 6 with PM loading 2 g/L in the SCRF®

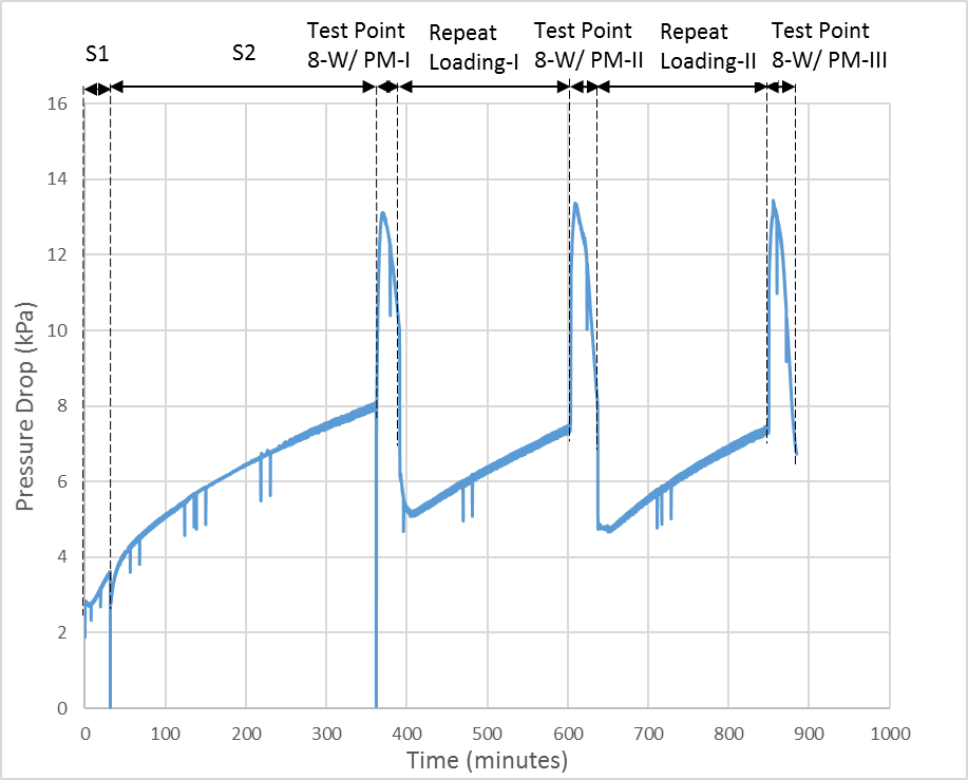

Figure E.8 Pressure drop curve for test point 8 with PM loading 2 g/L in the SCRF®

Loading at 4 g/L

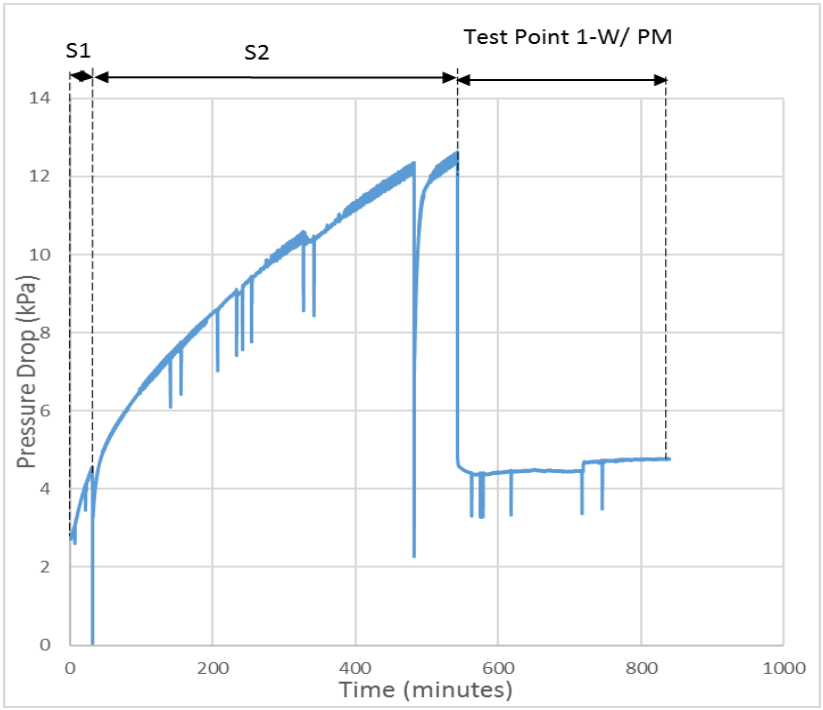

Figure E.9 Pressure drop curve for test point 1 with PM loading 4 g/L in the SCRF®

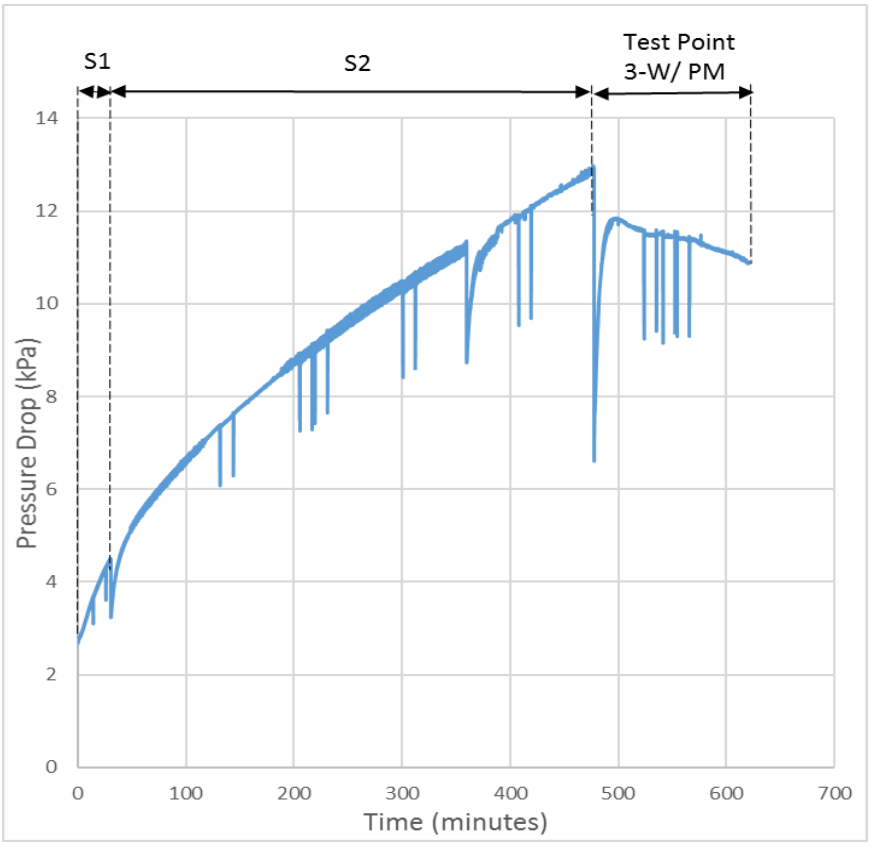

Figure E.10 Pressure drop curve for test point 3 with PM loading 4 g/L in the SCRF®

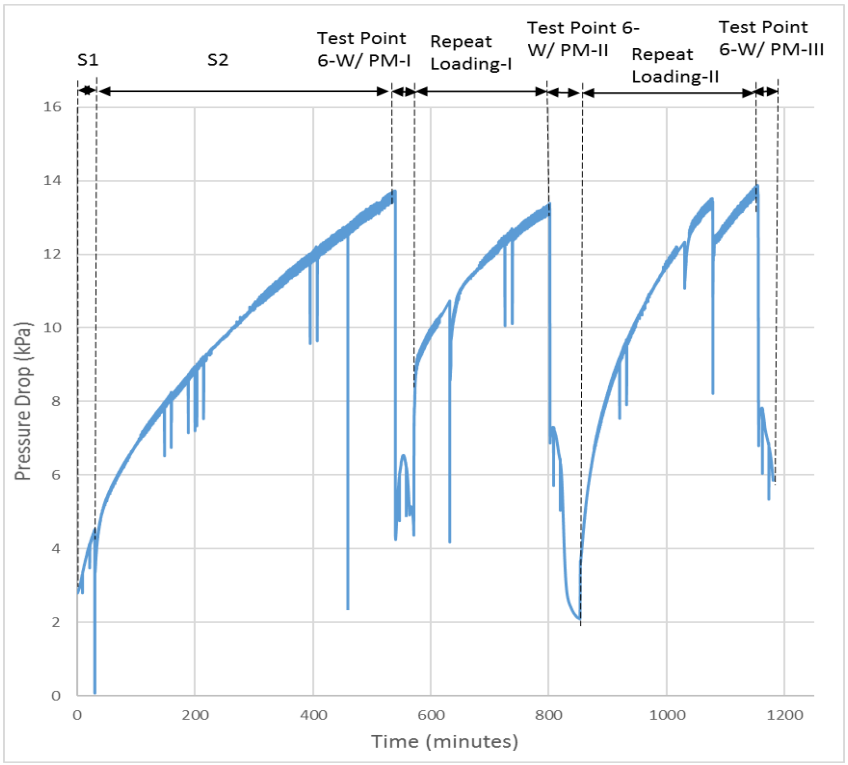

Figure E.11 Pressure drop curve for test point 6 with PM loading 4 g/L in the SCRF®

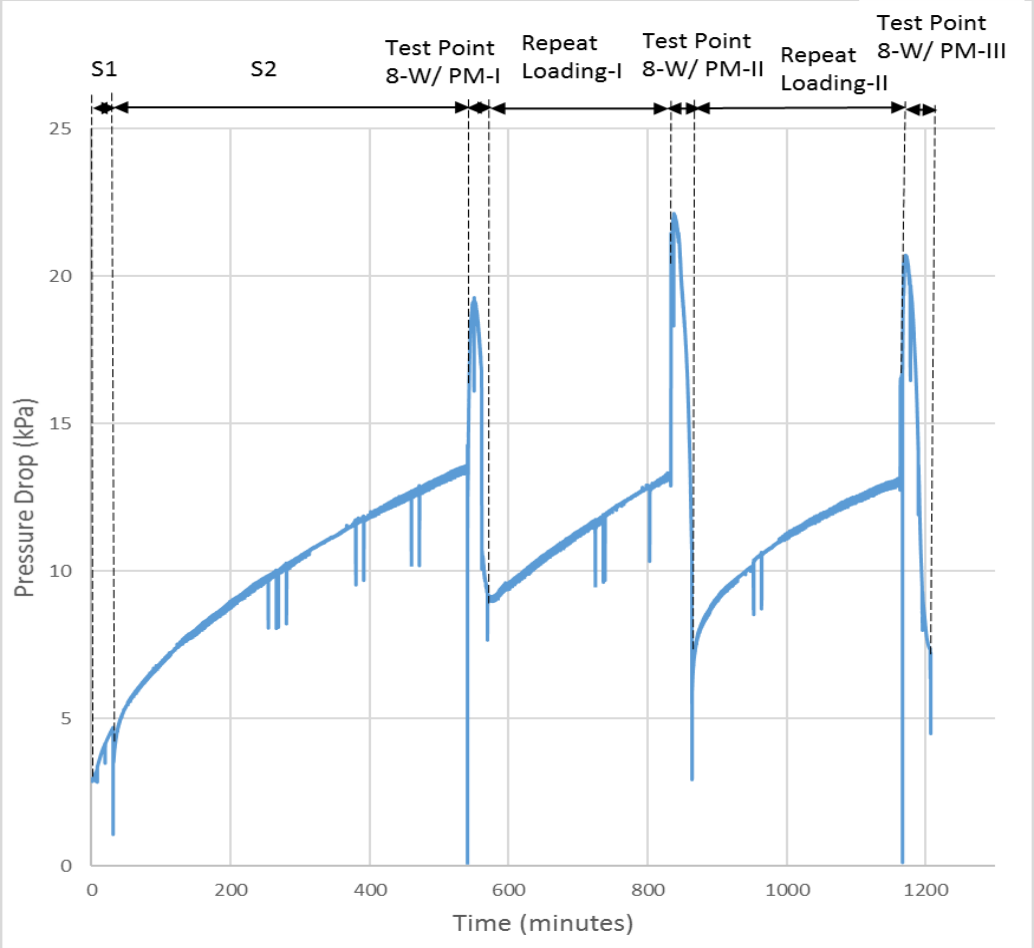

Figure E.12 Pressure drop curve for test point 8 with PM loading 4 g/L in the SCRF®

Appendix F. SCRF® Temperature Distributions

In this appendix, the temperature distribution in the radial and axial positions in the SCRF® is presented. The study of temperature distribution is critical to calibrate the model being developed at MTU. Figure F-1 shows the K-type thermocouple positions in the SCRF® at specific radial and axial locations. The thermocouples were placed to measure gas temperature at four axial locations (at a distance of 32, 152, 207 and 273 mm, from the inlet end of the SCRF®) and five radial locations (at a distance of 0, 55, 95, 122, and 131 mm from the center of the SCRF® block).

The temperature in the SCRF® is monitored at loading and NO_x reduction stages, with or without PM loading in the SCRF®. The 20 thermocouples labeled from S1 to S20 with their axial and radial positions were used to plot the temperature profiles. Thermocouples S1 to S5 and S16 to S20 are located in radial positions at the inlet and outlet of the SCRF® respectively. The radially varying temperature is attributed to external ambient heat transfer from the filter and the axially varying temperature is attributed to PM oxidation in the SCRF® along with heat flow distribution in radial and axial direction.

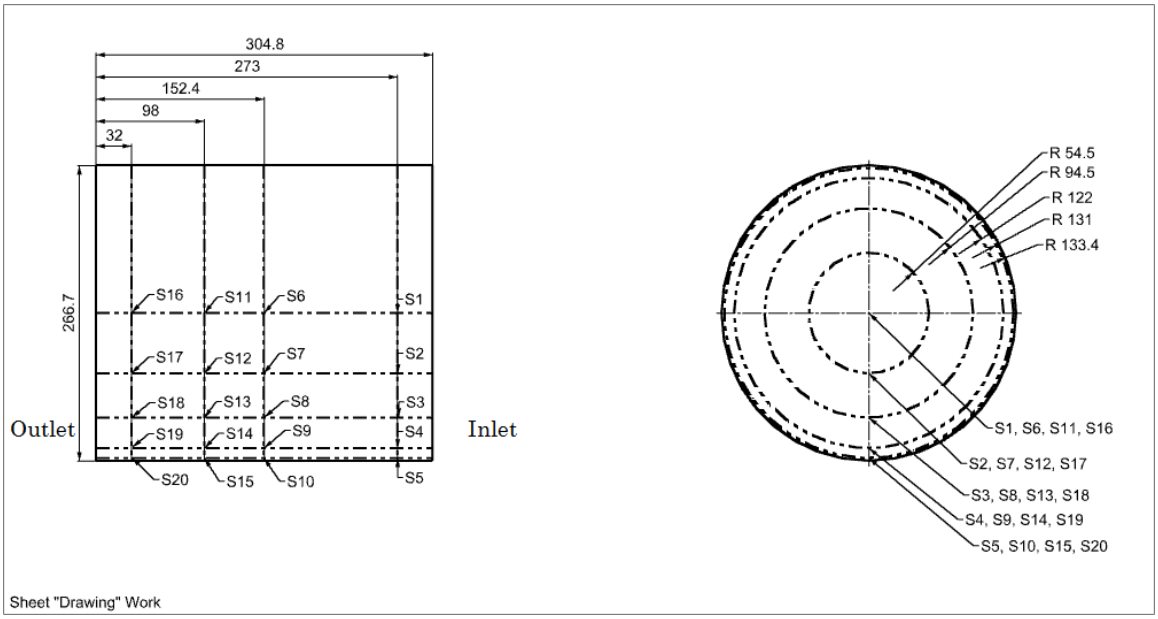

Figure F.1 Thermocouple arrangement for the SCRF® - dimensions in mm

Stage 2 Loading at 2 g/L and 4 g/L

Figures show the temperature boundary layer at the SCRF® inlet and temperature distribution in the complete SCRF® during Stage 2 loading for test point 1, 3, 6, and 8. The time (in hrs.) from the start of experiment at which the temperature distribution is plotted during Stage 2 loading is shown in Tables F.1 and F.2. It is observed from the temperature distribution plots that the temperatures are consistent along the axial locations of the SCRF®. A slight drop in temperature has been observed for 4 g/L tests along the axial position, in Figures F.16, F.17, F.18, and F.19.

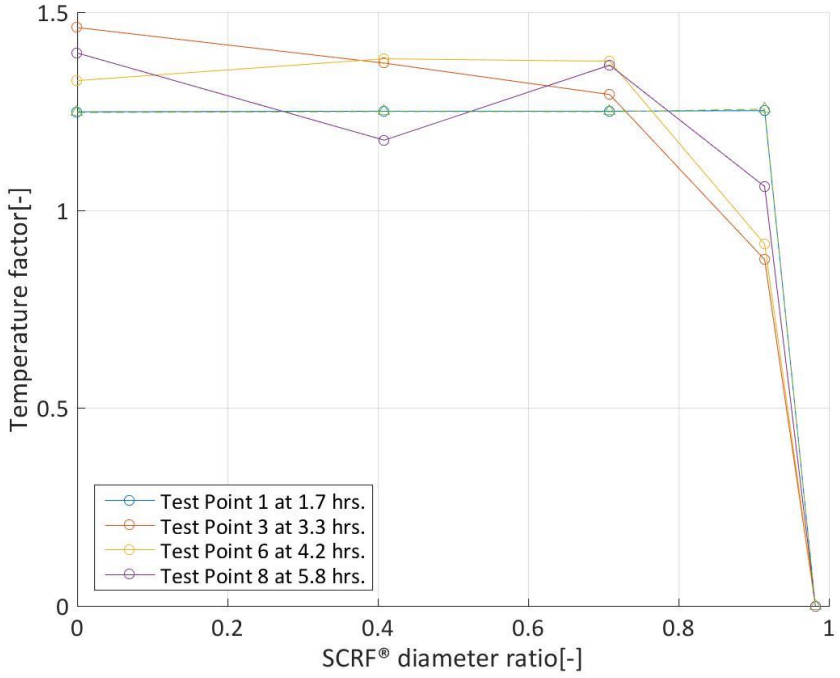

Figure F.2 Temperature boundary layer at SCRF® inlet during Stage 2 loading of 2 g/L.

Table F.1 Thermocouple temperatures at Stage 2 loading at 2 g/L

Stage 2 - 2 g/L	Time [hr.]	SCRF® Thermocouple Temperature [°C]																			
		S1	S2	S3	S4	S5	S6	S7	S8	S9	S10	S11	S12	S13	S14	S15	S16	S17	S18	S19	S20
1	1.7	290[1]	287	287	285	295[1]	289	288	287	283[1]	276	288	288	286	282	268	287	287	287	283	263
3	3.3	282	282	281	279	273[1]	283	282	280	275[1]	269	282	281	280	275	261	281	281	281	277	258
6	4.2	283	283	283	279	272	284	284	283	278[1]	271	283	283[1]	283[1]	277	263	282	283	283	278	262
8	5.8	283	282[1]	283	281	275	285	282	282	280[1]	271	286[1]	283	283	279	263	286	283	283	276	261

Table F.2 Thermocouple temperatures at Stage 2 loading at 4 g/L

Stage 2 - 4 g/L	Time [hr.]	SCRF® Thermocouple Temperature [°C]																			
		S1	S2	S3	S4	S5	S6	S7	S8	S9	S10	S11	S12	S13	S14	S15	S16	S17	S18	S19	S20
1	4.4	300[1]	300	300	297	289	299	300	300	295[1]	291	299	299	298	294[1]	279	300	299	299	292	279
3	5.0	297	296	296	294	287	298	298	298	292[1]	283	297	297	296	291	275	300[1]	297	296	289[1]	276
6	6.6	306[1]	307	305	305	297	306	307	307	302[1]	297	307	307	307[1]	301	287	308[1]	307	307	301	287
8	6.6	308	306[1]	307	305	299	308	307	308	303[1]	291[1]	308	308	308[1]	302	287	308	308[1]	308	302	286

[1] The highlighted thermocouple temperatures have been approximated on the basis of the trend of thermocouple temperatures in other test points.

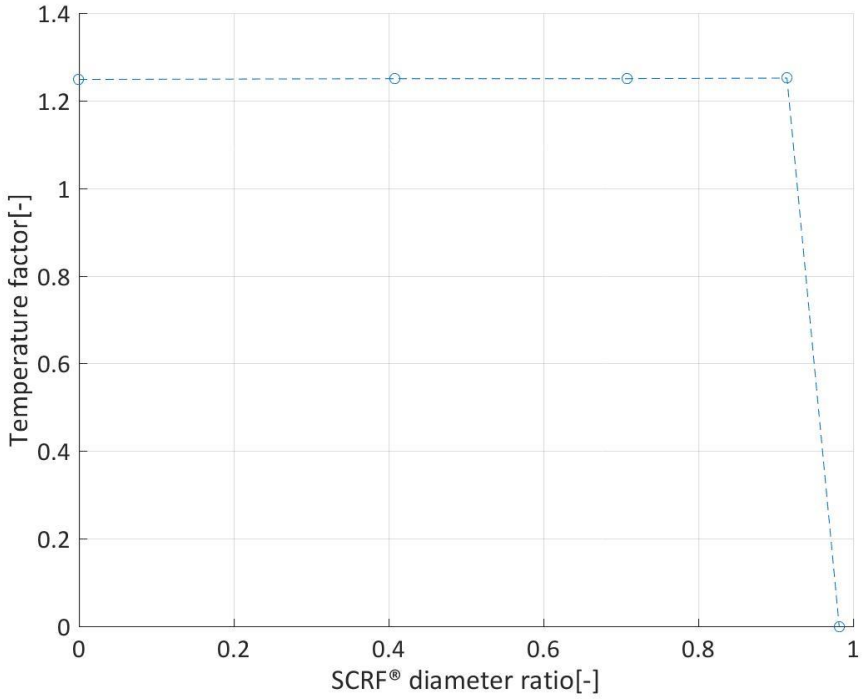

Figure F.3 Temperature boundary layer at SCRF® inlet at 1.7 hrs. for test point 1 during Stage 2 loading of 2 g/L

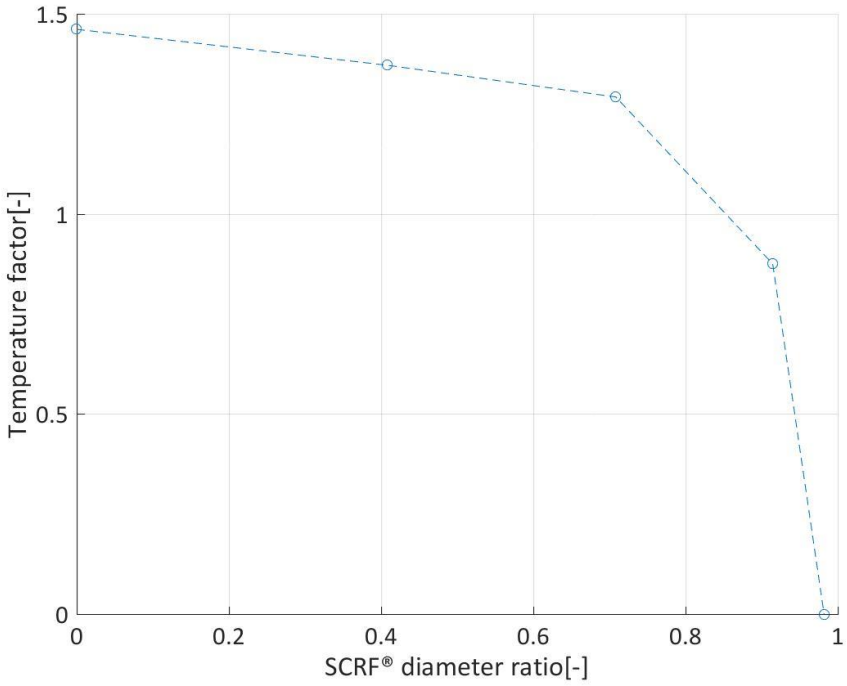

Figure F.4 Temperature boundary layer at SCRF® inlet at 3.3 hrs. for test point 3 during Stage 2 loading of 2 g/L

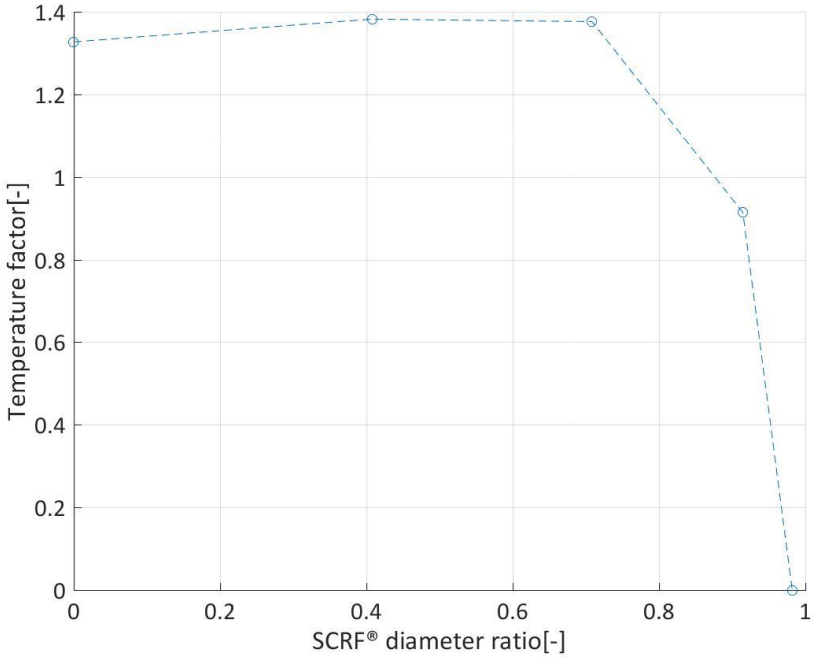

Figure F.5 Temperature boundary layer at SCRF® inlet at 4.2 hrs. for test point 6 during Stage 2 loading of 2 g/L

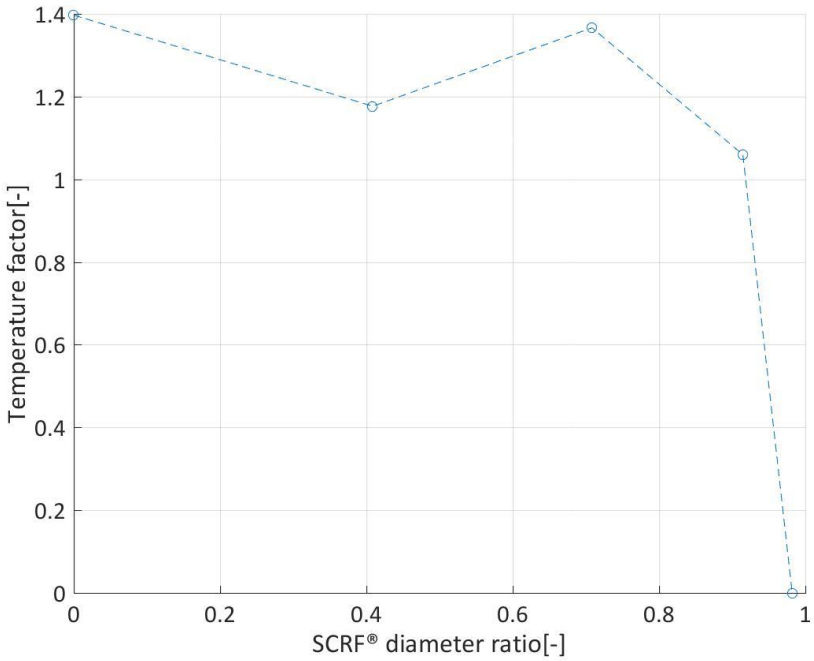

Figure F.6 Temperature boundary layer at SCRF® inlet at 5.8 hrs. for test point 8 during Stage 2 loading of 2 g/L

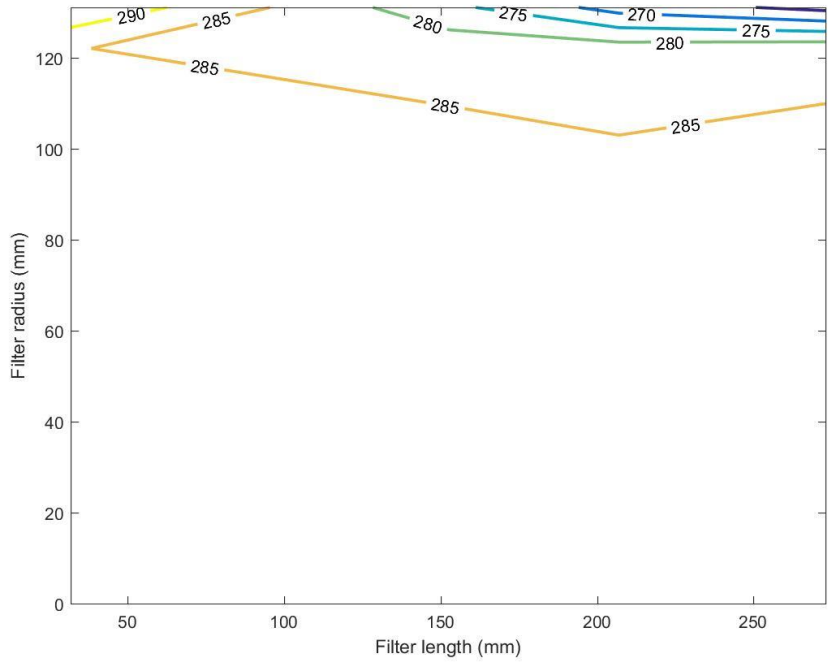

Figure F.7 Temperature distribution in the SCRF® for test point 1 at 1.7 hrs. during Stage 2 loading of 2 g/L

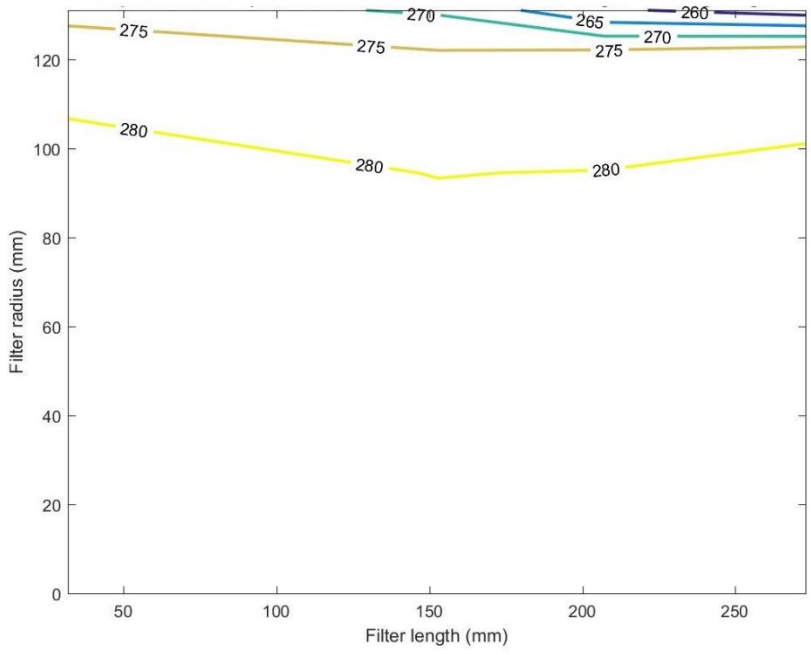

Figure F.8 Temperature distribution in the SCRF® for test point 3 at 3.3 hrs. during Stage 2 loading at 2 g/L

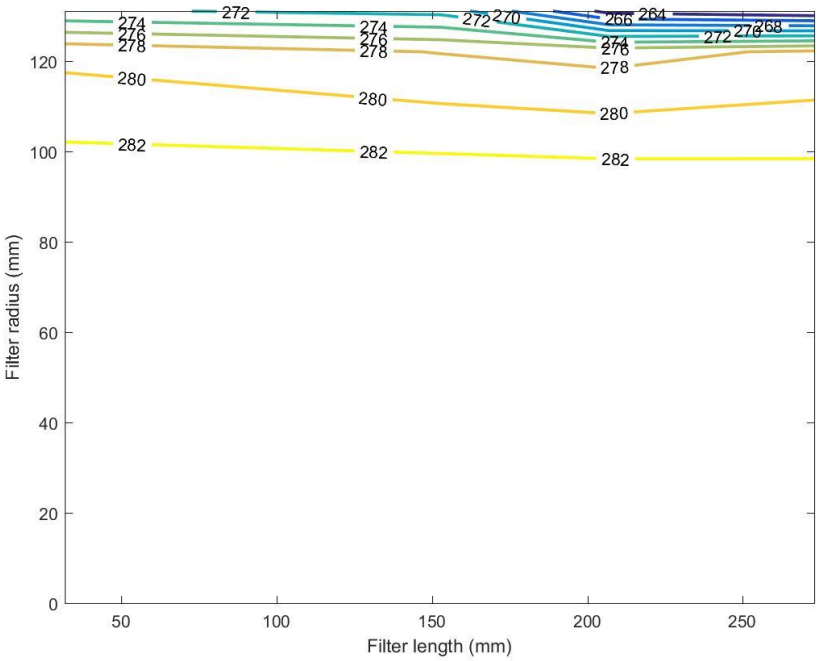

Figure F.9 Temperature distribution in the SCRF® for test point 6 at 4.2 hrs. during Stage 2 loading at 2 g/L

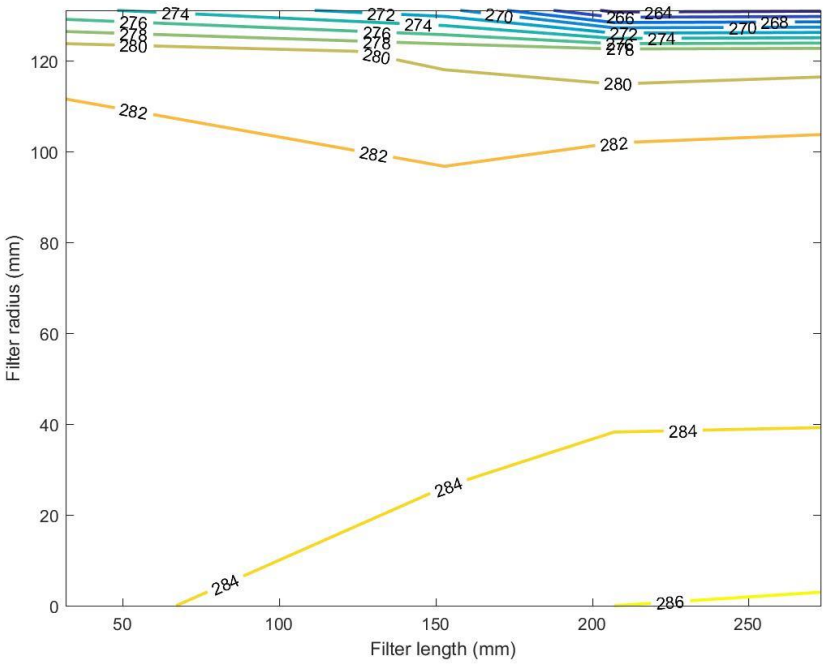

Figure F.10 Temperature distribution in the SCRF® for test point 8 at 5.8 hrs. during Stage 2 loading at 2 g/L

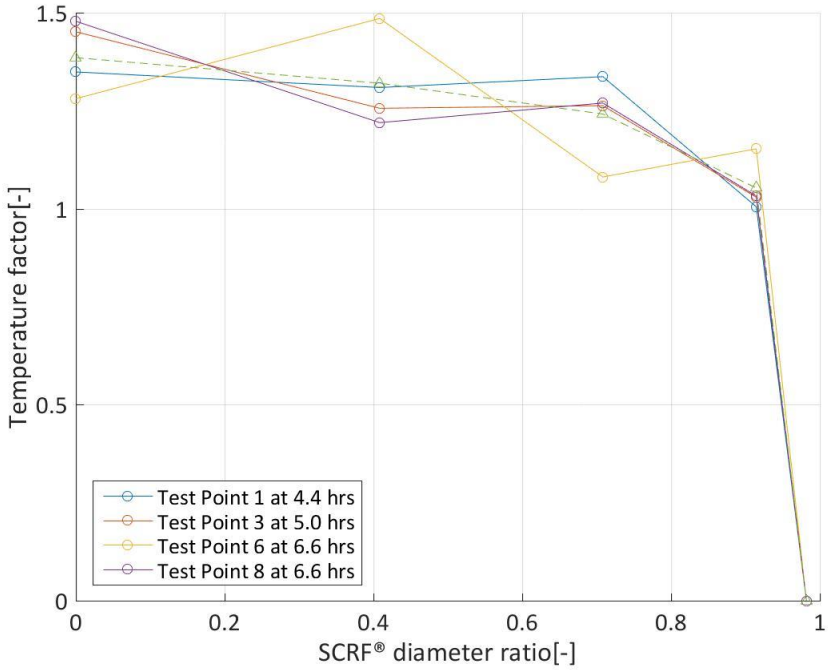

Figure F.11 Temperature boundary layer at SCRF® inlet for Stage 2 loading at 4 g/L

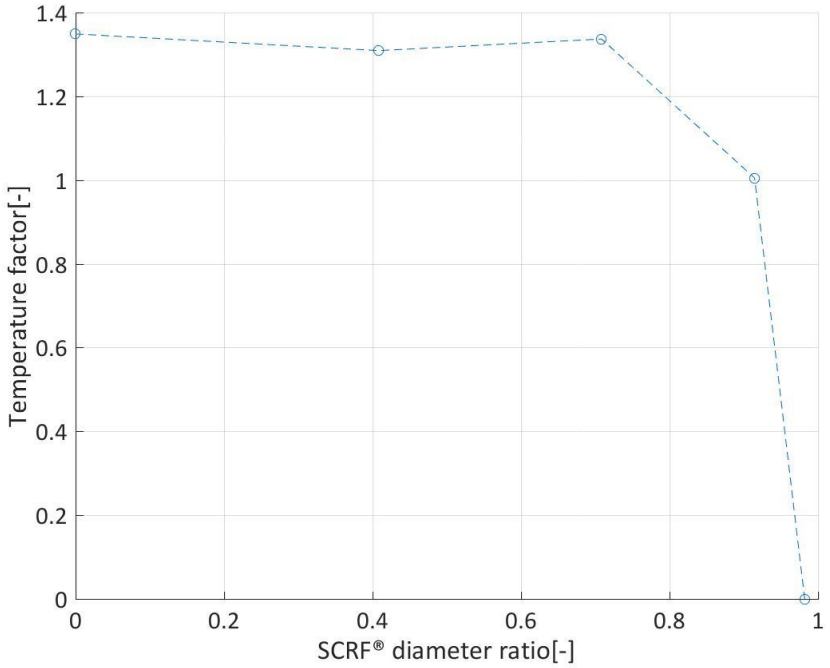

Figure F.12 Temperature distribution at SCRF® inlet for test point 1 at 4.4 hrs. during Stage 2 loading at 4 g/L

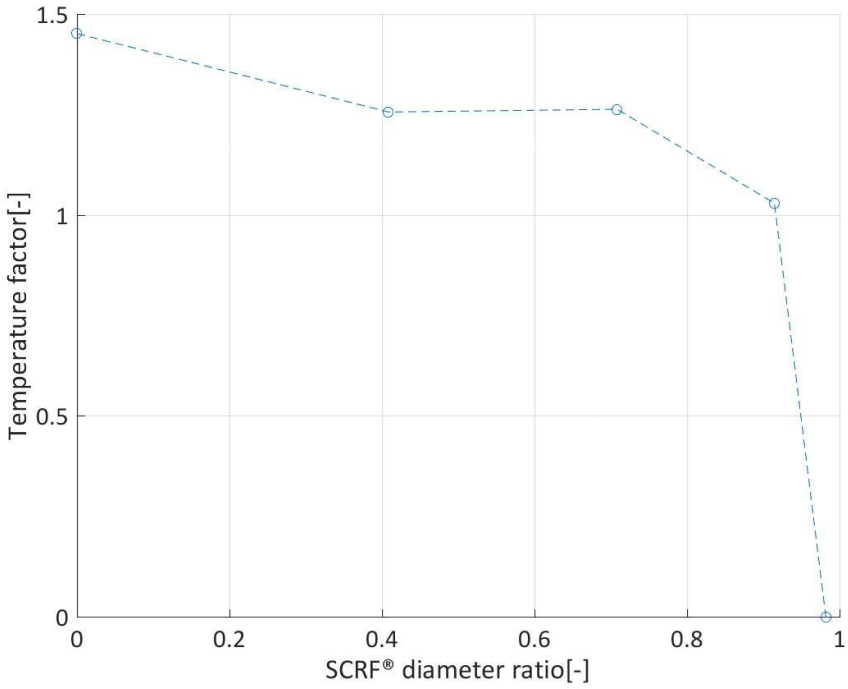

Figure F.13 Temperature distribution at SCRF® inlet for test point 3 at 5.0 hrs. during Stage 2 loading at 4 g/L

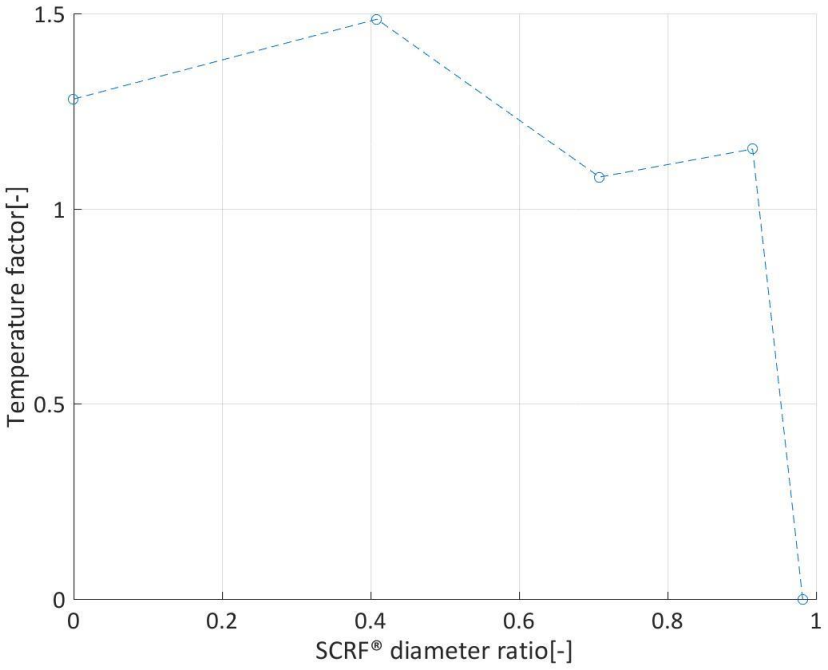

Figure F.14 Temperature distribution at SCRF® inlet for test point 6 at 6.6 hrs. during Stage 2 loading at 4 g/L

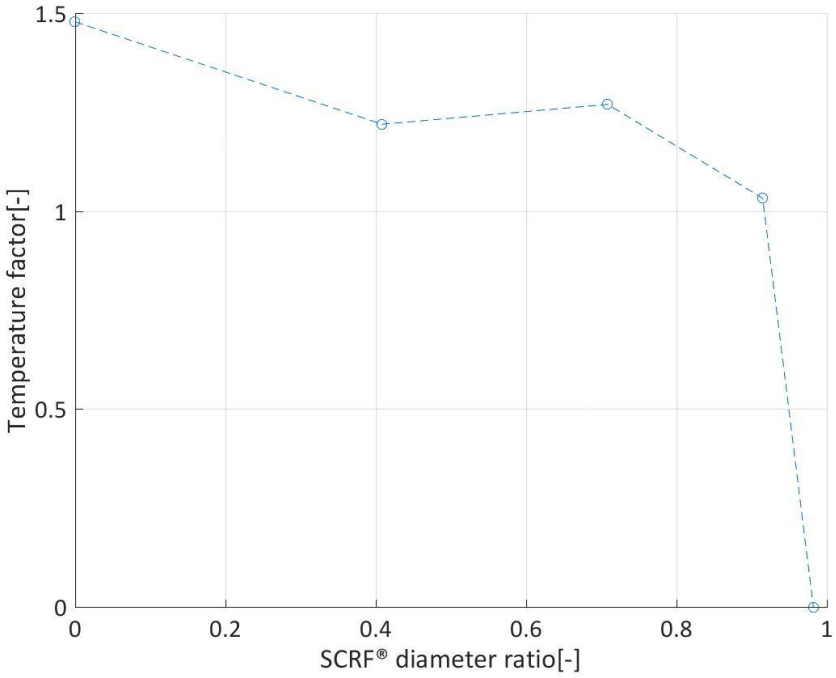

Figure F.15 Temperature distribution at SCRF® inlet for test point 8 at 6.6 hrs. during Stage 2 loading at 4 g/L

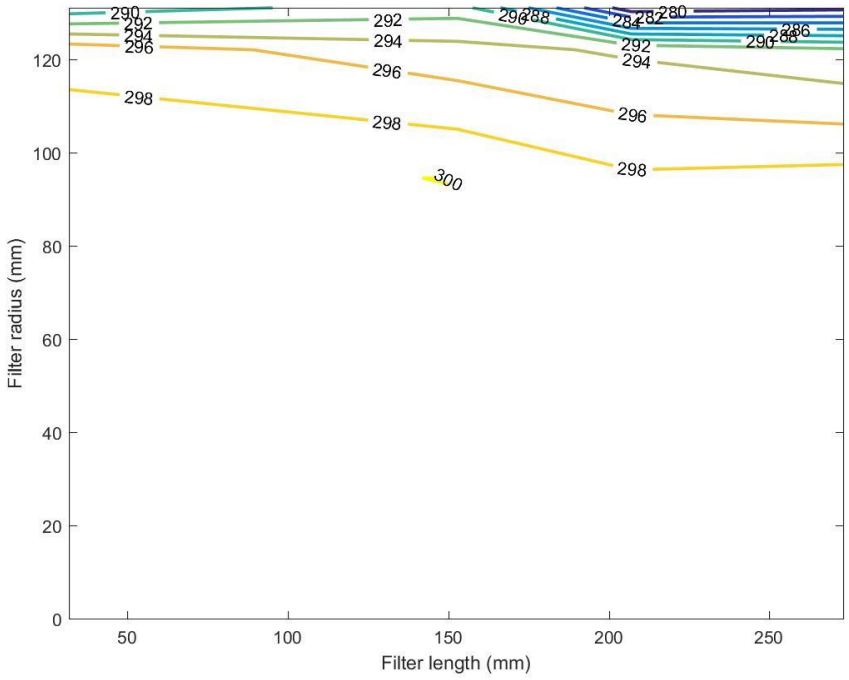

Figure F.16 Temperature distribution in the SCRF® for test point 1 at 4.4 hrs. during Stage 2 loading at 4 g/L

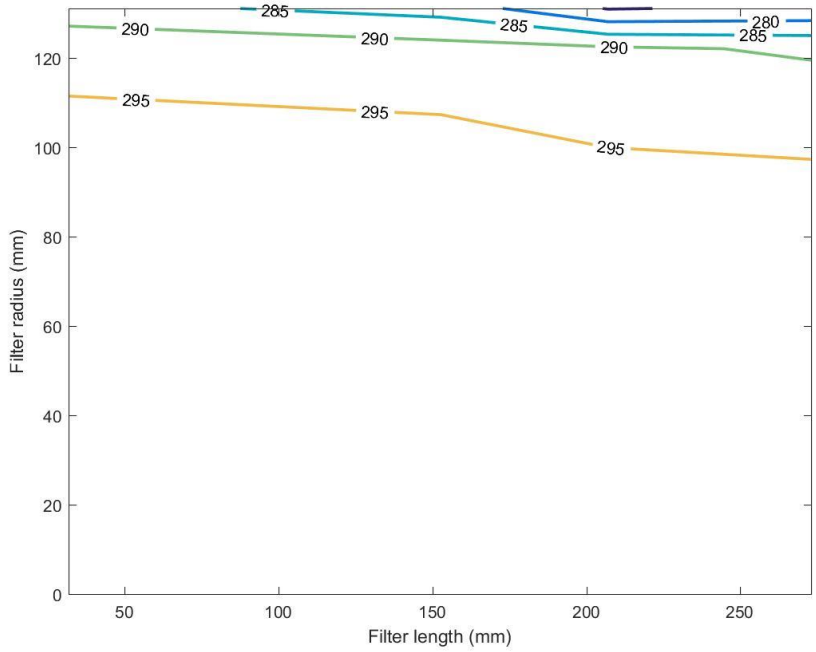

Figure F.17 Temperature distribution in the SCRF® for test point 3 at 5.0 hrs. during Stage 2 loading at 4 g/L

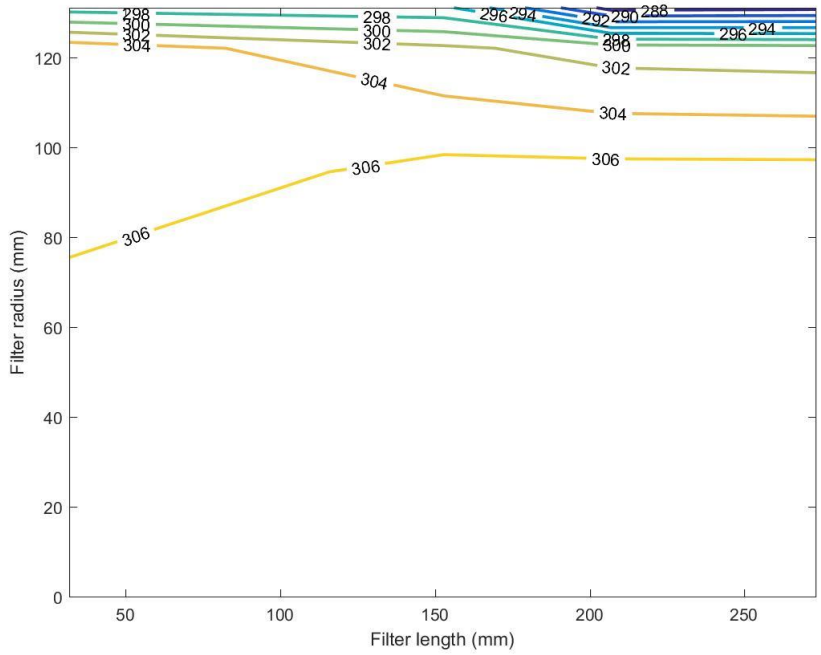

Figure F.18 Temperature distribution in the SCRF® for test point 6 at 6.6 hrs. during Stage 2 loading at 4 g/L

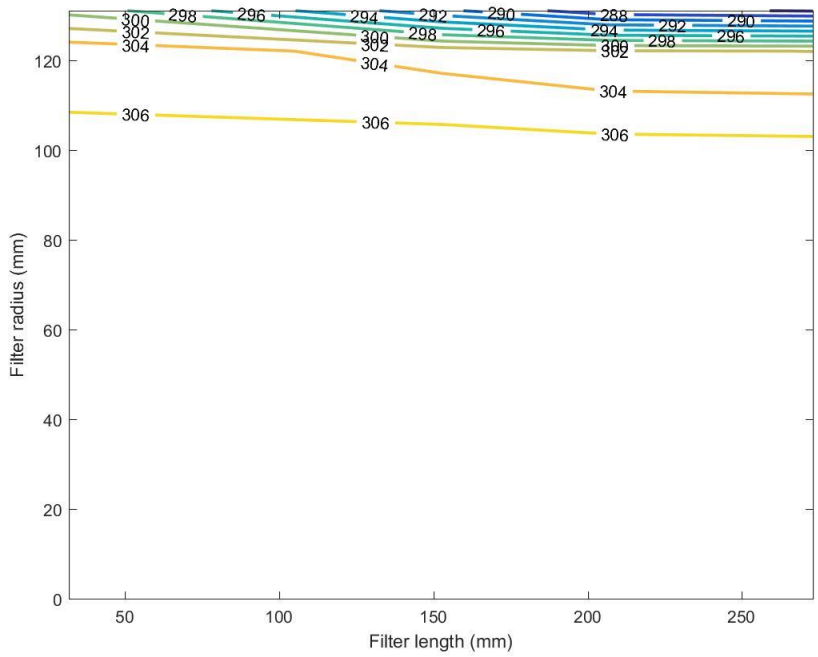

Figure F.19 Temperature distribution in the SCRF® for test point 8 at 6.6 hrs. during Stage 2 loading at 4 g/L

NO_x Reduction Stage

Figures in this section show the temperature distribution in the axial and radial position of the SCRF® for different NOx Reduction test points when dosed with ANR – 1. The temperature reading were considered for the time at the end of ANR – 1 dosing cycle to get stabilized temperature values. The plots of temperature boundary at the inlet of the SCRF® show the radially decreasing temperature for all tests of NO_x reduction stage. The temperature profiles depict axially increasing temperatures across the SCRF® as can be seen in figures for different loading condition. This can be attributed to the PM oxidation in PM loaded SCRF® at respective temperatures. It is shown in Figures F.27, F.36, and F.45, that for test point 6 with 0, 2, and 4 g/L PM loading in the SCRF® with urea dosing, the axial temperatures gradient across the SCRF® is high as compared to other test points. The time at which temperature boundary at inlet SCRF® and temperature distribution in the SCRF® is plotted is given in Figures F.3, F.4, and F.5.

Loading at 0 g/L

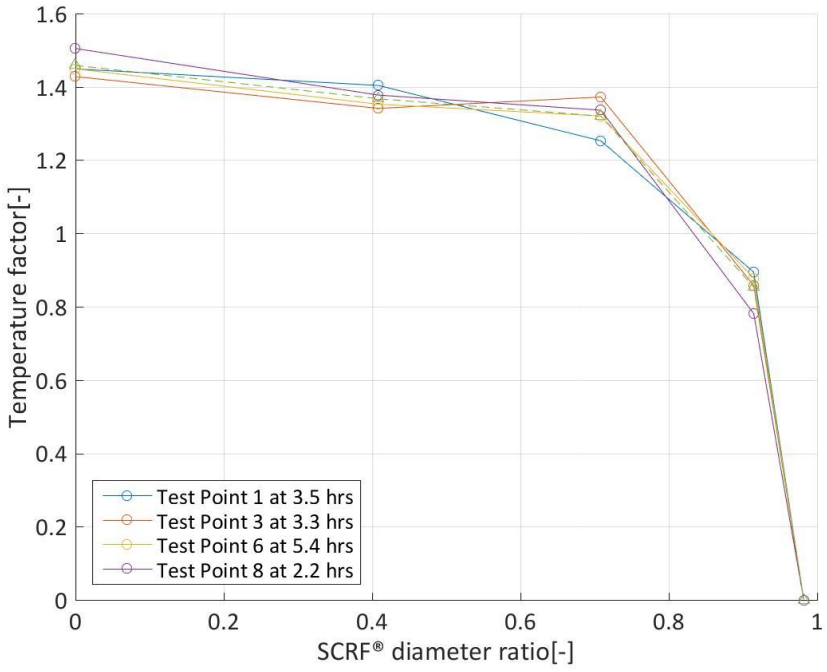

Figure F.20 Temperature boundary layer at SCRF® inlet for NO_x Reduction Stage (loading at 0 g/L)

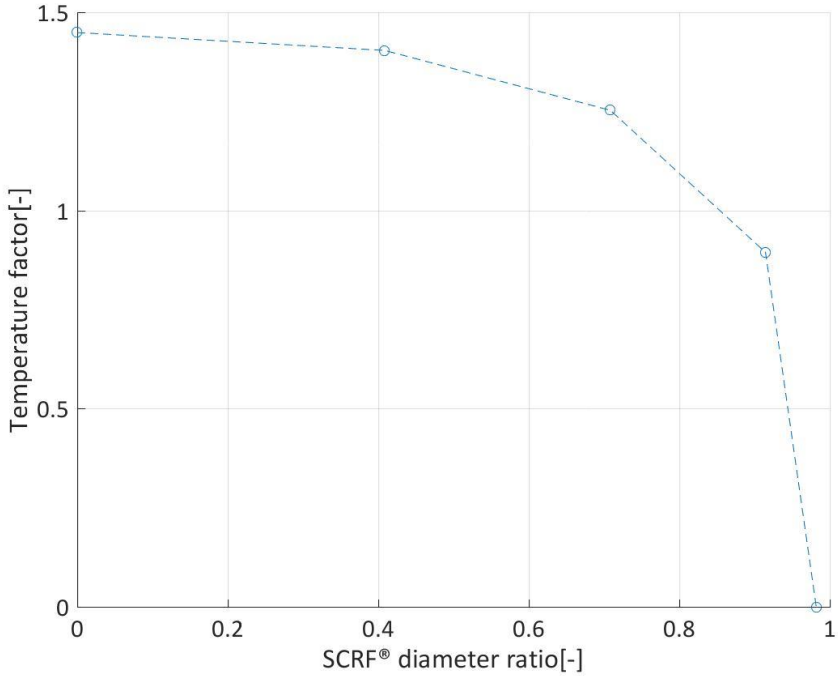

Figure F.21 Temperature distribution at SCRF® inlet for test point 1 at 3.5 hrs. during NO_x Reduction Stage (loading at 0 g/L)

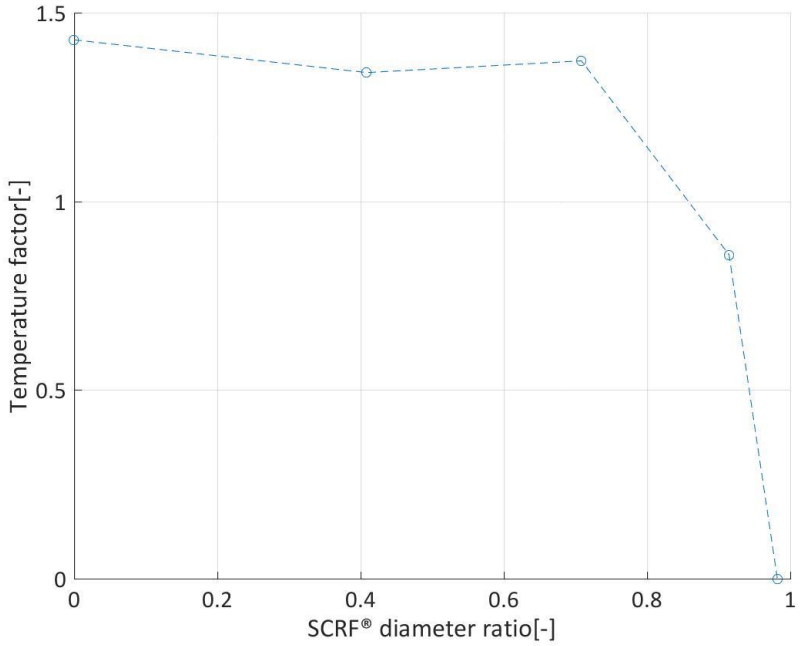

Figure F.22 Temperature distribution at SCRF® inlet for test point 3 at 3.3 hrs. during NO_x Reduction Stage (loading at 0 g/L)

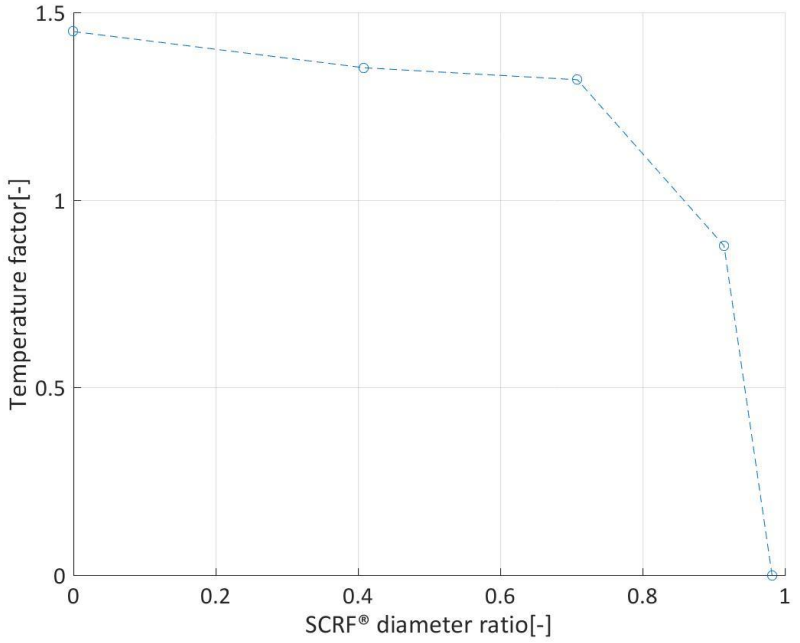

Figure F.23 Temperature distribution at SCRF® inlet for test point 6 at 5.4 hrs. during NO_x Reduction Stage (loading at 0 g/L)

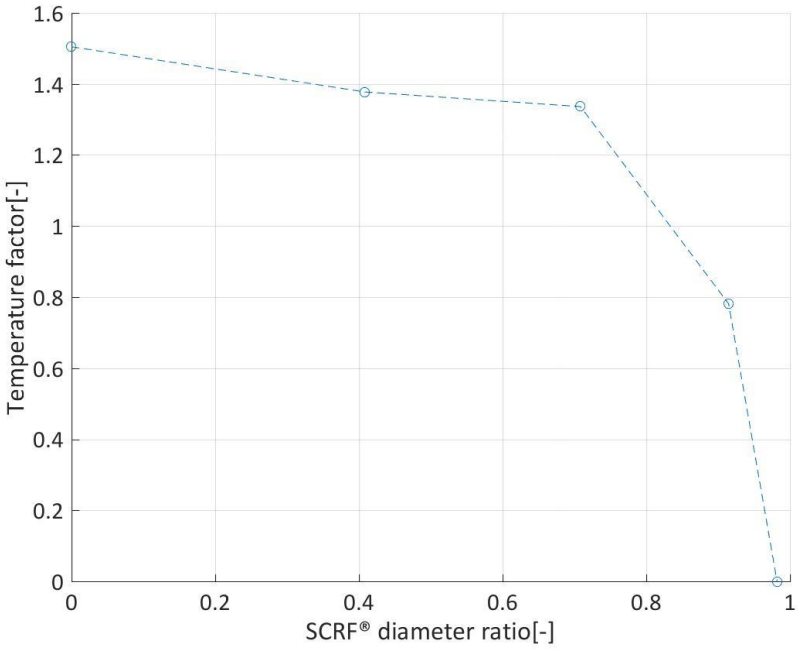

Figure F.24 Temperature distribution at SCRF® inlet for test point 8 at 2.2 hrs. during NO_x Reduction Stage (loading at 0 g/L)

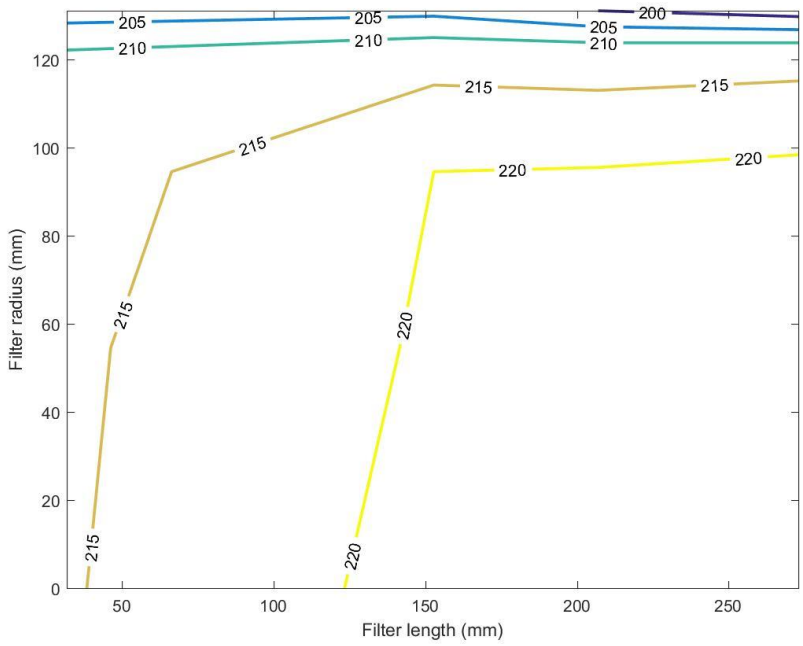

Figure F.25 Temperature distribution in the SCRF® for test point 1 at 3.5 hrs. during NO_x Reduction Stage (loading at 0 g/L)

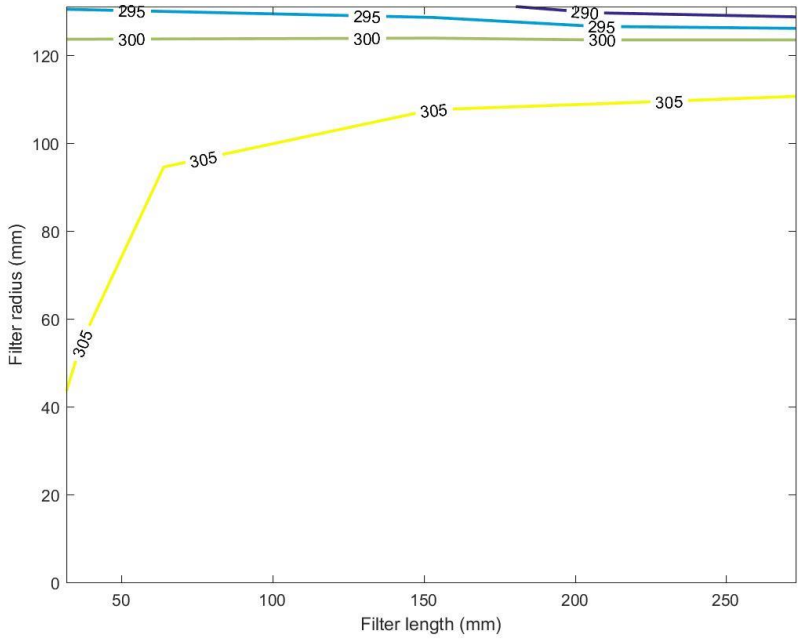

Figure F.26 Temperature distribution in the SCRF® for test point 3 at 3.3 hrs. during NO_x Reduction Stage (loading at 0 g/L)

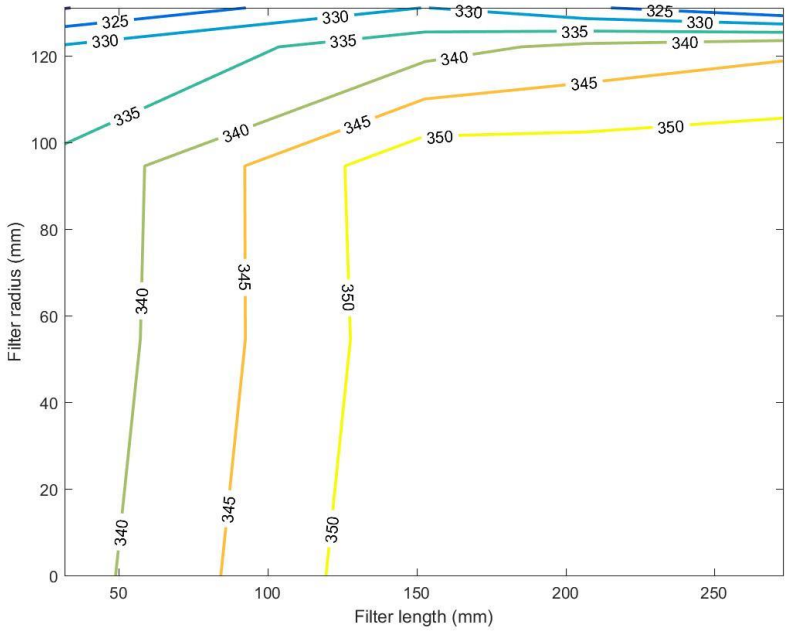

Figure F.27 Temperature distribution in the SCRF® for test point 6 at 5.4 hrs. during NO_x Reduction Stage (loading at 0 g/L)

Table F.3 Thermocouple temperatures at NO_x reduction stage at 0 g/L

NOx Reduction Stage - 0 g/L	Time [hr.]	SCRF® Thermocouple Temperature [°C]																		
		S1	S2	S3	S4	S5	S6	S7	S8	S9	S10	S11	S12	S13	S14	S15	S16	S17	S18	S19	S20
1	3.5	215	214	213[1]	210	203	222	221	220[1]	213[1]	204	222	221	220	212	200[1]	222	222	221	213	198
3	3.3	306	305	305	301	295	310	308	308	302[1]	292	309	308	308	302[1]	288	308	308[1]	308[1]	303	286
6	5.4	338	336	336[1]	331	320	355	354	354[1]	338[1]	330	355	354	353	341	326[1]	355	355	354	344	320
8	2.2	444	442	442[1]	437	430	451	448	448[1]	439[1]	430	450	449	449	440	426[1]	449	449	449	443	422

[1]The highlighted thermocouple temperature have been approximated on the basis of the trend of thermocouple temperatures in other test points.

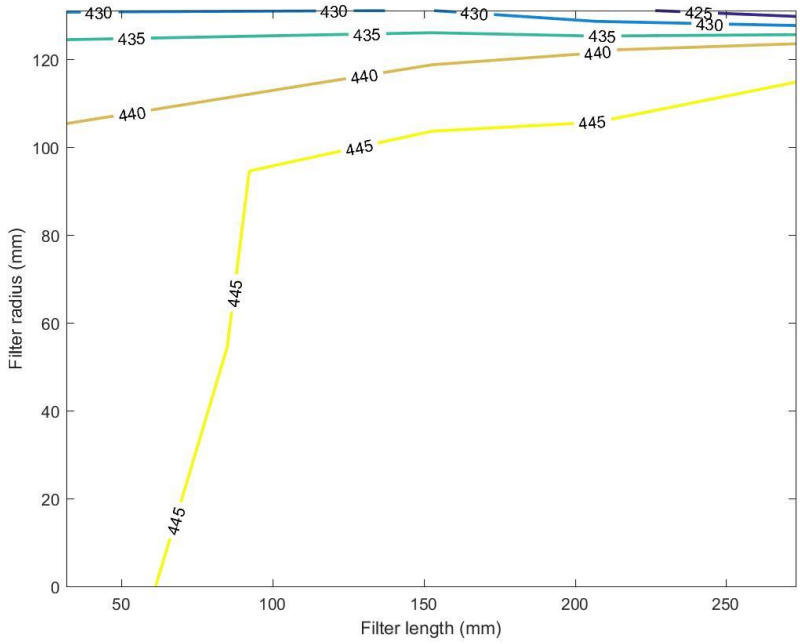

Figure F.28 Temperature distribution in the SCRF® for test point 8 at 2.2 hrs. during NO_x Reduction Stage (loading at 0 g/L)

Loading at 2 g/L

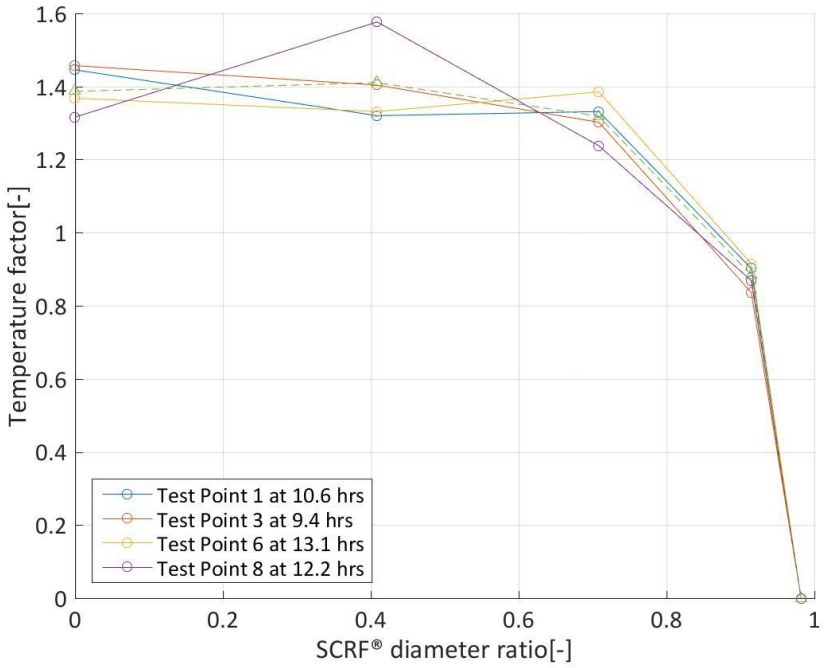

Figure F.29 Temperature boundary layer at SCRF® inlet for NO_x Reduction Stage (loading at 2 g/L)

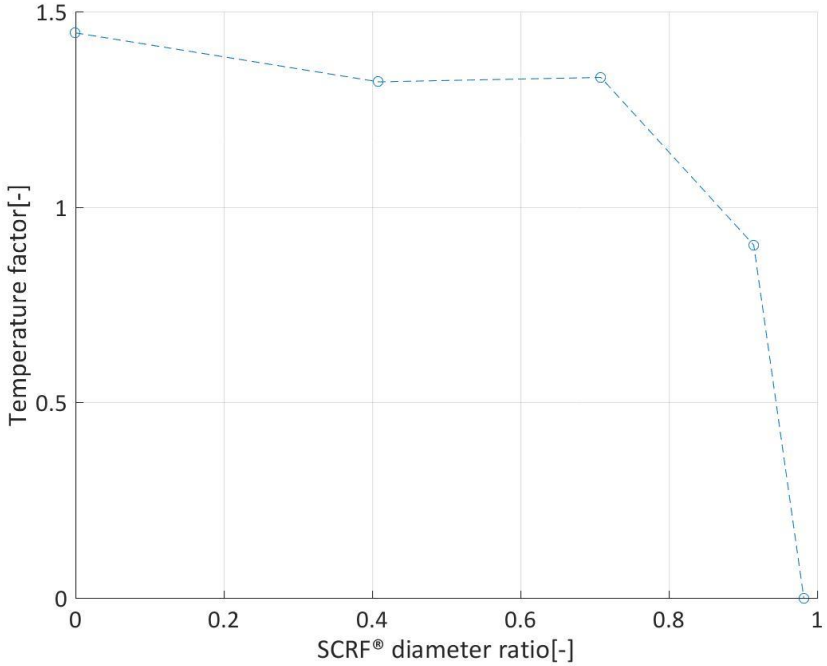

Figure F.30 Temperature distribution at SCRF® inlet for test point 1 at 10.6 hrs. during NO_x Reduction Stage (loading at 2 g/L)

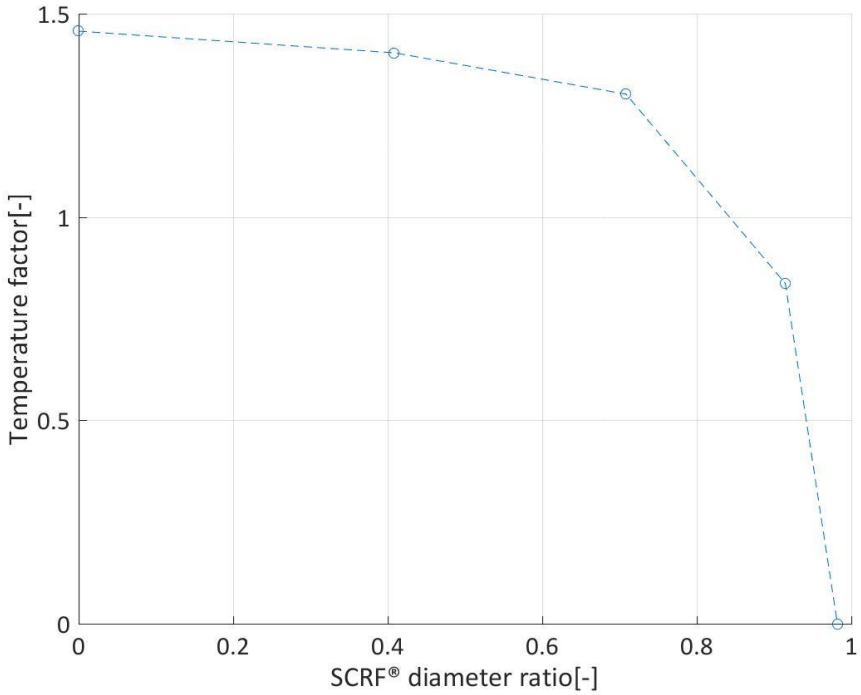

Figure F.31Temperature distribution at SCRF® inlet for test point 3 at 9.4 hrs. during NO_x Reduction Stage (loading at 2 g/L)

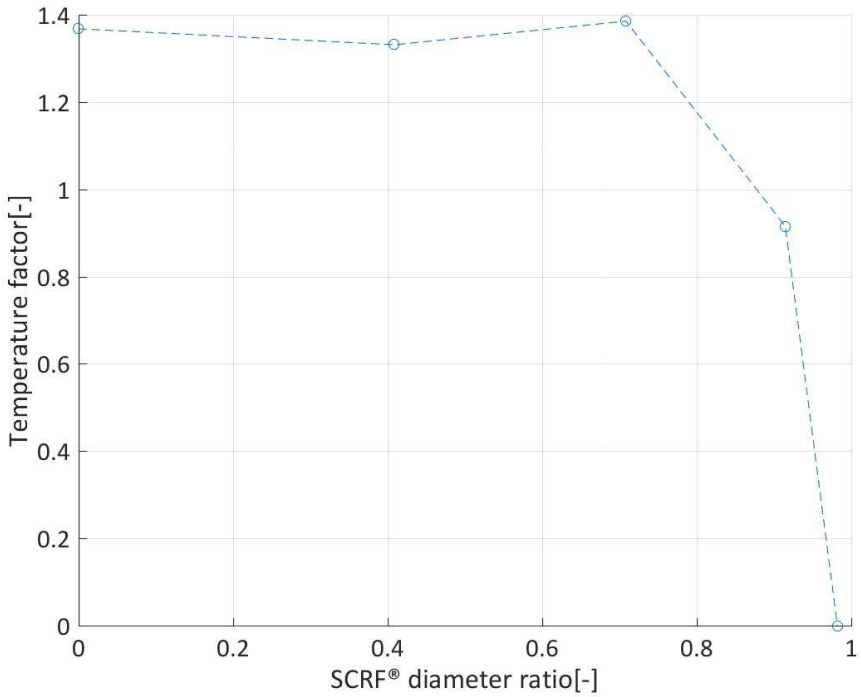

Figure F.32 Temperature distribution at SCRF® inlet for test point 6 at 13.1 hrs. during NO_x Reduction Stage (loading at 2 g/L)

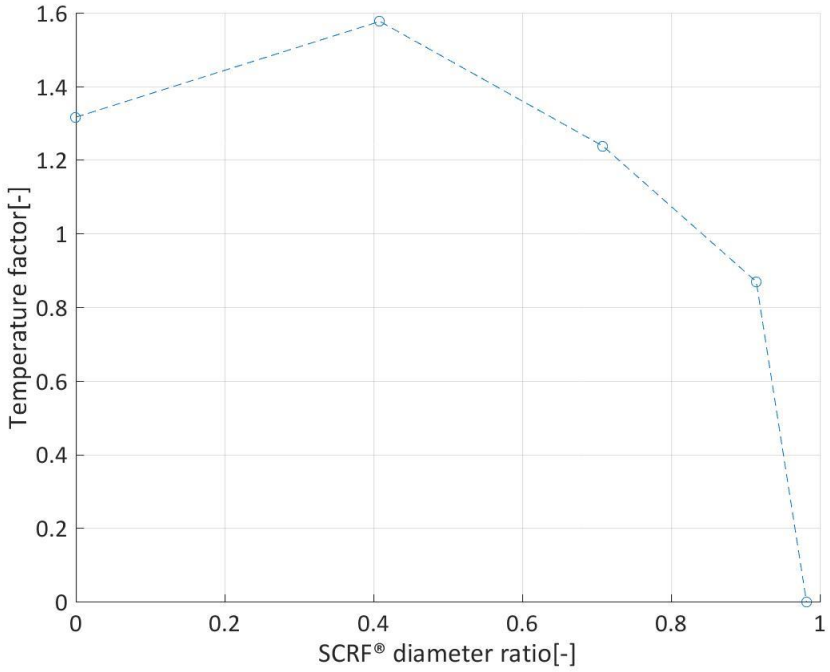

Figure F.33 Temperature distribution at SCRF® inlet for test point 8 at 12.2 hrs. during NO_x Reduction Stage (loading at 2 g/L)

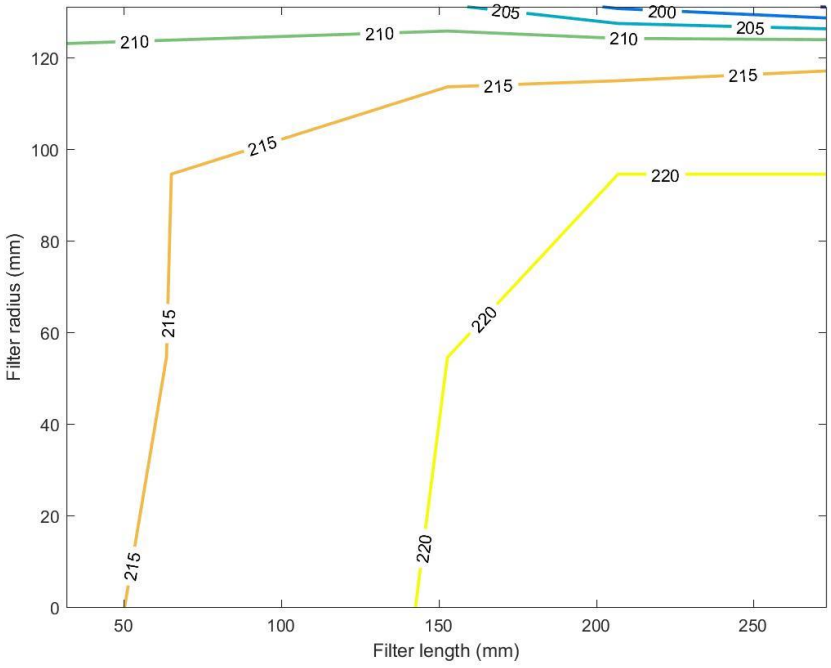

Figure F.34 Temperature distribution in the SCRF® for test point 1 at 10.6 hrs. during NO_x Reduction Stage (loading at 2 g/L)

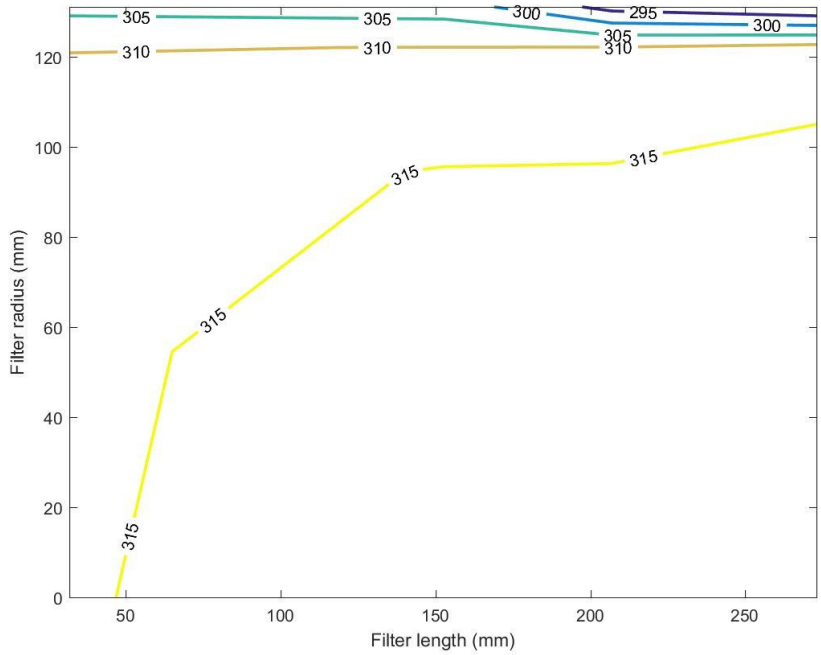

Figure F.35 Temperature distribution in the SCRF® for test point 3 at 9.4 hrs. during NO_x Reduction Stage (loading at 2 g/L)

Table F.4 Thermocouple temperatures at NO_x reduction stage at 2 g/L

NOx Reduction Stage - 2 g/L	Time [hr.]	SCRF® Thermocouple Temperature [°C]																			
		S1	S2	S3	S4	S5	S6	S7	S8	S9	S10	S11	S12	S13	S14	S15	S16	S17	S18	S19	S20
1	10.6	214[1]	213	213	211	205[1]	221	220[1]	220	213[1]	206	220	220	220	213	199	221[1]	221[1]	220	214	195
3	9.4	314	314	313	310	304	319	317	315	310[1]	303	318	318	315	310	293	317	318	317	312	290
6	13.1	344	344	345	339[1]	328[1]	360	360	360	350[1]	337	361	361	360	348	325	362	361	361	350	323
8	12.2	441	444[1]	441	437	429	447	446	445	440[1]	430	445	446	446	441	418	447	447	448[1]	442	422

[1]The highlighted thermocouple temperatures have been approximated on the basis of the trend of thermocouple temperatures in other test points.

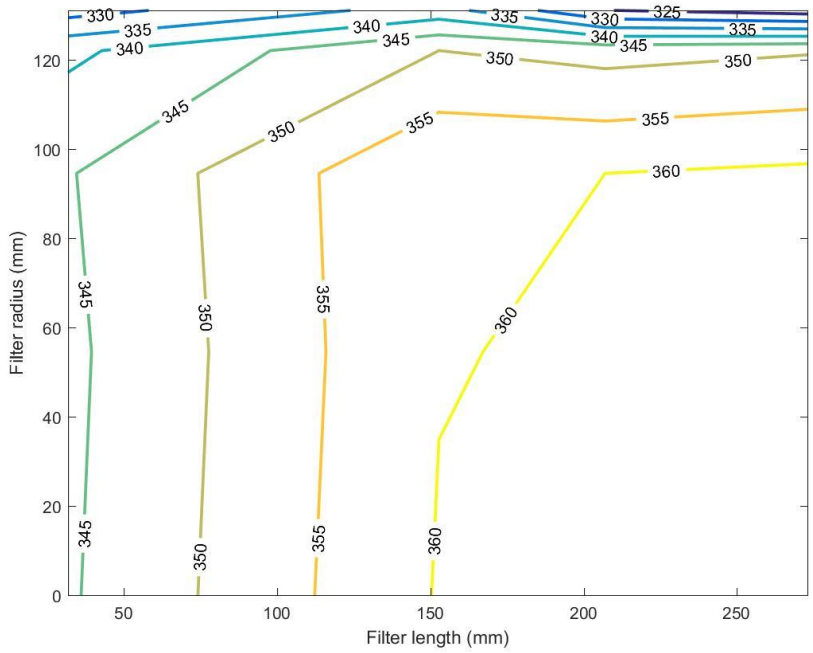

Figure F.36 Temperature distribution in the SCRF® for test point 6 at 13.1 hrs. during NO_x Reduction Stage (loading at 2 g/L)

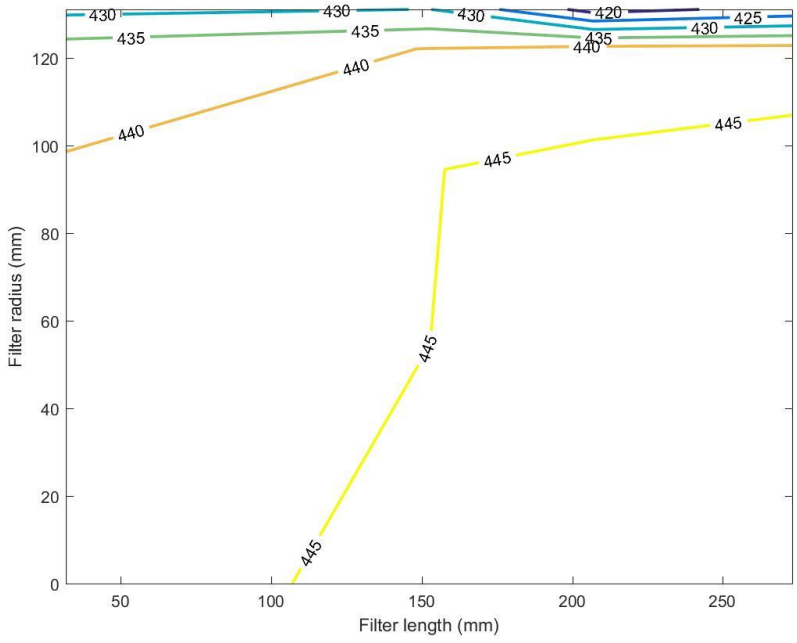

Figure F.37 Temperature distribution in the SCRF® for test point 8 at 12.2 hrs. during NO_x Reduction Stage (loading at 2 g/L)

Loading at 4 g/L

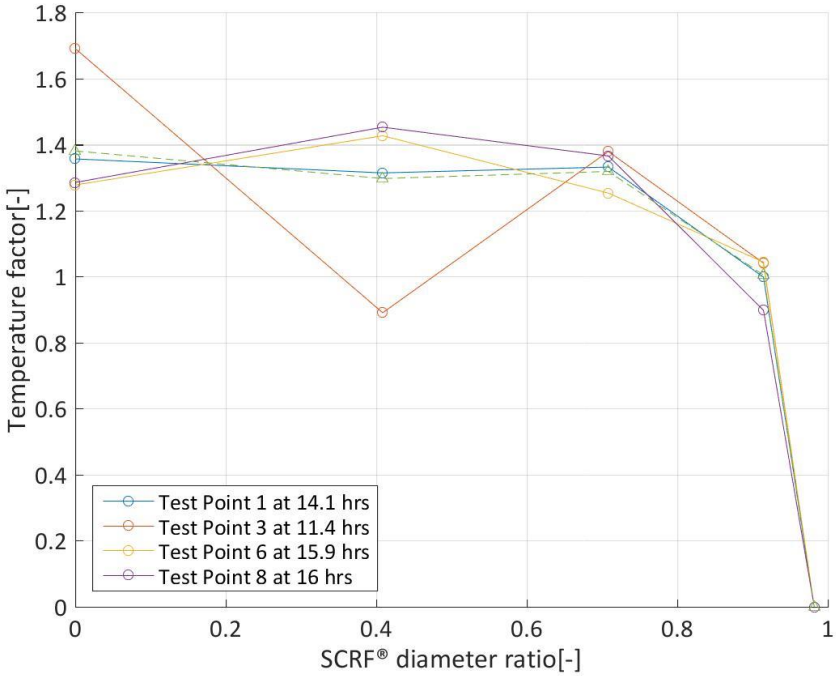

Figure F.38 Temperature boundary layer at SCRF® inlet for NO_x Reduction Stage (loading at 4 g/L)

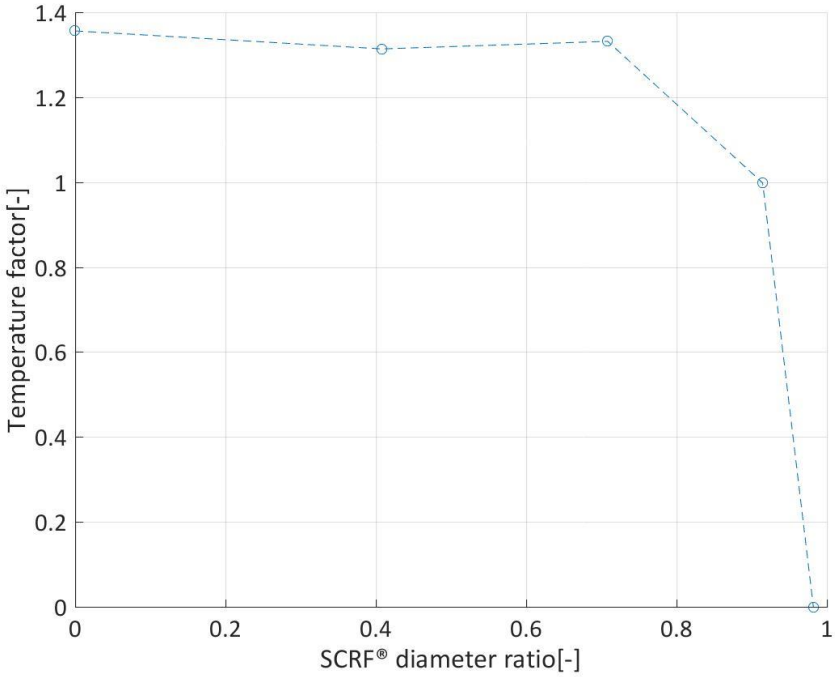

Figure F.39 Temperature distribution at SCRF® inlet for test point 1 at 14.1 hrs. during NO_x Reduction Stage (loading at 4 g/L)

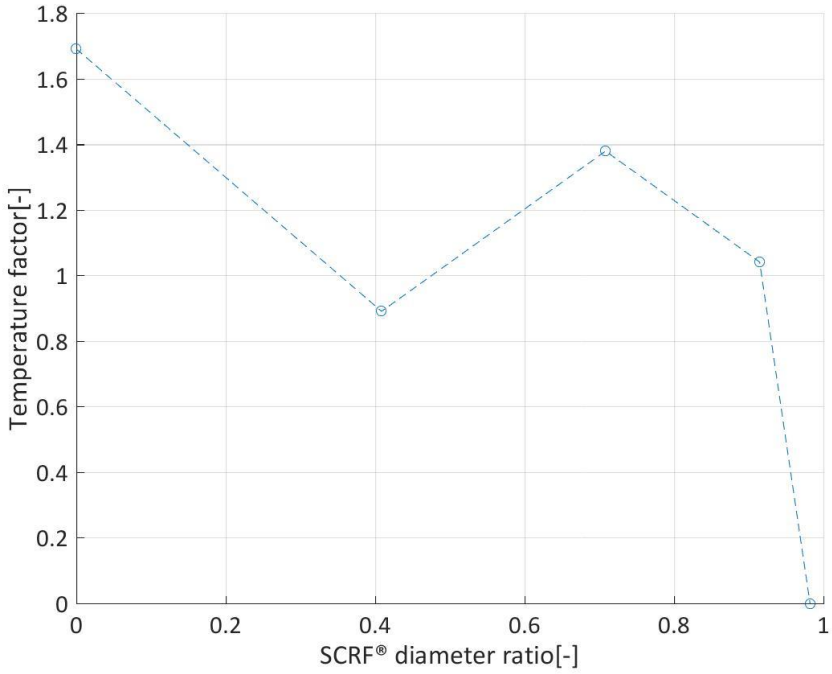

Figure F.40 Temperature distribution at SCRF® inlet for test point 3 at 11.4 hrs. during NO_x Reduction Stage (loading at 4 g/L)

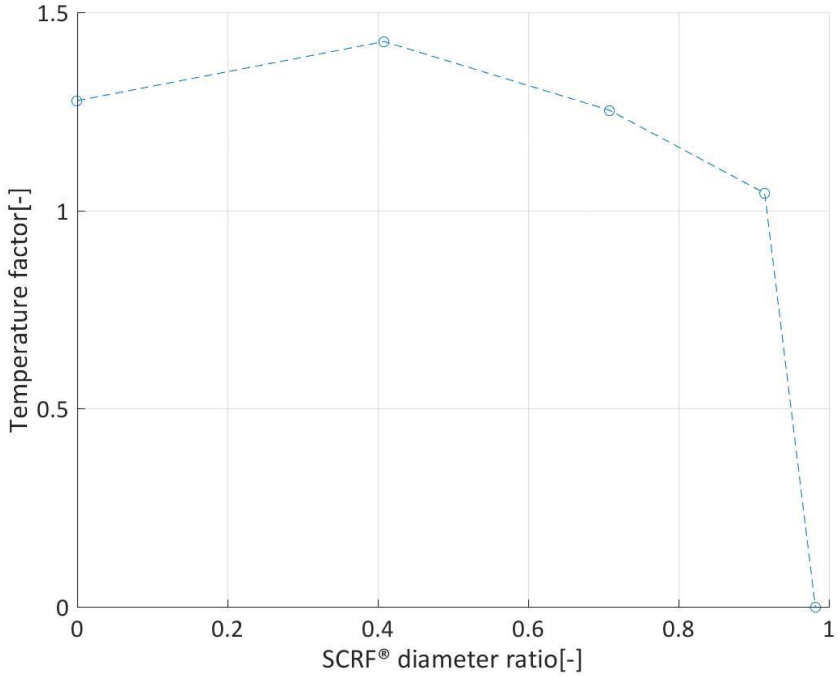

Figure F.41Temperature distribution at SCRF® inlet for test point 6 at 15.9 hrs. during NO_x Reduction Stage (loading at 4 g/L)

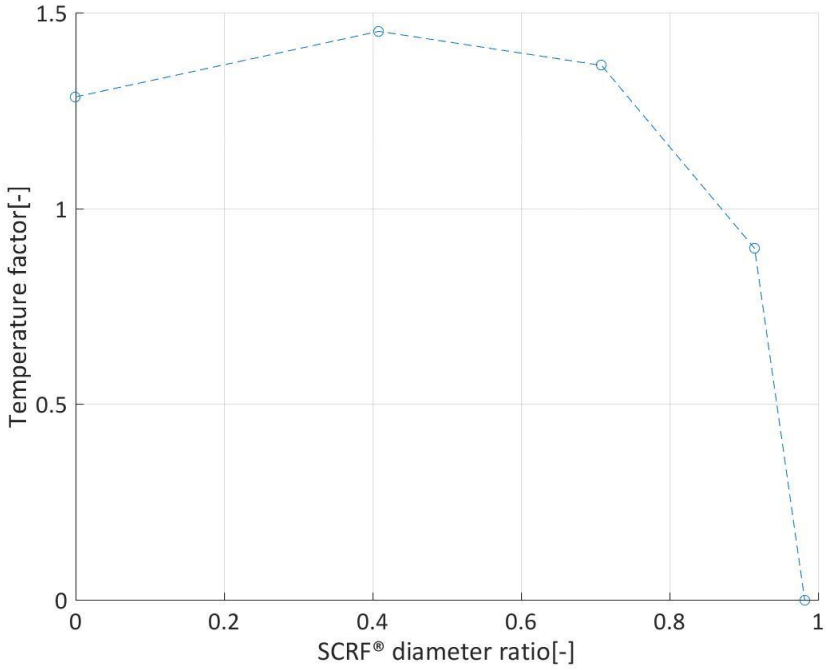

Figure F.42 Temperature distribution at SCRF® inlet for test point 8 at 16.0 hrs. during NO_x Reduction Stage (loading at 4 g/L)

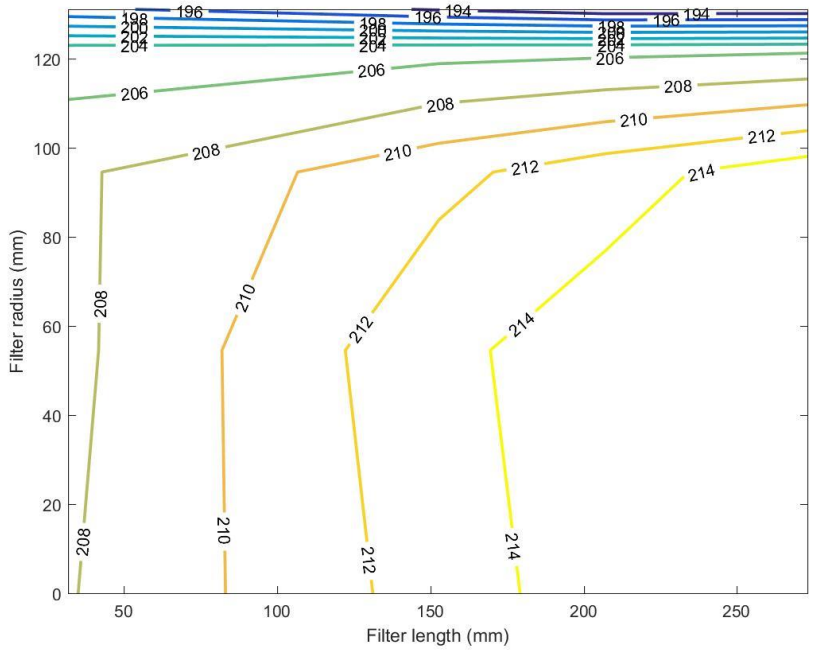

Figure F.43 Temperature distribution in the SCRF® for test point 1 at 14.1 hrs. during NO_x Reduction Stage (loading at 4 g/L)

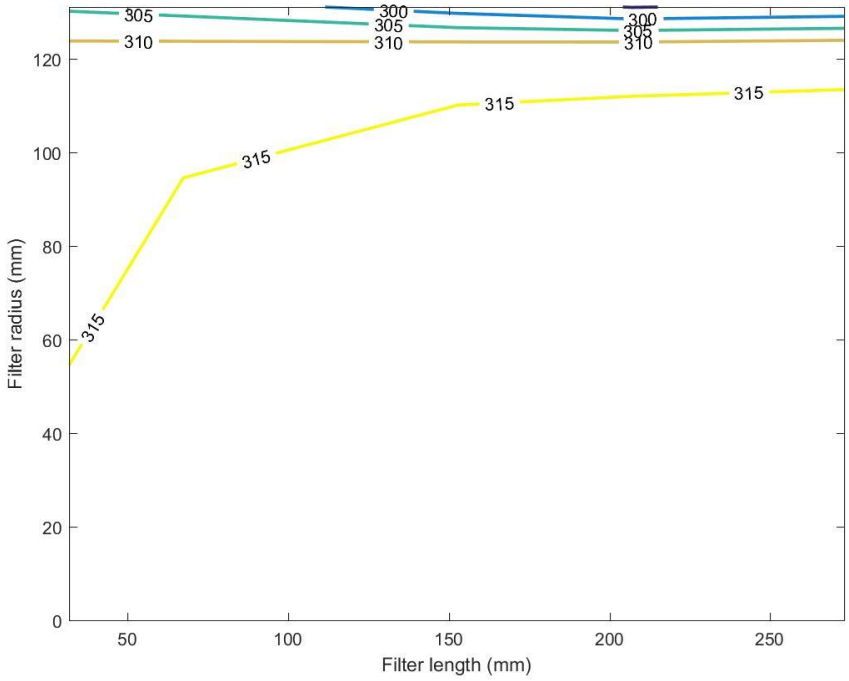

Figure F.44 Temperature distribution in the SCRF® for test point 3 at 11.4 hrs. during NO_x Reduction Stage (loading at 4 g/L)

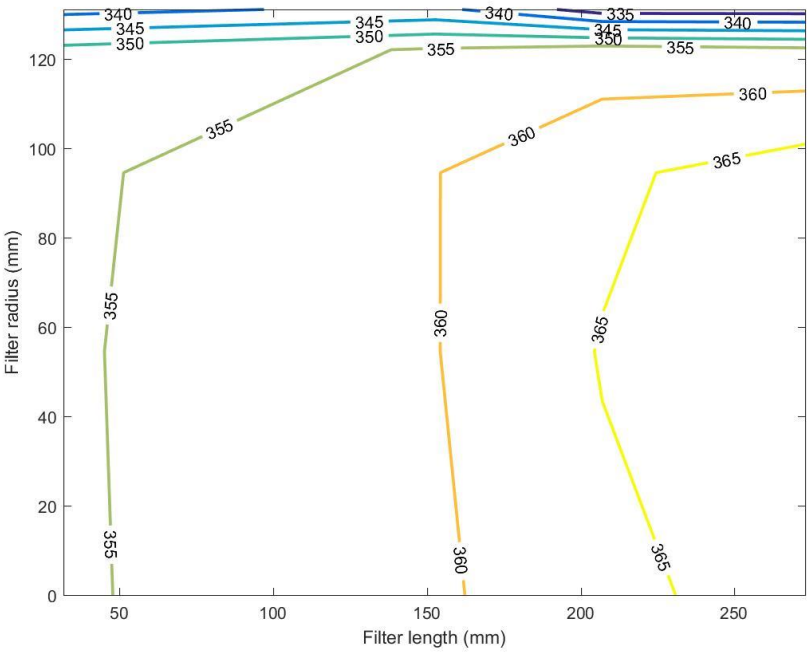

Figure F.45 Temperature distribution in the SCRF® for test point 6 at 15.9 hrs. during NO_x Reduction Stage (loading at 4 g/L)

Table F.5 Thermocouple temperatures at NO_x reduction stage at 4 g/L

NOx Reduction Stage - 4 g/L	Time [hr.]	SCRF® Thermocouple Temperature [°C]																			
		S1	S2	S3	S4	S5	S6	S7	S8	S9	S10	S11	S12	S13	S14	S15	S16	S17	S18	S19	S20
1	14.1	208[1]	208	208	205	196	213	214	211[1]	205[1]	194[1]	215	215	213[1]	205[1]	193	216	215	215	206	193
3	11.4	316	310	314	311	304	320	319	318	313[1]	298[1]	319	325	318	313	295	320[1]	318[1]	318	314[1]	296
6	15.9	354	356	354	351	338	359	360	360	355[1]	341	364	365	364	357	333	367	369	368	356	333
8	16.0	447	448	447	444	439	454	453	453	447[1]	430[1]	454[1]	454	449	448	426	454	455	454	447	426

[1]The highlighted thermocouple temperatures have been approximated on the basis of the trend of thermocouple temperatures in other test points.

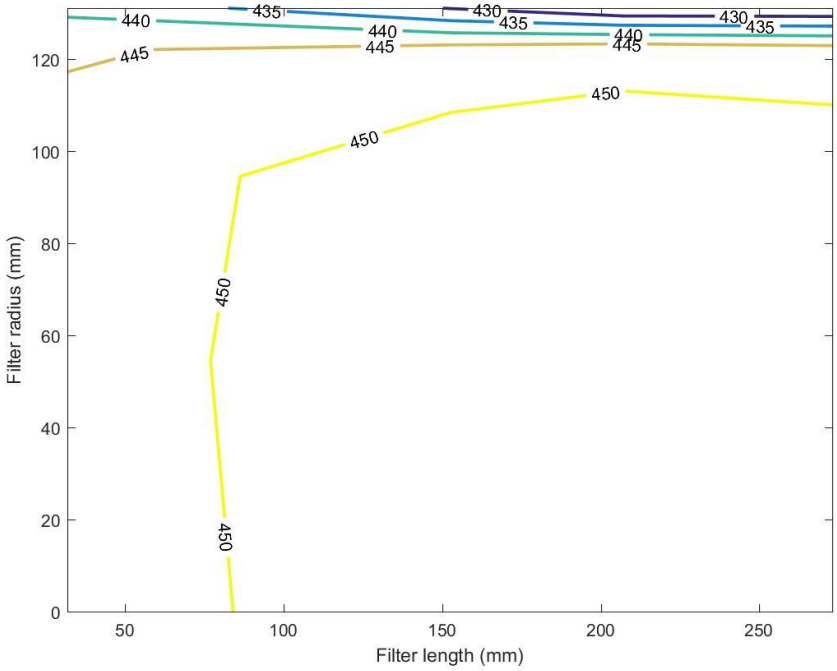

Figure F.46 Temperature distribution in the SCRF® for test point 8 at 16.0 hrs. during NO_x Reduction Stage (loading at 4 g/L)

Appendix G. Permission to Use Copyrighted Material

Michigan Tech

Saksham Gupta <sakshamg@mtu.edu>

Permission to use figure and tables from your MS Thesis

Krishnan Raghavan <kgraghav@mtu.edu> Tue, May 3, 2016 at 11:23 PM
To: Saksham Gupta <sakshamg@mtu.edu>

Hi Saksham,

Please go ahead and use any required figures and/or tables from my thesis. Best wishes for your report.

Regards,
Krishnan Raghavan

On Tue, May 3, 2016 at 11:12 PM, Saksham Gupta <sakshamg@mtu.edu> wrote:

> Hi Krishnan,
>
> I would like to request for your permission to adapt and use **Figure 3.2, Table 3.3, Table 3.11, and Table 3.12** from your Master's Thesis in my MS Report titled "*An Experimental Investigation into the Effect of Particulate Matter on NOx Reduction in a SCR Catalyst on a DPF*" to detail about experimental setup, fuel properties, and test cell instruments.
>
> Kindly respond with a text in your reply.
>
> Thanks,
> **Saksham Gupta**
> *Graduate Student*
> *Mechanical Engineering-Engineering Mechanics*
> *Michigan Technological University*
> *MI-49931*
> *Mobile: 906.370.7029*
> *Email: sakshamg@mtu.edu*